

Synthetic Efforts Toward New Splicing Modulators

by

Paulo Markaj

B.S. Biochemistry, Manhattan College, 2016

Submitted to the Graduate Faculty of the
Dietrich School of Arts and Sciences in partial fulfillment
of the requirements for the degree of
Master of Science

University of Pittsburgh

2021

UNIVERSITY OF PITTSBURGH

DIETRICH SCHOOL OF ARTS AND SCIENCES

This thesis was presented

by

Paulo Markaj

It was defended on

August 5, 2021

and approved by

Alex Deiters, Professor, Department of Chemistry

Paul Floreancig, Professor, Department of Chemistry

Thesis Advisor/Dissertation Director: Kazunori Koide Professor, Department of Chemistry

Copyright © by Paulo Markaj

2021

Synthetic Efforts Toward New Splicing Modulators

Paulo Markaj, MS

University of Pittsburgh, 2021

FR901464 is a natural product isolated in 1996. It's activity in a variety of cancer cells lines has made it placed it in the attention of chemists. It has since been synthesized by a number of different groups who have also synthesized new analogs of it. Analogs have been put forth with the goal of finding a compound more potent and having more favorable pharmacokinetics as well. The Koide group had synthesized an analog of FR901464 with low nanomolar activity called meayamycin B. Here are my attempts to synthesize an analog of meayamycin B with the C12 methyl removed, the nitrogen of the enamide methylated, and the C4'' acetyl group replaced with an O-methoxymethyl ether group. This new analog was designed to hopefully have better pharmacokinetics and take the conformation of the natural product, making it just as potent if not more then meayamycin B.

Table of Contents

Preface.....	xii
1.0 Introduction.....	1
1.1 Splicing and Disease	4
1.2 FR901464.....	5
1.3 Cyclopropyl Motif in Drug Design.....	13
2.0 Cyclopropyl MAMB Analog	15
3.0 N-methyl-C12-desmethyl MAMD	21
Appendix A Supporting Information.....	24
Appendix A.1 Experimentals.....	25
Appendix B NMR Spectra.....	43
Bibliography	72

List of Tables

Table 1: Conditions explored for Simmons Smith reaction.....	16
---	-----------

List of Figures

Figure 1: Mechanism of two transesterification reactions (called the branching and ligation reactions) in the splicing event.....	1
Figure 2: Alternative splicing patterns. Introns represented in blue, exons represented by red, green, and yellow.....	2
Figure 3: Structure of meayamycin B.....	10
Figure 4: Numbering scheme of FR901464	11
Figure 5: Proposed analogs to study the effect of the conformation of the left pyran ring .	12
Figure 6: BMS-791325 (right) and lead compound (left).....	13
Figure 7: Top row; GSK136070F (left) and previous analog. Bottom row; Spironolactone (left) and Drospironone (right)	14
Figure 8: HMBC and NOE correlations.....	17
Figure 9: Calculated conformers of Nicolaou intermediates (top and bottom left) and the cyclopropyl intermediate (bottom right)	18
Figure 10: Structures of meayamycin D and N-methyl meayamycin D.....	20
Appendix Figure 1: ¹H NMR spectrum of ethyl 2-(bis(2-(tert-butyl)phenoxy)phosphoryl)acetate (CDCl₃, 400MHz, 1H 298 K).....	43
Appendix Figure 2: ¹H NMR spectrum of ethyl 2-(bis(2-(tert-butyl)phenoxy)phosphoryl)propanoate (CDCl₃, 400MHz, 1H 298 K).....	44
Appendix Figure 3: ¹H NMR spectrum of ethyl 2-(triphenyl-λ5-phosphaneylidene)acetate (CDCl₃, 400MHz, 1H 298 K).....	45

Appendix Figure 4: ¹ H NMR spectrum of 3-(tert-butyl) 4-methyl (4S,5R)-2,2,5-trimethyloxazolidine-3,4-dicarboxylate (C ₆ D ₆ , 400MHz, 1H 338 K)	46
Appendix Figure 5: ¹ H NMR spectrum of tert-butyl (4R,5R)-4-(hydroxymethyl)-2,2,5-trimethyloxazolidine-3-carboxylate (C ₆ D ₆ , 400MHz, 1H 338 K)	47
Appendix Figure 6: ¹ H NMR spectrum of tert-butyl (4S,5R)-4-formyl-2,2,5-trimethyloxazolidine-3-carboxylate (C ₆ D ₆ , 400MHz, 1H 338 K)	48
Appendix Figure 7: ¹ H NMR spectrum of tert-butyl (4R,5R)-4-((Z)-3-ethoxy-3-oxoprop-1-en-1-yl)-2,2,5-trimethyloxazolidine-3-carboxylate (C ₆ D ₆ , 400MHz, 1H 343 K)	49
Appendix Figure 8: ¹ H NMR spectrum of tert-butyl ((2R,3R)-2-methyl-6-oxo-3,6-dihydro-2H-pyran-3-yl)carbamate (CDCl ₃ , 500MHz, 1H 298 K)	50
Appendix Figure 9: ¹ H NMR spectrum of tert-butyl ((2R,3R,6S)-6-allyl-2-methyl-3,6-dihydro-2H-pyran-3-yl)carbamate (CDCl ₃ with /1% CD ₃ OD, 400MHz, 1H 298 K).....	51
Appendix Figure 10: ¹³ C NMR spectrum of tert-butyl ((2R,3R,6S)-6-allyl-2-methyl-3,6-dihydro-2H-pyran-3-yl)carbamate (CDCl ₃ with /1% CD ₃ OD, 500400MHz, 1H 298 K) 52	
Appendix Figure 11: HMBC NMR spectrum of tert-butyl ((2R,3R,6S)-6-allyl-2-methyl-3,6-dihydro-2H-pyran-3-yl)carbamate (CDCl ₃ with /1% CD ₃ OD, 500MHz, HMBC 298 K)53	
Appendix Figure 12: HSQC NMR spectrum of tert-butyl ((2R,3R,6S)-6-allyl-2-methyl-3,6-dihydro-2H-pyran-3-yl)carbamate CDCl ₃ with /1% CD ₃ OD, 500MHz, HSQC 298 K). 54	
Appendix Figure 13: NOE irradiated at 1.15 ppm NMR spectrum of tert-butyl ((2R,3R,6S)-6-allyl-2-methyl-3,6-dihydro-2H-pyran-3-yl)carbamate CDCl ₃ with /1% CD ₃ OD, 400MHz, 298 K)	55

Appendix Figure 14: NOE irradiated at 2.25 ppm NMR spectrum of tert-butyl ((2R,3R,6S)-6-allyl-2-methyl-3,6-dihydro-2H-pyran-3-yl)carbamate (CDCl ₃ with 1% CD ₃ OD, 400MHzpp, 298 K)	56
Appendix Figure 15: NOE irradiated at 3.85 ppm NMR spectrum of tert-butyl ((2R,3R,6S)-6-allyl-2-methyl-3,6-dihydro-2H-pyran-3-yl)carbamate (CDCl ₃ with /1% CD ₃ OD, 400MHz, 298 K)	57
Appendix Figure 16: NOE irradiated at 4.15 ppm NMR spectrum of tert-butyl ((2R,3R,6S)-6-allyl-2-methyl-3,6-dihydro-2H-pyran-3-yl)carbamate (CDCl ₃ with /1% CD ₃ OD, 400MHz, 298 K)	58
Appendix Figure 17: NOE irradiated at 4.25 ppm NMR spectrum of tert-butyl ((2R,3R,6S)-6-allyl-2-methyl-3,6-dihydro-2H-pyran-3-yl)carbamate (CDCl ₃ with /1% CD ₃ OD, 400MHz, 298 K)	59
Appendix Figure 18: ¹ H NMR of (S)-1-ethoxy-1-oxopropan-2-yl morpholine-4-carboxylate (CDCl ₃ , 400MHz, 298 K)	60
Appendix Figure 19: ¹ H NMR of (S)-(Z)-5-ethoxy-5-oxopent-3-en-2-yl morpholine-4-carboxylate (CDCl ₃ , 500MHz, 298 K)	61
Appendix Figure 20: ¹ H NMR of tert-butyl (4R,5R)-4-((E)-3-ethoxy-3-oxoprop-1-en-1-yl)-2,2,5-trimethyloxazolidine-3-carboxylate (C ₆ D ₆ , 400MHz, 338 K)	62
Appendix Figure 21: ¹ H NMR of tert-butyl tert-butyl (4R,5R)-4-(3-ethoxy-3-oxopropyl)-2,2,5-trimethyloxazolidine-3-carboxylate (C ₆ D ₆ , 400MHz, 338 K)	63
Appendix Figure 22: ¹ H NMR of tert-butyl ((2R,3R)-2-methyl-6-oxotetrahydro-2H-pyran-3-yl)carbamate (CDCl ₃ , 500MHz, 298 K)	64

Appendix Figure 23: ^1H NMR of tert-butyl ((2R,3R,6R)-6-allyl-2-methyltetrahydro-2H-pyran-3-yl)carbamate (CDCl_3 , 500MHz, 298 K).....	65
Appendix Figure 24: ^1H NMR of S)-2-(methoxymethoxy)propanoate (CDCl_3 , 500MHz, 298 K)	66
Appendix Figure 25: ^1H NMR of (S)-(Z)-4-(methoxymethoxy)pent-2-enoate (CDCl_3 , 400MHz, 298K)	67
Appendix Figure 26: ^1H NMR of ((S)-(Z)-4-(methoxymethoxy)pent-2-enoic acid (CDCl_3 , 400MHz, 298 K)	68
Appendix Figure 27: ^1H NMR of (((S)-(Z)-)-N-((2R,3R,6R)-)-6-allyl-2-methyltetrahydro-2H-pyran-3-yl)-4-(methoxymethoxy)-N-methylpent-2-enamide (CDCl_3 , 400MHz, 298 K)	69
Appendix Figure 28: ^{13}C NMR of (((S)-(Z)-)-N-((2R,3R,6R)-)-6-allyl-2-methyltetrahydro-2H-pyran-3-yl)-4-(methoxymethoxy)-N-methylpent-2-enamide (CDCl_3 , 400MHz, 298 K)	70
Appendix Figure 29: NOE irradiated at 3.7623ppm NMR of (((S)-(Z)-)-N-((2R,3R,6R)-)-6-allyl-2-methyltetrahydro-2H-pyran-3-yl)-4-(methoxymethoxy)-N-methylpent-2-enamide (CDCl_3 , 400MHz, 298 K)	71

List of Schemes

Scheme 1: Retrosynthetic analysis by Jacobsen	6
Scheme 2: Kitahara retrosynthetic analysis	7
Scheme 3: Koide retrosynthetic analysis	8
Scheme 4: Ghosh retrosynthetic analysis	9
Scheme 5: Start of new route	15
Scheme 6: Strategies to overcome over reduction	15
Scheme 7: Steps toward cyclopropyl LF	16
Scheme 8: Positive control SSC	18
Scheme 9: Synthesis of side chain material	19
Scheme 10: Scheme towards enamide 31	21
Scheme 11: Synthesis of acid 30	22

Preface

I would like to thank My committee members Dr Paul Floreancig and Dr Alex Dieters for their guidance. I would also like to thank the Koide group for all their support and guidance over the years. I would like to especially thank Dr Kazunori Koide for his help, guidance, and teaching over the years. This wouldn't be possible without them.

1.0 Introduction

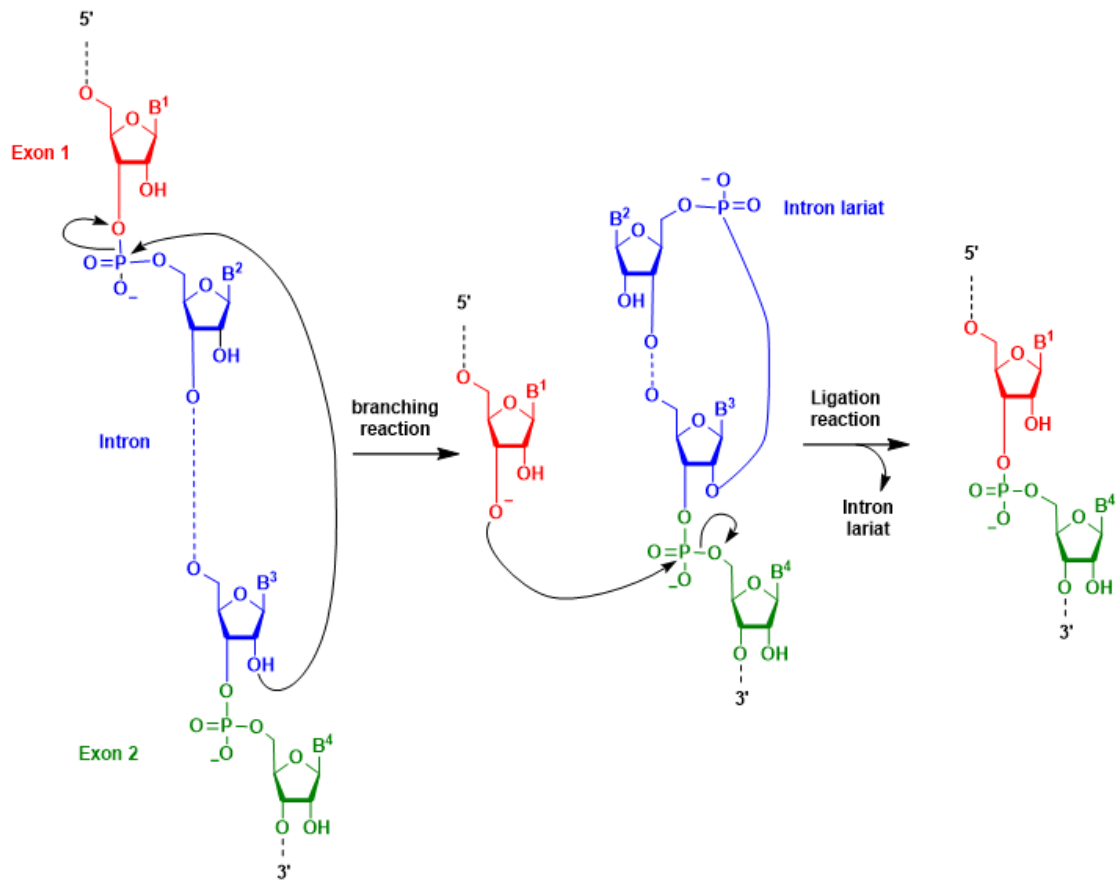


Figure 1: Mechanism of two transesterification reactions (called the branching and ligation reactions) in the splicing event.

The central dogma of molecular biology is DNA undergoes transcription to create RNA, which then undergoes translation to create proteins. During that first step premature RNA, pre-mRNA, is converted to messenger RNA or mRNA. The conversion of pre-mRNA to mRNA involves removal of sequences that do not code for the protein. These sequences are called introns.

This process leaves behind the segments that are used for the protein synthesis which are called exons. The process of removing introns from the pre-mRNA to yield the mature mRNA is called splicing. This is done by two transesterification reactions, Figure 1, the free hydroxy group on the 3' end of the intron attacks the phosphate just after the 3' end of the first exon. This removes the first exon in an S_N2 fashion. This is referred to as the branching reaction. The subsequent alkoxide of the 3' end of the first exon then attacks the phosphate of the 5' end of the second exon in a similar S_N2 fashion, called the ligation reaction which connects the two exons and frees the intron lariat. The biological machinery that catalyzes this process is called the spliceosome.

This phenomenon is commonplace throughout many organisms, including humans. In fact, approximately 92-95% of the human genome is spliced.¹ In 1977 studies done in adenovirus 2 discovered RNA strands with noncontiguous sequences of

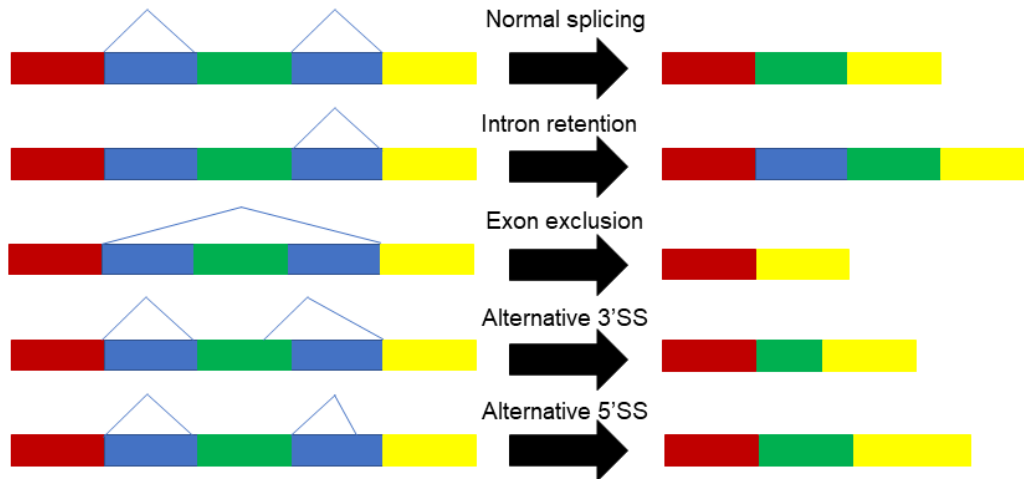


Figure 2: Alternative splicing patterns. Introns represented in blue, exons represented by red, green, and yellow

the viral genome.^{2,3} The discovery of these RNA strands leads to the hypothesis that a single pre-mRNA sequence could code for multiple mRNA sequences. This hypothesis was later confirmed

by the discovery of similar RNA strands in eukaryotic cells and experiments done on yeast tRNA.^{4,5} Since then, splicing patterns have been studied more in depth. The phenomenon of one premRNA strand being spliced into different mRNA strands is termed alternative splicing (Figure 2).

The spliceosome is comprised of small ribonucleoproteins (snRNPs) and other protein splicing factors.^{6,7} The spliceosome forms onto the pre-mRNA in stages as the splicing process occurs. Splicing begins with the formation of the E complex to recognize the target intron. This is initiated by the U1snRNP recognizing the 5' splice site (5'SS), the splicing factor SF1 recognizing the branch point site (BPS), the U2AF65 factor recognizing the polypyrimidine tract (PYT), and U2AF35 factor recognizing the 3' splice site (3'SS).⁸⁻¹¹ The U2snRNP then replaces SF1 at the BPS converting the E complex into the A complex.^{12,13} The pre-formed U4/U5/U6 tri-snRNP then binds to the A complex causing a conformation change and converting the A complex to the pre-B complex.¹² The interaction between the 5'SS and U1snRNP is distorted by the helicase Prp28, releasing the U1snRNP converting the pre-B complex into the B complex.¹⁴ Helicase Brr2 removes the U4snRNP and other protein splicing factors are recruited to stabilize the newly formed catalytic core of the B^{act} complex.^{15,16} Helicase Prp2 then rearranges the B^{act} to the B* complex.¹⁷ The B* complex catalyzes the cleavage of the 5' exon from the intron in the branching reaction.^{18,19} The freed 5'SS and intron lariat bound to the U2, U5, and U6 snRNPs are called the C complex. Prp 16 rearranges the C complex to the C* complex which catalyzes the second step of splicing known as the ligation reaction.²⁰⁻²² The 5' exon and 3' exon are joined and the intron is removed yielding the P complex. The joined exons are released by Prp 22, forming the Intron Lariat Spliceosome complex (ILS). The ILS is released, and the complex is unraveled with the help of Prp 43.^{23,24}

The U2snRNP is further comprised of 2 subcomplexes, SF3a and SF3b.^{25,26} The SF3b subcomplex is made up of 4 subunits the SAP 49, 130, 145, and 155.²⁶ All of which are required to form the A complex. SF3b1, also known as SAP 155, plays a crucial role in the 3'SS selection in homeostatic cells.²⁷

The spliceosome, like other biological processes, is susceptible to error and disease. There are two categories of diseases associated with splicing mistakes; “in cis” mutations are errors that arise from mutations in the machinery of splicing that cause errors, while “in trans” mutations are mutations that arise from misspliced RNA.

1.1 Splicing and Disease

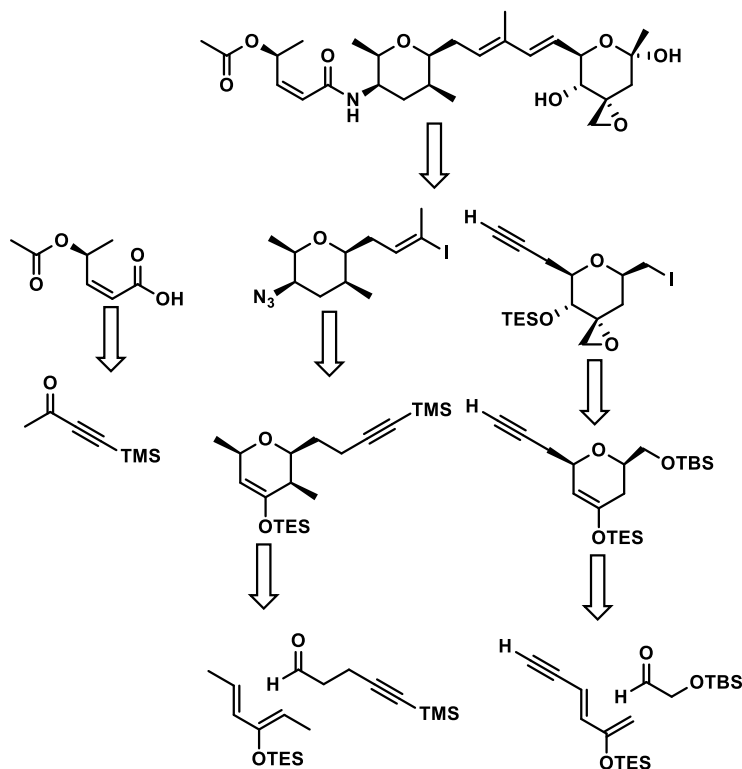
Myelodysplastic syndrome (MDS) are a group of disorders where normal blood cell production in the bone marrow is affected or hindered. One sub type of MDS is refractory anemia is characterized by erythroid dysplasia with bone marrow ring sideroblasts (RARS). Recently it was shown that RARS and other subtypes of MDS have mutations in splicing factors, DNA methylators, chromatin modifiers, and transcription factors. Specifically, it was shown that 129 cases of 159 cases had SF3B1 mutations.²⁸ SF3B1 is involved in the alternative splicing of apoptosis-related gene myeloid cell leukemia-1 (Mcl-1).²⁹ Mcl-1 has two isoforms; proapoptotic Mcl-1S and antiapoptotic Mcl-1L.³⁰⁻³¹ Recently, SF3b1 has also been identified as a copy number alterations yielding cancer liabilities owing to partial loss (CYCLOPS) gene.³² CYCLOPS genes are non-driver mutations in genes that lead to partial loss of expression but not cell death. A portion of these genes are essential genes to cell viability with little feedback regulation. The partial loss makes these cells sensitized to gene suppression of their paralogs. 16% of the genome is lost in the

average cancer and CYCLOPs genes are frequently lost. 71.6% of the 10,570 cancers spanning 31 cancer types harbor loss of at least one CYCLOPs gene. CYCLOPs genes tend to be spliceosome or proteasome genes. CYCLOPs gene expression upon copy loss decreases by 28% on average, whereas non-CYCLOPs genes experienced an 18% decrease. This difference in gene expression concludes that cancers with copy loss of CYCLOPs genes are expressed at lower levels than normal cells. This decrease in paralogs, specifically the SF3b complex, is what allows for the preferential targeting of cancer cells over healthy cells.³² Targeting cancer cells specifically while not damaging healthy cells is a large issue in cancer therapy to this day. The unique nature of CYCLOPs genes allows for the spliceosome to be a viable drug target. H3B8800 small molecule drug.

1.2 FR901464

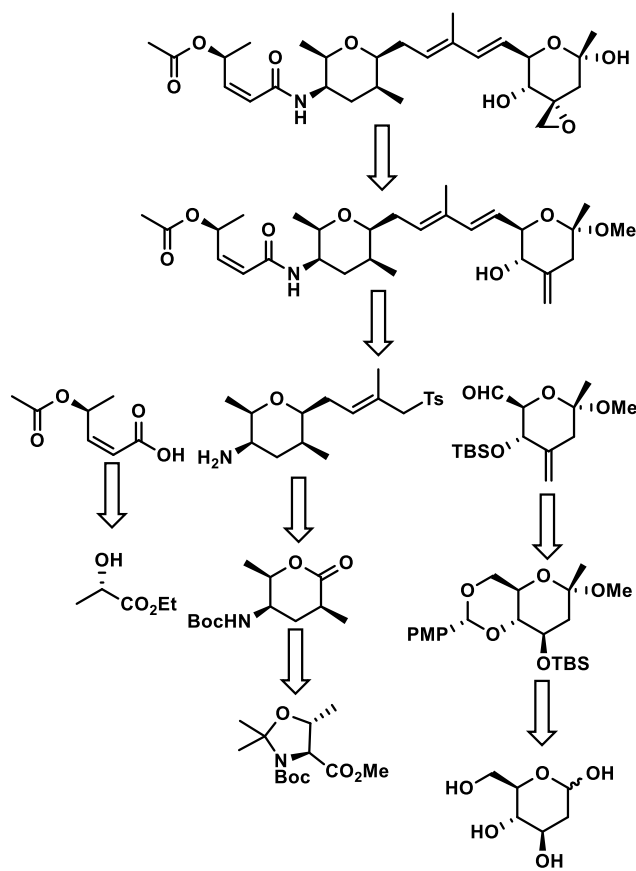
There are many compounds that fall in the class of compounds that is now called splicing inhibitors. FR901464 (Scheme 1) is a natural product first reported in 1996.³³ It was isolated in a bacterium originally described as *Pseudomonas* sp. 2663. However, based on 16S rRNA sequence analysis, it has since been shown to be a *Burkholderia* sp. FERM BP-3421.³⁴ FR901464 induced G1 and G2/M phase arrest and reduced the expression of endogenous genes related to cell cycle transition and cell death while not affecting the expression of other genes. This transcriptional control was shown to be related to its antitumor activity in a variety of cancer cell lines.³³ The Yoshida group determined the target of FR901464 and related compounds using a biotinylated analog.³⁵ They found that SAP155, 145, and 130 were isolated, concluding that SF3B is the target.

This is corroborated by the fact that herboxidiene and pladienolide, known splicing modulators, also target SF3B.^{36,37} The activity of FR901461 has drawn the attention of synthetic chemists.



Scheme 1: Retrosynthetic analysis by Jacobsen

Since its isolation, it has been synthesized by 4 groups. The Jacobsen group (Scheme 1)^{38,39} was the first to synthesize the compound in 2000 using their hetero Diels-Alder reaction conditions to build the two pyran rings and set the stereocenters early. The pyran rings were combined via a hydrozirconation-transmetalation -Negishi coupling sequence. The synthesis was then rounded out via an azide reduction to do a classic HBTU coupling reaction. They also confirmed the absolute stereochemistry of FR901464 and synthesized two analogs. The methyl amide confirmed the biological necessity of the enamide side chain and the cyclopropane analog confirmed the necessity of the epoxide. The deshydroxy analog showed that the hemiketal on the right pyran ring is not favorable.

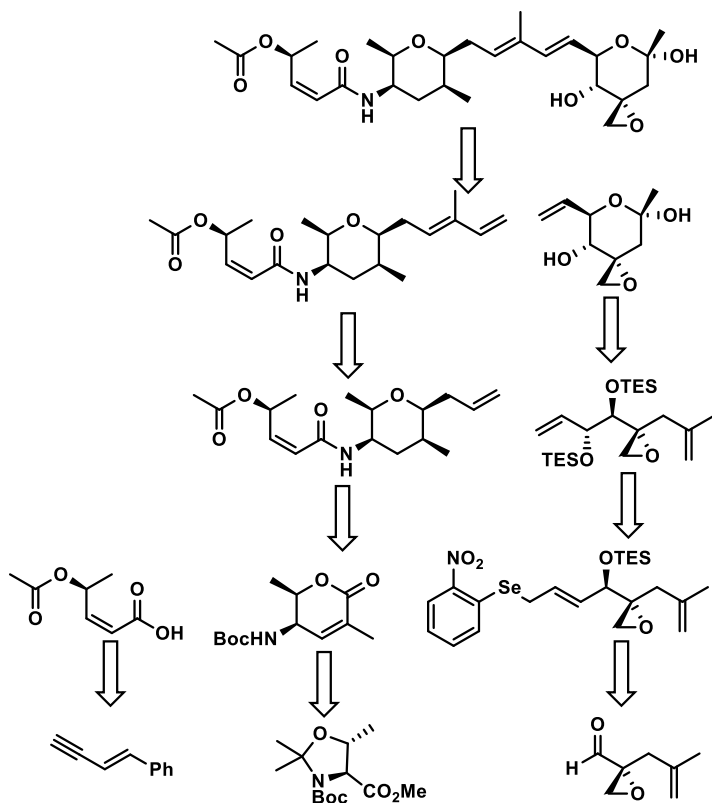


Scheme 2: Kitahara retrosynthetic analysis

The Kitahara group synthesized the natural product in 2001.⁴⁰⁻⁴² They had made similar disconnections as the Jacobsen group did, although they sought to utilize the chiral pool rather than asymmetric catalysts. The left fragment was synthesized from Garner's ester in a 14-step sequence. The side chain enamide was then coupled to the left pyran ring via HBTU coupling. The right pyran ring was synthesized in a 14-step sequence. The left and right pyran rings were combined via a Julia olefination. The final stage of their synthesis was deprotection, acetalation of the side chain, and epoxidation of the right pyran ring.

The Koide group^{43,44} retrosynthetically disconnected the molecule in a similar fashion but looked to make a more concise synthesis to find analogs via newly functionalized left and right tetrahydropyran fragments. The left tetrahydropyran synthesis started with the chiral pool L-

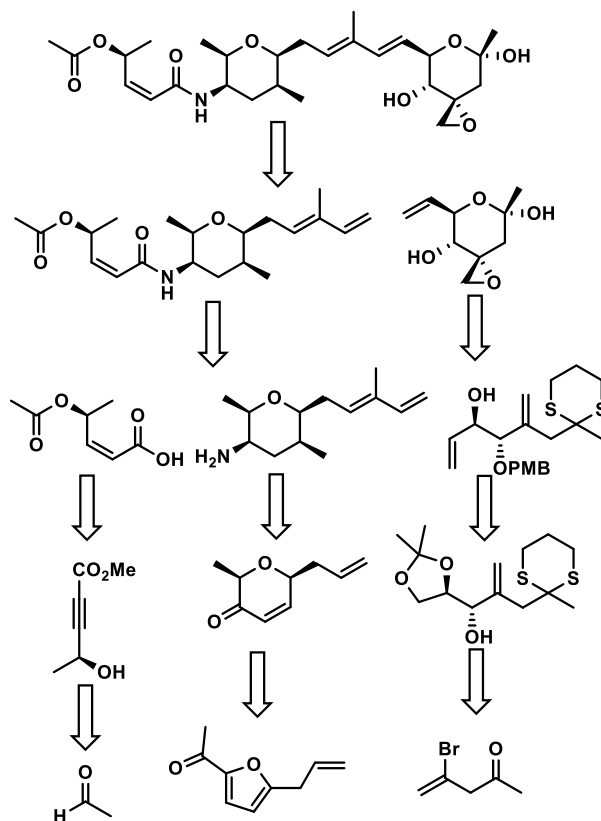
threonine which in a few steps yielded Garner's ester, which could then be opened and a ring closing metathesis then oxidation would lead to enone shown, which would then be diastereoselectively hydrogenated.



Scheme 3: Koide retrosynthetic analysis

Allylation followed by silane reduction lead to tetrahydropyran intermediate which would then be combined with the acid side chain, formed in a 4-step sequence, in a HATU coupling to form the enamide intermediate. Cross metathesis with methacrolein followed by a Wittig reaction yielded the diene that would be combined with the right fragment in a cross metathesis. The key steps in the synthesis of the right tetrahydropyran ring synthesis are the stereoselective C-C bond formation was done using the Zr/Ag alkynylation developed by the Koide group,⁴⁵ followed by RED-Al reduction⁴⁶ and TES protection lead to the allylic alcohol. DIBALH reduction of the

available ester to the alcohol then allowed conversion to the *o*-nitrophenylselenide which allowed for the Mislow-Evans rearrangement⁴⁷ to the allylic alcohol in the presence of H₂O₂.



Scheme 4: Ghosh retrosynthetic analysis

The Ghosh group⁴⁸⁻⁵⁰ retrosynthetically broke up FR901464 in a similar fashion; left tetrahydropyran, right tetrahydropyran, and side chain acid fragment. The right tetrahydropyran ring started with chiral pool (R)-isopropylidene glyceraldehyde. Attack by the carbanion and protection lead to thioacetal which was then converted to allylic alcohol after a deprotection and tosylation with Corey-Chaykovsky dimethylsulfonium methylide. The dithiane was removed with Hg(ClO₄)₂ and cyclization with lutidine. Finally mCPBA lead to epoxy tetrahydropyran. The left tetrahydropyran ring was synthesized starting with commercially available acetyl furan. The selective reduction then Achmatowicz rearrangement furnished a hemiketal that was then reduced to enone. 1,4-Addition furnished the installation of the missing methyl group with excellent

diastereoselectivity. From the pyranone, a metathesis-elimination sequence attached the diene then reductive amination and HATU coupling with the side chain acid, made in a 4-step sequence starting from acetic aldehyde, to get the enamide needed for the 2nd cross methatesis which led to spliceostatin A which could be deprotected to yield FR901464.

The structure activity relationship studies done by the different groups has revealed important details. Beginning with the right fragment the Jacobsen group and Koide group showed that the epoxide at C3 is required through their cyclopropyl analog and their hydroxy analog, respectively.^{39,51} The hydroxy group at C1 was shown to decrease the half-life. This was concluded by exchanging the hydroxy group for a methyl group to create meayamycin which is 100-fold more potent.^{42,44} The hydroxy group at C4 was found to be necessary for potency, as the methoxy analog was less potent. The Z-enamide was shown to be necessary for potency.³⁹ The olefin between C2' and C3' is an important structural component as the trans and saturated analogs were 5-fold and 20-fold less potent respectively.⁵¹ Analogs replacing the acetyl group at the C4' with a hydroxy group were 400-fold less potent, concluding that the hydrolysis of the acetyl group in biological conditions would decrease the compounds potency over time.⁵² Replacing the acetyl group with a morpholine carbamate increased potency leading to meayamycin B.⁵² Left fragment SAR began with the diene across C6-C9, showing necessity for potency as analogs with one olefin replaced with a cyclopropane ring were 10-fold less potent. Finally, it was showed that positions C12 and C15 prefer to be hydrophobic.⁵¹ Not much further has been probed about the structure and impact of the left fragment.

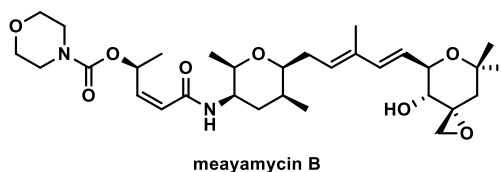


Figure 3: Structure of meayamycin B

Meayamycin B was shown to be two orders of magnitude more potent making it the most potent analog to date.⁵² Meayamycin B has also been shown to alter the splicing of Mcl-1 to decrease the expression of Mcl-1_L and increase the expression of Mcl-1_S inducing apoptosis.⁵³ Recently, the Pena group obtained the crystal structure of the SF3b1 complex bound to pladienolide B, a potent antitumor splicing modulator.⁵⁴ Their work has shown that splicing modulators bind to the hinge region of SF3b1. This binding causes a conformational change in SF3b1. The conformational change prevents proper U2 binding to the splice site. Analysis of the binding of different splicing modulators concludes that more sterically demanding analogs are more effective at destabilizing the interaction, allowing splicing to be modified and not completely inhibited.

The SAR studies of FR901464 and its analogs have probed many questions; one that has not been probed efficiently is if the conformation that is shown in the characterization is the conformation that leads to activity. It is important to probe this question because understanding what conformer the compound takes when active can allow for proper analog design to fully take advantage of how the compound sits in the active site.

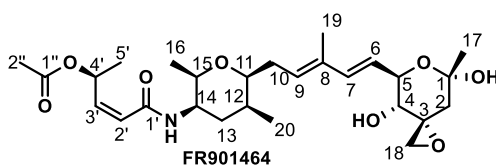


Figure 4: Numbering scheme of FR901464

Probing the necessity of the conformation can be done by designing a new analog that takes a different conformation (Figure 5). If said analog showed the same, or better, activity then the conformation of the natural product then the taking the conformation of the natural product is not necessary for activity. If the new analog is not active, then the conformation of the natural product is necessary. The conformation of the left fragment pyran ring has been concluded to be a chair

conformation. The reported coupling constants between the C14 and C15 hydrogens (Figure 4) was 2.0 Hz, indicative of a chair. The Nicolaou group synthesized analogs of FR901464 and used nuclear overhauser effect (NOE) experiments to confirm the stereochemistry of the C11 and C12 positions. The NOE experiments also allowed for conformation of the chair conformer of the pyran ring.

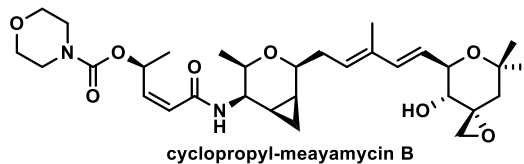


Figure 5: Proposed analogs to study the effect of the conformation of the left pyran ring

More information is needed on the conformation of the left pyran ring in order to design a splicing modulating drug. This knowledge would allow for the development of more active analogs. This goal in mind, cyclopropyl-meayamycin B was designed (Figure 6). The fused ring system will lock the rings in a half chair conformation without imposing great change in the steric bulk of the natural product. The activity of these compounds will determine if the conformation of the left fragment influences potency.

1.3 Cyclopropyl Motif in Drug Design

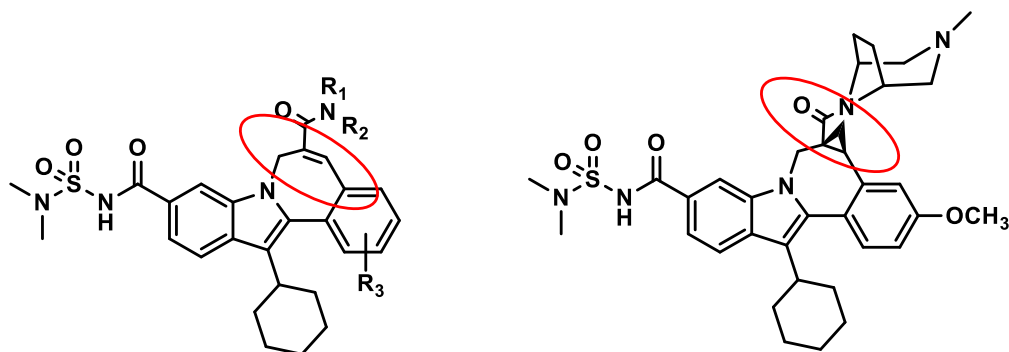


Figure 6: BMS-791325 (right) and lead compound (left)

There are many examples of cyclopropane rings in natural products and natural product synthesis. The cyclopropyl ring motif has been used to increase selectivity, microsomal stability, lock noncyclic alkenes, and eliminate Michael acceptors.⁵⁵ Cyclopropyl rings have been used to make a compound more resistant to metabolism. The carbon hydrogen bonds in cyclopropane rings are stronger (106 kcal/mol) than those in regular alkanes (101 kcal/mol in ethane).^{55,56} The locked staggered geometry of the ring prevents the proper alignment of orbitals to allow for hyperconjugation. This increased bond strength prevents the oxidative metabolism of the drug.⁵⁵ The cyclopropyl ring motif has also been used to increase potency as well.

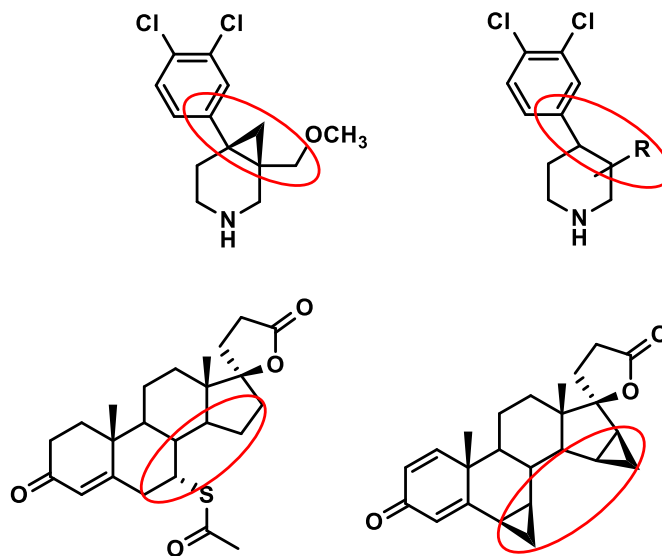
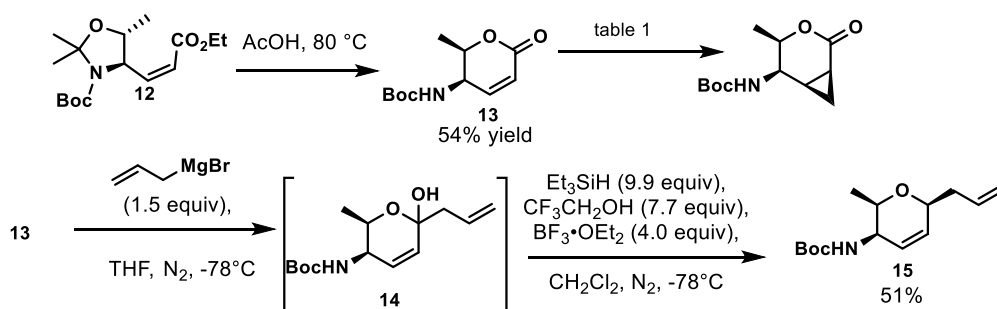


Figure 7: Top row; GSK136070F (left) and previous analog. Bottom row; Spirolactone (left) and Drospironone (right)

Fused ring systems with cyclopropyl ring motif are common as well. BMS-791325 is an HCV non-structural protein 5B (NS5B) polymerase inhibitor, currently in clinical trials with other HCV NS5B pol inhibitors.^{55,57,58} The incorporation of the cyclopropyl motif increased potency over the lead compound due to a conformational rigidity and better interactions with the Leu(492) residue.

borohydride conditions showed little to no conversion. Switching to lithium aluminum hydride (LAH) yielded full conversion, was completed in 2 h, and did not require a column. These results were reproduced when scaled up to 4 g. With the alcohol in hand, I began searching for oxidation conditions. Attempts with tempo and sodium hypochlorite showed little conversion of starting material. Swern oxidation of **10** to the aldehyde **2**, was successful but the yield was not satisfactory. The influence the temperature of the DIBALH solution was also studied in tandem. Initial cooling to -98°C for addition and then warming to -78°C prevented overreduction and allowed for increased yields of the 2-step process. Phosphonate **11** is used to yield the z-disubstituted olefin **12**.



Scheme 7: Steps toward cyclopropyl LF

Table 1: Conditions explored for Simmons Smith reaction.

ZnEt ₂ (equiv)	CH ₂ I ₂ (equiv)	Solvent	Temp.	Time
1.4	1.6	Et ₂ O	23	4
50	50	Et ₂ O	23	8
50	50	Et ₂ O	35	8
50	50	CH ₂ Cl ₂	45	8

The unsaturated ester **12** (scheme 7) was then exposed to the same oxazolidinone opening and cyclization conditions to yield lactone **13** in 48 % yield. With lactone **13** in hand Simmons-Smith chemistry (SSC) was attempted. Different equivalences of ZnEt₂ and CH₂I₂ were used with no success. Changing solvent, temp, and time didn't show improvement in yield either. Attempting

Simmons-Smith chemistry on a more activated olefin could be attempted a few steps later in the synthesis. Lactone 13 was exposed to Grignard conditions to form hemiketal 14 which was reduced to tetrahydropyran 15. Before SSC can be done confirmation of stereoselectivity is necessary. Determining the stereochemistry of the C11 position of tetrahydropyran 15 began by assigning the protons in the ^1H NMR spectra. The assignments can be confirmed by comparison to chemical shifts from previous intermediates synthesized and the coupling constants (see data for 15). The lactone signal at 4.65 ppm with a J values of 6.5 Hz and 3.5 Hz represents the hydrogen at C15. The signal at 4.33 ppm with J values of 3.5 Hz, 3.0 Hz, and 2.5 Hz represents the C14 hydrogen. These coupling constants account for coupling with the hydrogens at the C15 and C13 positions, and the N-H. These assignments are correlated to the signals at 3.72 ppm (C15 hydrogen) and 3.92 ppm (C14 hydrogen) based on J values and previously synthesized intermediates. The new peak at 4.13 ppm with J values of 6.4 Hz, 5.6 Hz, and 1.6 Hz corresponds to the new proton at C11. This chemical shift lines up with previous intermediates synthesized by the group. The J values correspond to the 2 diastereotopic protons at C10 and the vinyl proton at C12. HSQC experiments confirmed these assignments (Figure 8). To confirm the stereochemistry of the C11 position I did NOE experiments. NOE experiments show

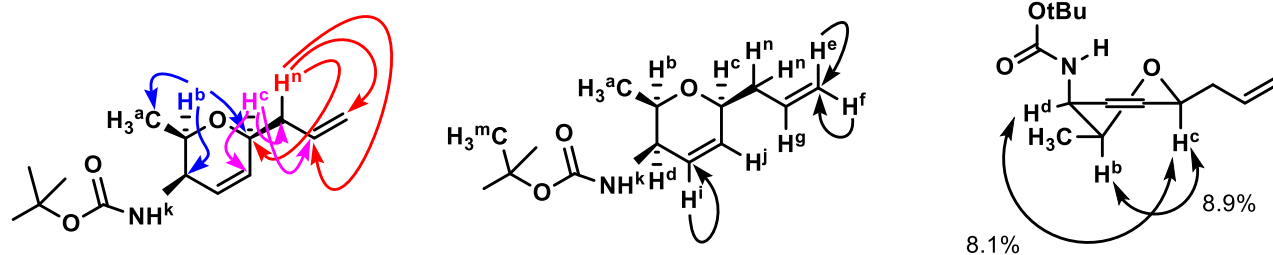
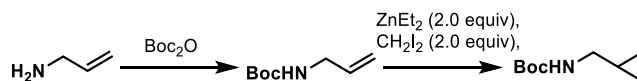


Figure 8: HMBC and NOE correlations

correlations between the C15 proton and the C11 proton. It also showed a strong correlation between C11 and C14. These correlations indicate that the compound may not be in the twist

boat conformation as one would expect, but they do support the desired stereochemistry. HSQC also allowed for proper olefin assignment which is vital for the SSC studies. The signal at 5.89 correlates to the C13 therefore, that signal represents Hⁱ. The signal at 5.11 ppm correlates to C8 and therefore represents H^e and H^f. The signal at 5.81 correlates to both C12 and C9 and therefore represents both H^j and H^g, respectively.



Scheme 8: Positive control SSC

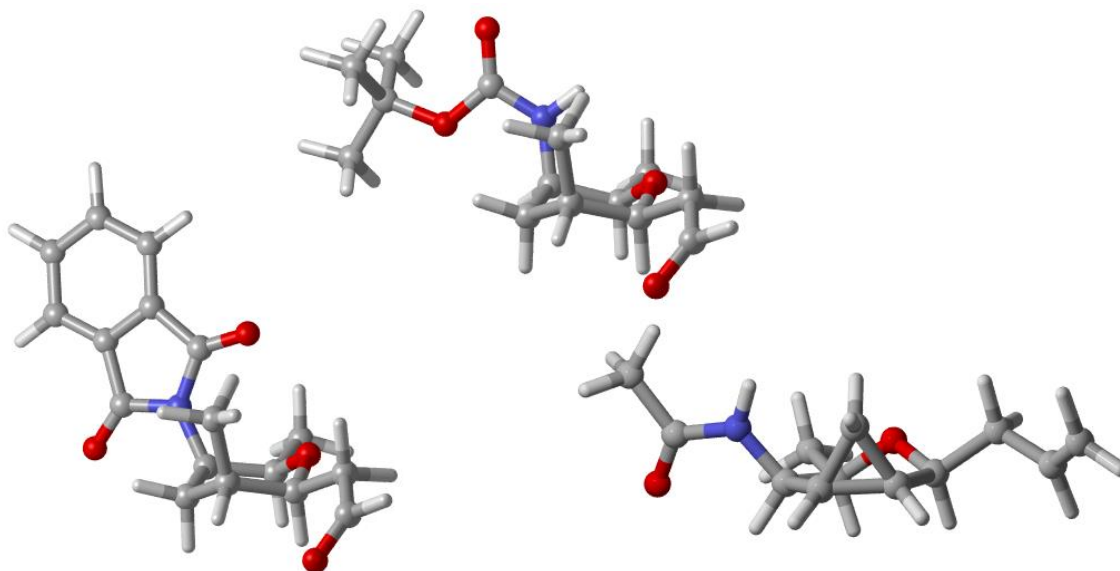
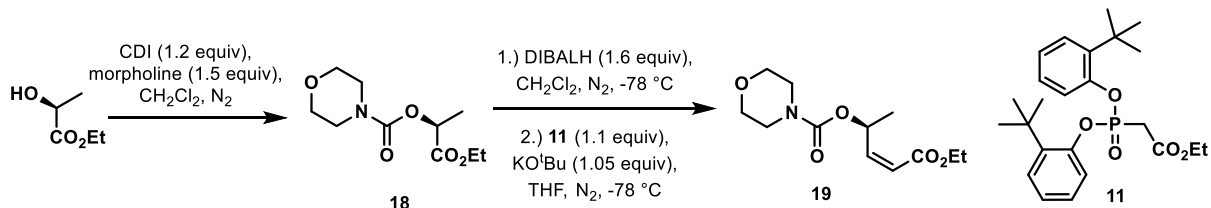


Figure 9: Calculated conformers of Nicolaou intermediates (top and bottom left) and the cyclopropyl intermediate (bottom right)

With the characterized tetrahydropyran **15** in hand efforts to cyclopropanate the disubstituted olefin began. Positive control experiments ruled out technical errors from previous trials (scheme 8). Initial experiments showed both olefins reacted at room temperature. Inconsistent yields and difficulty isolating the desired product prevented me from fully characterizing the fused ring intermediate. The conformers of the desired cyclopropanated intermediates proposed by DFT, B3LYP/6-31G(d) calculations (done by Wei Chuen Chan) using

Gaussian 09, Revision D. 01. As shown in Figure 7 the natural product will most likely take a chair conformation while the cyclopropyl analog would take a conformation closer to a boat conformation. The boc-protected amine is more representative of the natural product. All calculated conformers of the cyclopropyl analog took a half chair conformer. This would allow for the analog to test if the conformation of the left fragment is required for binding.



Scheme 9: Synthesis of side chain material

The side chain was synthesized using the same strategy put forth by our group (Scheme 9). Starting with ethyl-(S)-lactate CDI and morpholine yields the carbamate **18**. The carbamate is then subjected to DIBALH conditions followed by Horner-Wadsworth-Emmons reaction to yield the z-enoate, **19**. The ester is then hydrolyzed to the acid, which is used crude in the amide coupling. The synthesis was halted once the analogs synthesized by Dr Robert Bressin were tested. He explored the necessity of the N-H bond as well as sought to improve the pharmacokinetics of MAMB. Dr Bressin synthesized meayamycin D and N-methyl meayamycin D (Figure 12). Meayamycin D showed growth inhibition similar to that of meayamycin B, while the N-methylated version however did not perform as well. Differences of note between the two analogs is the coupling constants between H-14 and H-15. MAMD has a coupling constant of 2.1 Hz while the coupling constant of N-methyl MAMD is 4.9 Hz. This difference in coupling constants can be attributed to a difference in conformation of the left pyran ring. The decrease in activity can therefore mean that the active compound must take the chair conformation, yielding the 2.1 Hz J value. The other conformations are not as active. Comparing the structures made by the

computational models suggests that the cyclopropyl analogs would not take the optimal conformation to be active. The hypothesis then shifted to modifying MAMD to take the active conformation. Removing the C12 methyl group would relieve some of the strain and allow the chair conformation to be favored. This lead to the design of the new analog, N-methyl-C-12-desmethyl MAMD

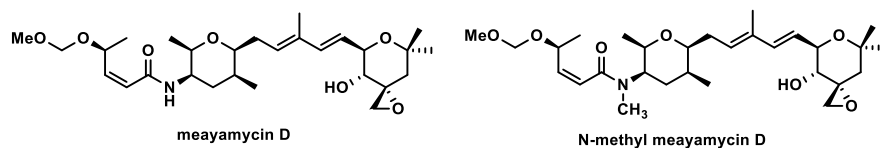
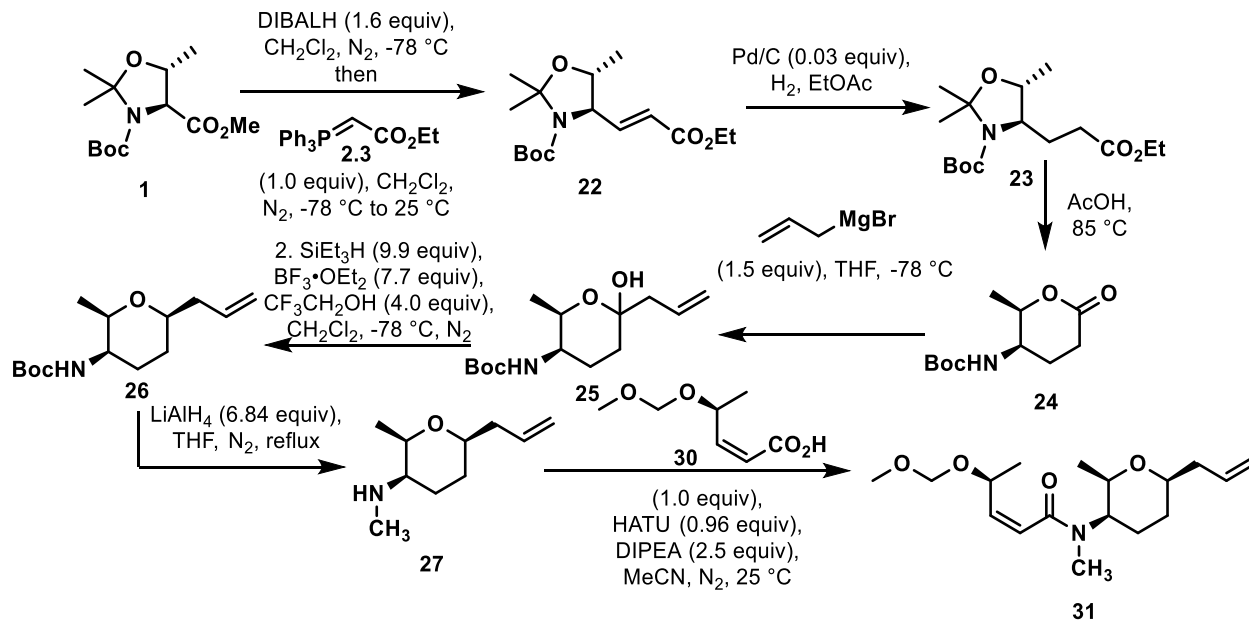


Figure 10: Structures of meayamycin D and N-methyl meayamycin D

3.0 N-methyl-C12-desmethyl MAMD

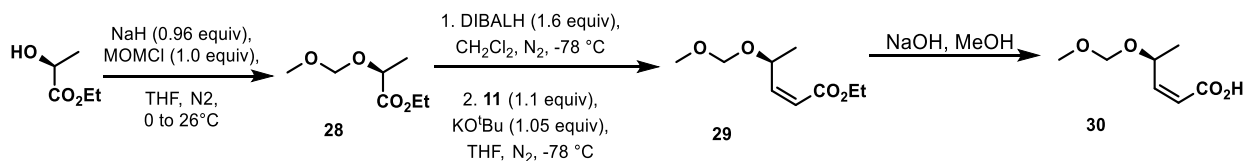


Scheme 10: Scheme towards enamide 31

The synthesis to the new analog would be similar to that of meayamycin B with minor alterations. LAH reduction of the boc group would allow for the N-methyl installation and deprotection of the amine for the following amide coupling step. This would allow for the amide coupling to the side chain to yield the completed left fragment. The completed left fragment, following the same sequence previously established by our group, would yield the desired analog in 3 steps.

Reduction of Garner's ester to the aldehyde followed by Wittig reaction with ylide **2.3** yields the enoate **22**. This enoate was easier to purify than the previous olefination. The enoate was then exposed to standard hydrogenation conditions to yield the saturated ester **23** which was carried forward to the lactone, **24**, using the same oxazolidine deprotection, cyclization conditions

previously discussed. The lactone was then converted to the hemiketal **25** using the Grignard addition, followed by silyl reduction to get pyran **26**. The next step was the boc reduction to the secondary amide **27**. Crude NMR and LCMS analysis supported the formation of the amine and was carried forward crude.



Scheme 11: Synthesis of acid 30

The side chain material was synthesized in a similar fashion as stated prior. Ethyl-(S)-lactate was subjected to standard MOM protection conditions. The ether **28** was then subjected to the DIBALH/HWE conditions to yield enoate **29**. The ester was hydrolyzed to acid **30** and used in the amide coupling. With the tertiary enamide synthesized two challenges arose. Confirming the presence of rotamers in the characterization and determining the conformation of the left pyran ring.

The tertiary enamide caused the appearance of rotamers in the HNMR spectra. Rotamers are isomers that differ only in their rotation around a bond. The presence of each rotamer on the NMR spectra makes it difficult to determine the presence of diastereomers or impurities. Techniques to distinguish the rotamers range from variable temperature NMR or 1D NOE gradient NMR. NOE gradient experiments give a quick qualitative answer to the identification of rotamers and diastereomers present. Hu et al showed that when protons are irradiated their rotamers peaks can be identified because the chemical exchange property also irradiates their rotamer peak in the spectra. Diastereomers present do not show up using this method.

Enamide **31** was irradiated their rotamers will also be irradiated. Compiling all of the NOE data confirms the presence of rotamers and no presence of diastereomers. The next challenge is

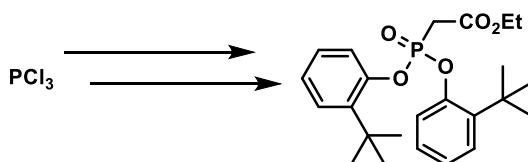
confirming the conformation of the left pyran ring. The dq at 3.75 ppm with coupling constants of 6.5 Hz and 3.3 Hz corresponds to the C15 hydrogen of enamide **31**. It couples with the C16 methyl group with a coupling constant of 6.5 Hz, leaving the coupling constant of 3.3 Hz to be the coupling constant between the hydrogens of C15 and C14. This is confirmed by the coupling constant of 2.9 Hz found in the signal at 3.64 ppm which correlates to the C14 hydrogen. While this coupling constant varies from the natural products coupling constant of 2.5 Hz, it is much smaller than the 4.9 Hz of MAMD and well within the range to support the compound taking a chair conformation.

Appendix A Supporting Information

All reactions were carried out with freshly distilled solvents under anhydrous conditions, unless otherwise stated. All flasks used to carry out reactions were dried in an oven at 80 °C prior to use. Unless specifically stated, the temperature of a water bath during the evaporation of organic solvents using a rotary evaporator was about 40 + 5 °C. All the syringes in this study were dried in an oven at 80 °C and stored in a dessicator over drierite. Tetrahydrofuran (THF) was distilled over Na metal and benzophenone. Methylene chloride (CH₂Cl₂) was stored over 3Å molecular sieves. Yields refer to chromatographically and spectroscopically (¹H NMR) homogenous materials, unless otherwise stated. All reactions were monitored by thin-layer chromatography (TLC) carried out on 0.25mm Merck silica gel plates (60F-254) using UV light (254 nm) for visualization or anisaldehyde in ethanol or 0.2% ninhydrin in ethanol as a developing agent and heat for visualization. Silica gel (230-400 mesh) was used for column chromatography. A rotary evaporator was connected to PIAB system that produced a vacuum system of about 60 mmHg when it was connected to the evaporator. NMR spectra were recorded on a Bruker Advance spectrometer at 300 MHz, 400 MHz, or 500 MHz. The chemical shifts are given in parts per million (ppm) on a delta (δ) scale. The solvent peak was used as a reference value, for ¹H NMR: CHCl₃ = 7.26 ppm, CH₃OH = 3.31 ppm, and C₆D₆ = 7.16 ppm, for ¹³C NMR: CDCl₃ = 77.00 ppm, CD₃OD = 49.00 ppm, and C₆D₆ = 128.06 ppm. The following abbreviations are used to indicate the multiplicities: s = singlet; d = doublet; t = triplet; q = quartet; m = multiplet; br = broad, apt = apparent. High-resolution mass spectra were recorded on a Shimadzu LCMS-2020. Infrared (IR) spectra were collected on a Mattson Cygnus 100 spectrometer. Samples for acquiring IR spectra

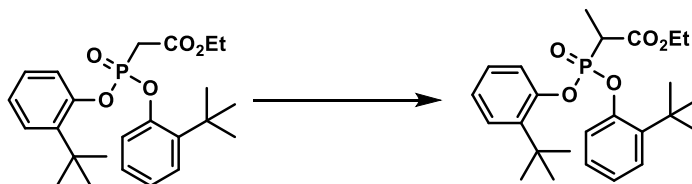
were prepared as a thin film on a NaCl plate by dissolving the compound in CH₂Cl₂ and then evaporating the CH₂Cl₂.

Appendix A.1 Experimentals



Preparation of ethyl 2-(bis(2-(tert-butyl)phenoxy)phosphoryl)acetate: To a 4 L erlenmeyer flask with a side arm, 500 mL addition funnel, and PCl₃ (175.0 mL, 2.01 mmol) under a nitrogen atmosphere was added toluene (1.023 L) and 2-t-butylphenol (605.79 mL, 3.95 mol) and stirred with a mechanical stirrer. The solution was cooled to -10 °C, and Et₃N (844.4 mL, 6.06 mmol) was added dropwise. The reaction was monitored by TLC. After 4 h EtOH (111.7 mL, 1.926 mmol) was added dropwise at -10 °C. The solution was warmed to 25 °C and stir for 13 h. H₂O (1000 mL) was added and the solution was allowed to stirred for 1 h. The layers were separated, and the aqueous layer was extracted with EtOAc/hexanes (2 x 1.5 L) mixture. The combined organic layers were washed with brine and dried over NaSO₄, and then concentrated under reduced pressure. The crude material was then added dropwise to a 3-neck 3-L round bottom flask with ethylbromoacetate at 130 °C (internal temperature) under a nitrogen atmosphere. The solution was stirred at 130 °C for 6 h. The solution was then cooled down to 25 °C. The crude mixture was recrystallized from hexanes to yield ethyl 2-(bis(2-(tert-butyl)phenoxy)phosphoryl)acetate (196.0 g, 23%) as a white solid.

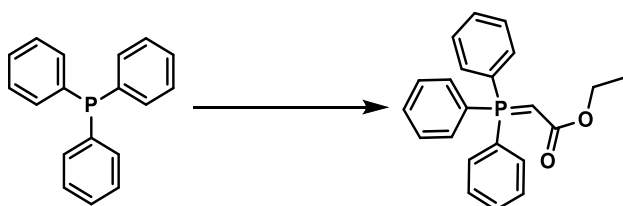
Spectroscopic data for ethyl 2-(bis(2-(*tert*-butyl)phenoxy)phosphoryl)acetate matches known literature; Touchard, F. P., *Euro. J. Org. Chem.*, **2005**, 1790.



*Preparation of ethyl 2-(bis(2-(*tert*-butyl)phenoxy)phosphoryl)propanoate:* To a round bottom flask charged with starting phosphonate (53.30 g, 123.3 mmol) under a nitrogen atmosphere was added THF (123.3 mL). The solution was stirred and cooled to 0 °C (external temperature). MeI (7.630 mL, 123.3 mmol) was added dropwise followed by KO^tBu (13.83 g, 123.3 mmol) in four portions at 0 °C. The solution was stirred at 0 °C for 1 h. An aliquot was taken for ¹H NMR analysis and used to monitor reaction progress. DBU (18.42 mL, 246.6 mmol) was added dropwise followed by MeI (7.630 mL, 123.3 mmol) at 0 °C. After 2 h, saturated NH₄Cl (aq) (30 mL) was added dropwise and the solution was warmed to 23 °C. THF was removed at reduced pressure; the aqueous residue was extracted with EtOAc (2 x 200 mL). The organic extracts were washed with brine, dried over NaSO₄, and then concentrated under reduced pressure. The crude mixture was purified by recrystallization from hot ethanol (100 mL) to yield ethyl 2-(bis(2-(*tert*-butyl)phenoxy)phosphoryl)propanoate as a white solid (26.96 g, 49%).

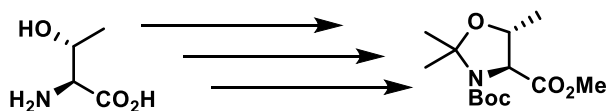
Spectroscopic data for ethyl 2-(bis(2-(*tert*-butyl)phenoxy)phosphoryl)propanoate: $R_f = 0.34$ (20% EtOAc in hexanes); IR (neat): $\nu_{\max} = 3391, 3032, 2958, 1738, 1672, 1488, 1442, 1300, 1257, 1180, 1086, 1056, 938, 757 \text{ cm}^{-1}$; ¹H NMR (400 MHz, 293K, CDCl₃): $\delta = 7.74$ (d, $J = 8.0$ Hz, 1H), 7.65 (d, $J = 8.0$ Hz, 1H), 7.36 (dd, $J = 7.6, 1.6$ Hz, 2H), 7.12 (m, 4H), 4.19 (dq, $J = 10.8, 7.2$ Hz, 1H), 4.05 (dq, $J = 10.8, 7.2$ Hz, 1H), 3.54 (dq, $J = 22.8, 7.2$ Hz, 1H), 1.73 (dd, $J = 19.6, 7.2$ Hz, 3H), 1.36 (s, 9H), 1.11 (t, $J = 7.2$ Hz, 3H); ¹³C NMR (300 MHz, 293K, CDCl₃): 168.4,

168.3, 150.9, 150.8, 150.6, 138.9, 138.8, 138.7, 138.7, 127.5, 127.4, 127.3, 127.2, 124.3, 124.3, 124.1, 119.7, 119.7, 119.5, 119.5, 61.9, 41.9, 41.9, 40.1, 34.6, 30.1, 30.0, 13.8, 12.0, 11.9 ppm; HRMS (ES+) calcd for C₂₅H₃₅O₅P [M+H]⁺ 447.2300, found 447.2305 matches those in literature;(use EndNote to cite) *Org. Proc. Dev.* **2019**, 23, 274.



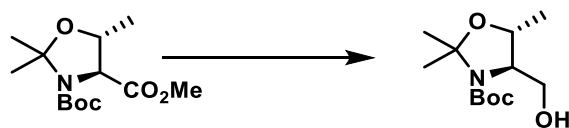
Preparation of ethyl 2-(triphenyl-λ5-phosphaneylidene)acetate: To a 1-L round bottom flask with PPh₃ (71.0 g, 270.5 mmol) in toluene (300.5 mL) and a 500-mL addition funnel was added ethylbromoacetate dropwise (40.0 mL, 360.7 mmol) and began stirring open to air at 25 °C (external temperature). The reaction was monitored by TLC. The solution was stirred for 7 h. The solid was then filtered and washed with hexanes (2 x 100 mL). The solid was transferred to a 2-L round bottom flask and CH₂Cl₂ (750 mL) was added followed by phenolphthalin (20.0 mg). NaOH_(aq) (20% wt) was added dropwise until the indicator endpoint. The solution was then allowed to stir for another 30 mins and the layers were separated, the aqueous layer was extracted with EtOAc/hexanes mixture (2 x 600 mL) and the combined organic layers were washed with brine, dried over Na₂SO₄, and concentrated under reduced pressure yielding ethyl 2-(triphenyl-λ5-phosphaneylidene)acetate (97.69 g, 96 %) as a white solid.

Spectroscopic data for ethyl 2-(triphenyl-λ5-phosphaneylidene)acetate matches known literature; *Angew. Chem. Int. Ed.* **2018**, 57, 7240.



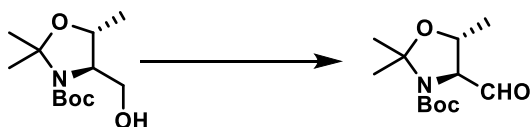
Preparation of 3-(tert-butyl) 4-methyl (4S,5R)-2,2,5-trimethyloxazolidine-3,4-dicarboxylate: To a 3-neck 3-L round bottom flask equipped with a reflux condenser and a 500-mL addition funnel under a nitrogen atmosphere was added MeOH (1.80 L). The solution was cooled to 0 °C and AcCl (623.4 mL, 8.73 mol) was added dropwise. L-threonine (400.6 g, 3.36 mol) was added in portions at 0 °C (internal temperature). The solution was raised to 68 °C and stirred for 5 days. The reaction was monitored by TLC. The solvent was removed under reduced pressure and the crude material then dissolved in a 6:1 CH₂Cl₂:MeOH (460 mL) in a 4-L Erlenmeyer flask. The solution was cooled to 0 °C and then brought to pH 8 with NaHCO_{3(aq)} and stirred. Boc₂O was added (366.6 g, 1.68 mol) in 3 portions and allowed to stir for 21 h. The reaction was monitored by TLC. The solution was quenched with NH₄Cl_(aq) until neutral pH. The layers were separated, and the organic layer was washed with brine, dried over NaSO₄, and then concentrated under reduced pressure. The crude material was then added to a 3-L round bottom flask with an addition funnel under a nitrogen atmosphere. CH₂Cl₂ (1.89 L) was added, and the solution was cooled to 0 °C. CSA (3.95 g, 0.017 mol) was added in one portion at 0 °C, followed by 2-methoxypropene (314.3 mL, 3.4 mol) dropwise at 0 °C, then allowed to warm to 25 °C. The reaction was monitored by TLC. After 20h Et₃N (15 mL) was added dropwise. The solvent was removed under reduced pressure and the crude material was purified by flash chromatography (5% →20% EtOAc/Hexanes) on silica gel (1 L) to yield *tert*-butyl (4*S*,5*R*)-4-formyl-2,2,5-trimethyloxazolidine-3-carboxylate (305.6 g, 66 %) a colorless oil.

Spectroscopic data for *tert*-butyl (4*S*,5*R*)-4-formyl-2,2,5-trimethyloxazolidine-3-carboxylate match known literature; Garner, P., *et. al. J. Org. Chem.* **1987**, 52, 2361.



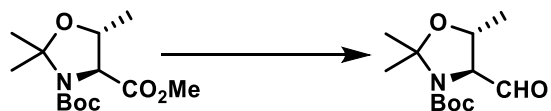
Preparation of tert-butyl (4R,5R)-4-(hydroxymethyl)-2,2,5-trimethyloxazolidine-3-carboxylate: To a 3-neck 250-mL round bottom flask charged with LAH (1.85 g, 48.7 mmol) under a nitrogen atmosphere was added Et₂O (50.0 mL). The solution was cooled to -30 °C. Garner's ester (10.0 g, 36.6 mmol) in Et₂O (15.25 mL) was added dropwise. The temperature was raised to 0 °C. The reaction was monitored by TLC. After 2 h, EtOAc was added dropwise until no gas was produced at 0 °C. The solution was warmed to 23 °C. Phosphoric acid (150 mL, 1.0 M) was added and stirred until the aqueous layer was clear (12 h). The organic layer was washed with water, then saturated NaHCO₃ (aq), then brine and then dried over sodium sulfate. The extracts were concentrated under reduced pressure to afford *tert*-butyl (4*R*,5*R*)-4-(hydroxymethyl)-2,2,5-trimethyloxazolidine-3-carboxylate (7.1 g, 79%) as a colorless oil.

Spectroscopic data for *tert*-butyl (4*R*,5*R*)-4-(hydroxymethyl)-2,2,5-trimethyloxazolidine-3-carboxylate matches known literature; Meffre, P. *et al.*, *Syn. Comm.* **1994**, *24*, 2147.

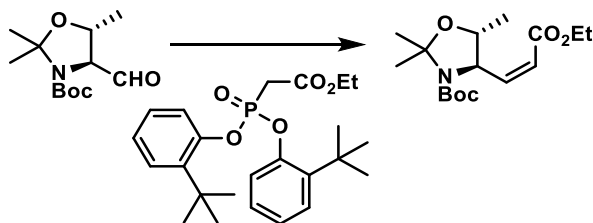


Preparation of tert-butyl (4S,5R)-4-formyl-2,2,5-trimethyloxazolidine-3-carboxylate: To a 50-mL 3-neck round bottom flask with a thermometer under a nitrogen atmosphere was added (COCl)₂ (0.107 mL, 1.22 mmol) followed by CH₂Cl₂ (30 mL). The solution was stirred and cooled to -78 °C. DMSO (0.116 mL, 1.63 mmol) was added dropwise. Once gas production halted, starting alcohol (100 mg, 0.408 mmol) in CH₂Cl₂ (5 mL) was added at -74 °C. After 1h Et₃N (0.455 mL, 3.264 mmol) was added dropwise at -78 °C and allowed to warm to 30 °C. Phosphoric acid (10 mL, 0.1 M) was added slowly at 30 °C. The solution was diluted with Et₂O. The layers were separated and the aqueous layer was extracted with EtOAc (2 x 10mL). The organic extracts were combined and washed with saturated NaHCO₃ (aq), brine, dried over sodium sulfate and

concentrated under reduced pressure. The crude mixture was used in the next step without purification.



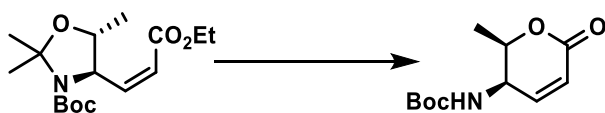
Preparation of tert-butyl (4S,5R)-4-formyl-2,2,5-trimethyloxazolidine-3-carboxylate: To a 3-L, 3-neck round bottom flask equipped with an addition funnel, a thermometer, and Garner's ester (40.00 g, 146.7 mmol) under a nitrogen atmosphere is added CH₂Cl₂: hexanes (2:1, 293.5 mL) and cooled to -92 °C (internal temperature). DIBALH (205.4 mL, 205.4 mmol) is added dropwise at -92 °C and raised to -78 °C. The reaction was monitored by TLC. After 4 h, saturated NH₄Cl (aq) (66 mL) was added dropwise at -78 °C and then warmed to 23 °C and stirred until the layers were clear (4 h). MgSO₄ (267.0 g) was added and then the mixture was filtered through a pad of celite. The solid was washed with CH₂Cl₂ and then concentrated under reduced pressure. The crude oil was used in the next step without further purification.



Preparation of tert-butyl (4R,5R)-4-((Z)-3-ethoxy-3-oxoprop-1-en-1-yl)-2,2,5-trimethyloxazolidine-3-carboxylate: To a 1-L round bottom flask (FLASK A) charged with starting aldehyde (31.84 g, 132.0 mmol) under nitrogen atmosphere was added CH₂Cl₂ (132.0 mL). The solution was stirred and cooled to 0 °C (external temperature). To a separate 500-mL round bottom flask (FLASK B) with phosphonate (65.66 g, 151.8 mmol) under a nitrogen atmosphere was added THF (151.8 mL). The solution was cooled to 0 °C (external temperature). KO^tBu (16.30 g, 145.2 mmol) was added in portions at 0 °C. After 0.5 h, FLASK B was transferred by cannula

to FLASK A at 0 °C and the combined solutions were warm to 23 °C. The reaction was monitored by TLC. After 24 h, saturated $\text{NH}_4\text{Cl}_{(\text{aq})}$ (72.62 mL) was added dropwise. THF was removed under reduced pressure and the aqueous residue was extracted with EtOAc (2 x 400 mL). The combined extracts were washed with brine, dried over Na_2SO_4 , and concentrated under reduced pressure. The crude mixture was purified via flash chromatography (2.5 \rightarrow 10% EtOAc/Hexanes) on silica gel (2 L) to afford *tert*-butyl (4*R*,5*R*)-4-((*Z*)-3-ethoxy-3-oxoprop-1-en-1-yl)-2,2,5-trimethyloxazolidine-3-carboxylate (27.57 g, 80%) as a colorless oil.

Spectroscopic data for *tert*-butyl (4*R*,5*R*)-4-((*Z*)-3-ethoxy-3-oxoprop-1-en-1-yl)-2,2,5-trimethyloxazolidine-3-carboxylate matches known literature; Koskinen, A. M. P. and Otsomaa, L. A., *Tetrahedron*, **1997**, 53, 6473.

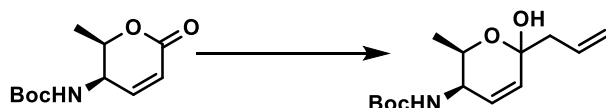


*Preparation of tert-butyl ((2*R*,3*R*)-2-methyl-6-oxo-3,6-dihydro-2*H*-pyran-3-yl)carbamate:*

To a 250-mL round bottom flask charged with starting enoate (1.65 g, 5.29 mmol) was added AcOH (98.9 mL). The solution was kept open to air and raised to 80 °C (internal temperature) in an oil bath. The reaction was monitored by TLC. After 22 h, the AcOH was removed under reduced pressure with the rotary evaporator bath at 80 °C. To the remaining oil was added saturated $\text{NaHCO}_3_{(\text{aq})}$ until the pH was approx. 8-9, then THF (16.7 mL) and Boc_2O (1.15 g, 16.5 mmol) were added at 25 °C and stirred for 3 h. Once the reaction is complete the THF was removed under reduced pressure. The aqueous residue was extracted with EtOAc (2 x 100 mL). The combined extracts were washed with brine, dried over Na_2SO_4 , and concentrated under reduced pressure. The crude oil was then purified by flash chromatography (10 \rightarrow 40% EtOAc/Hexanes) on silica gel

(250 mL) to afford *tert*-butyl ((2*R*,3*R*)-2-methyl-6-oxo-3,6-dihydro-2*H*-pyran-3-yl)carbamate (1.19 g, 98%) as a yellow solid.

Spectroscopic data for *tert*-butyl ((2*R*,3*R*)-2-methyl-6-oxo-3,6-dihydro-2*H*-pyran-3-yl)carbamate matches known literature; Koskinen, A. M. P. and Otsomaa, L. A., *Tetrahedron*, **1997**, *53*, 6473.



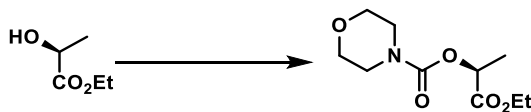
*Preparation of tert-butyl ((2*R*,3*R*)-6-allyl-6-hydroxy-2-methyl-3,6-dihydro-2*H*-pyran-3-yl)carbamate:* To a 100-mL round bottom flask charged with starting lactone (100 mg, 0.440 mmol) under a nitrogen atmosphere was added THF (2.02 mL). The solution was stirred and cooled to -78 °C (external temperature). Allyl magnesium bromide solution (0.66 mL, 1.0 M in THF) was added dropwise. The reaction was monitored by TLC. After 2 h, saturated NH₄Cl (aq) (2.0 mL) was added dropwise at -78 °C and then the solution was warm to 23 °C. The THF is removed under reduced pressure and the aqueous residue was extracted with EtOAc (2 x 10 mL). The combined extracts were washed with brine, dried over Na₂SO₄, and then concentrated under reduced pressure. The crude mixture was used in the next step without further purification.



*Preparation of tert-butyl ((2*R*,3*R*,6*S*)-6-allyl-2-methyl-3,6-dihydro-2*H*-pyran-3-yl)carbamate:* To a 100-mL round bottom flask charged with the crude mixture of hemiketal mentioned above (0.44 mmol) under a nitrogen atmosphere is added CH₂Cl₂ (2.767 mL). The solution was stirred and cooled to -75 °C (external temperature). Et₃SiH (0.695 mL, 4.356 mmol) is added dropwise followed by CF₃CH₂OH (0.247 mL, 3.39 mmol) and BF₃·OEt₂ (0.221 mL, 1.76

mmol) are added dropwise at -78 °C. The reaction was monitored by TLC. After 1 h, saturated NaHCO_{3(aq)} (10 mL) is added dropwise at -75 °C and the solution is warmed to 23 °C. Saturated NaHCO_{3(aq)} is added until pH 9 at which point THF (40 mL) and Boc₂O (96.0 mg, 0.44 mmol) is added and allowed to stir open to air for 12 h. The THF is removed under reduced pressure and the aqueous residue is extracted with EtOAc (2 x 20 mL). The extracts are washed with brine, dried over Na₂SO₄, and concentrated under reduced pressure. The crude mixture is then purified by flash chromatography (2.5 → 10% EtOAc/Hexanes) on silica gel (50 mL) to afford *tert*-butyl ((2*R*,3*R*,6*S*)-6-allyl-2-methyl-3,6-dihydro-2H-pyran-3-yl)carbamate (20 mg, 23%) as a colorless oil.

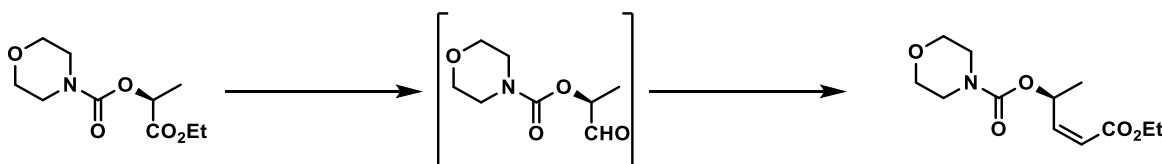
Spectroscopic data for *tert*-butyl ((2*R*,3*R*,6*S*)-6-allyl-2-methyl-3,6-dihydro-2H-pyran-3-yl)carbamate: *R_f* = 0.30 (20% EtOAc in hexanes); IR (neat): ν_{max} = 2979, 2932, 1713, 1496, 1393, 1367, 1212, 1163, 1117, 1064, 983, 916, 845, 774 cm⁻¹; [α]_D²⁴ -104.3 (1.0, CH₂Cl₂); ¹H NMR (400 MHz, CDCl₃ 1% CD₃OD, 298 K): δ = 5.91-5.87 (ddd, 1H, *J* = 10.0, 5.6, 2.0), 5.85-5.76 (m, 2H, *J* = 17.2, 10, 9.6 Hz), 5.14-5.09 (m, 2H, *J* = 17.2, 10.0, 1.4 Hz), 4.15-4.12 (m, 1H), 3.94-3.89 (m, 1H, *J* = 5.6, 2.8 Hz), 3.75-3.70 (dq, 1H, *J* = 6.4, 2.8 Hz), 1.44 (s, 9H), 1.19-1.18 (d, 3H, *J* = 6.4 Hz) ppm; ¹³C NMR (500 MHz, 293 K, CDCl₃) 155.7, 133.9, 133.3, 132.4, 126.3, 117.5, 79.3, 74.7, 72.9, 47.1, 39.5, 28.4, 16.9 ppm; HRMS (ES⁺) calcd for C₁₄H₂₄O₃N [M+H]⁺ 254.17507, found 254.17559.



Preparation of (S)-1-ethoxy-1-oxopropan-2-yl morpholine-4-carboxylate: To a 1-L round bottom flask with ethyl-(*L*)-lactate (25.3 g, 214.17 mmol) under a nitrogen atmosphere was added CH₂Cl₂ (214.7 mL). CDI (41.67 g, 252.00 mmol) was added dropwise at 25 °C. After 20 h, the

solution was cooled to 0 °C (external temperature) and morpholine (28.02 mL, 321.26 mmol) was added dropwise and the solution was warmed to 25 °C. After 2 h the solvent was removed under reduced pressure and the crude material was purified by flash chromatography (17.5% → 70% EtOAc/Hexanes) on silica gel (500 mL) yielding (*S*)-1-ethoxy-1-oxopropan-2-yl morpholine-4-carboxylate (47.25 g, 95%) as a colorless oil.

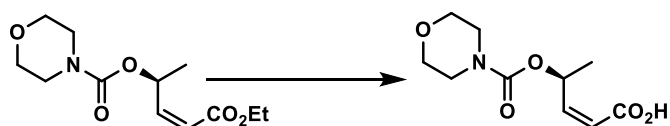
Spectroscopic data for (*S*)-1-ethoxy-1-oxopropan-2-yl morpholine-4-carboxylate matches known literature; *Chem. Eur. J.*, **2011**, *17*, 895.



Preparation of (S)-(Z)-5-ethoxy-5-oxopent-3-en-2-yl morpholine-4-carboxylate: To a 3-neck 250 mL round bottom flask (FLASK A) with morpholino carbamate mentioned above (2.10 g, 9.12 mmol) under a nitrogen atmosphere was added CH₂Cl₂ (11.40 mL) and cooled to -78 °C (external temperature). DIBALH (15.14 mL, 15.51 mmol) was added dropwise at -78 °C and the solution was allowed to stir at that temperature. The reaction was monitored by TLC. To a separate 100-mL round bottom flask (FLASK B) with phosphonate (4.34 g, 10.03 mmol) under a nitrogen atmosphere was added THF (10.32 mL) and cooled to 0 °C (external temperature). KO^tBu (1.04 g, 9.12 mmol) was added in one portion at 0 °C and the solution was allowed to stir at that temperature. After 6 h, the solution from FLASK B was added to FLASK A via cannula and the combined solution was warmed to 25 °C. The reaction was monitored by TLC. After 21 h Na₃C₆H₅O₇(aq) (17.06 mL, 1.0 M) was added and stirred until the layers were clear (5 h). The organic solvent was removed under reduced pressure and the aqueous residue was extracted with EtOAc/hexanes mixture (2 x 600 mL). The combined organic layers were washed with brine, dried over Na₂SO₄, and concentrated under reduced pressure. The crude residue was purified by flash

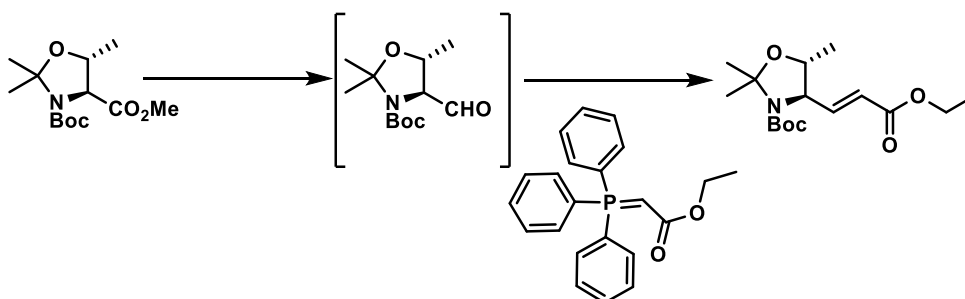
chromatography (10 → 50% EtOAc/Hexanes) on silica gel (45 mL) yielding (*S*)-(*Z*)-5-ethoxy-5-oxopent-3-en-2-yl morpholine-4-carboxylate (1.48 g, 63%) as a colorless oil.

Spectroscopic data for (*S*)-(*Z*)-5-ethoxy-5-oxopent-3-en-2-yl morpholine-4-carboxylate matches known literature; *Chem. Eur. J.*, **2011**, *17*, 895.



*Preparation of (*S*)-(*Z*)-4-((morpholine-4-carbonyl)oxy)pent-2-enoic acid:* To 25-mL round bottom flask with the starting morpholino enoate (0.0265 g, 0.1029 mmol) was added MeOH (0.1305 mL) and $\text{NaOH}_{(\text{aq})}$ (0.2610 mL, 1.0 M). The solution was stirred open to air at 25 °C. The reaction was monitored by TLC. After 1 h, the solution was acidified with $\text{HCl}_{(\text{aq})}$ (10% v/v) until pH 1 and stirred for 0.5 h. The solvent was removed under reduced pressure and the aqueous residue was extracted with CH_2Cl_2 (2 x 20 mL), washed with brine, and dried over Na_2SO_4 . The solvent was removed under reduced pressure and the crude material was used in the next step without further purification.

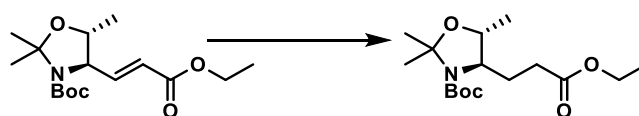
Spectroscopic data for (*S*)-(*Z*)-4-((morpholine-4-carbonyl)oxy)pent-2-enoic acid matches known literature, *Chem. Eur. J.*, **2011**, *17*, 895.



*Preparation of tert-butyl (4*R*,5*R*)-4-((*E*)-3-ethoxy-3-oxoprop-1-en-1-yl)-2,2,5-trimethylmorpholine-3-carboxylate:* To a 2-L round bottom flask with Garner's ester (25.5 g, 93.53

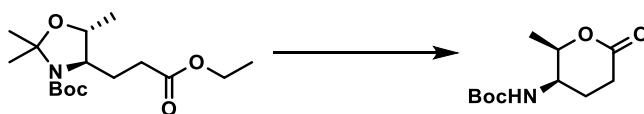
mmol) and a 500-mL addition funnel under a nitrogen atmosphere was added CH₂Cl₂ (233.8 mL). The solution was cooled to -78 °C (external temperature). DIBALH (149.7 mL, 149.7 mmol) was added dropwise at -78 °C and stirred at that temperature. The reaction progress was monitored by ¹H NMR. After 4.5 h, EtOH (60 mL) was added dropwise at -78 °C followed by a solution of ylide (32.6 g, 93.5 mmol) in CH₂Cl₂ (93.5 mL) and allowed to warm to room temperature. The reaction was monitored by TLC. After 20 h, Na₃C₆H₅O₇(aq) (610 mL, 1.0 M) was added and stirred until the layers were clear (5 h). The layers were separated, and the aqueous layer was extracted with EtOAc/hexanes mixture (2 x 500 mL). The combined organic layers were washed with brine, dried over Na₂SO₄, and concentrated under reduced pressure. The crude residue was purified by flash chromatography (2.5% → 10% EtOAc/Hexanes) on silica gel (900 mL) yielding *tert*-butyl (4*R*,5*R*)-4-((*E*)-3-ethoxy-3-oxoprop-1-en-1-yl)-2,2,5-trimethyloxazolidine-3-carboxylate (17.1 g, 65%) as a colorless oil.

Spectroscopic data for *tert*-butyl (4*R*,5*R*)-4-((*E*)-3-ethoxy-3-oxoprop-1-en-1-yl)-2,2,5-trimethyloxazolidine-3-carboxylate matches known literature; *Chem. Euro. J.*, **2011**, *17*, 895.



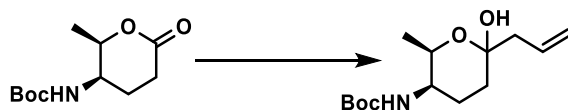
Preparation of tert-butyl (4R,5R)-4-(3-ethoxy-3-oxopropyl)-2,2,5-trimethyloxazolidine-3-carboxylate: To a 1-L round bottom flask with the starting enoate (17.1 g, 54.6 mmol) was added Pd/C (0.1744 g, 1.639 mmol), followed by EtOAc (325.5 mL). The flask was vacated and put under a hydrogen atmosphere and stirred vigorously. The reaction progress was monitored by TLC. After 5 h the Pd/C was filtered out and the filtrate was concentrated in vacuo. Yielding *tert*-butyl (4*R*,5*R*)-4-(3-ethoxy-3-oxopropyl)-2,2,5-trimethyloxazolidine-3-carboxylate (17.0 g, quantitative) a colorless oil.

Spectroscopic data for *tert*-butyl (4*R*,5*R*)-4-(3-ethoxy-3-oxopropyl)-2,2,5-trimethyloxazolidine-3-carboxylate matches known literature; *Chem. Euro. J.*, **2011**, *17*, 895.



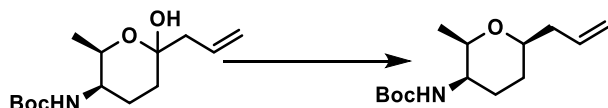
*Preparation of tert-butyl ((2*R*,3*R*)-2-methyl-6-oxotetrahydro-2*H*-pyran-3-yl)carbamate:* To a 250-mL round bottom flask with ethyl ester (7.81 g, 24.7 mmol) was added AcOH (148.3 mL). The solution was heated to 85 °C (internal temperature) and stirred open to air. The reaction progress was monitored by TLC. After 120 h, the solvent was removed under reduced pressure and the crude residue was basified to pH 9 with saturated NaHCO_{3(aq)}. THF (80 mL) and Boc₂O (5.41 g, 24.7 mmol) were added and the solution stirred at 25 °C open to air for 12 h. The solvent was removed under reduced pressure and the aqueous residue was extracted with EtOAc/hexanes mixture (2 x 750 mL). The combined organic layers were washed with brine, dried over Na₂SO₄, and concentrated under reduced pressure. The crude residue was purified with flash chromatography (12.5 to 50% EtOAc/Hexanes) on silica gel (140 mL) yielding *tert*-butyl ((2*R*,3*R*)-2-methyl-6-oxotetrahydro-2*H*-pyran-3-yl)carbamate (2.1 g, 52%) as a white solid.

Spectroscopic data for *tert*-butyl ((2*R*,3*R*)-2-methyl-6-oxotetrahydro-2*H*-pyran-3-yl)carbamate matches known literature; *Chem. Euro. J.*, **2011**, *17*, 895.



*Preparation of tert-butyl ((2*R*,3*R*)-6-allyl-6-hydroxy-2-methyltetrahydro-2*H*-pyran-3-yl)carbamate:* To a 250 mL round bottom flask with starting lactone (4.48 g, 19.54 mmol) under a nitrogen atmosphere was added THF (69.8 mL) and cooled to -78 °C (external temperature). A solution of allylmagnesium bromide in THF (31.3 mL, 1.0 M) was added dropwise at -78 °C and allowed to stir at temperature. The reaction process was monitored by

TLC. After 2 h saturated $\text{NH}_4\text{Cl}_{(\text{aq})}$ (30 mL) was added dropwise at $-78\text{ }^\circ\text{C}$ and allowed to warm to $25\text{ }^\circ\text{C}$. The solvent was removed under reduced pressure and the aqueous residue was extracted with EtOAc (2 x 400mL). The combined organic layers were washed with brine, dried over Na_2SO_4 , and concentrated in vacuo. The crude material was used in the next step.



Preparation of tert-butyl ((2R,3R,6R)-6-allyl-2-methyltetrahydro-2H-pyran-3-yl)carbamate: To a 1-L round bottom flask charged with the crude mixture of hemiketal prepared previously (16.033 mmol) under a nitrogen atmosphere was added CH_2Cl_2 (100 mL) and cooled to $-78\text{ }^\circ\text{C}$ (external temperature). Et_3SiH (25.35 mL, 158.727 mmol) was added dropwise at $-78\text{ }^\circ\text{C}$ followed by $\text{BF}_3\cdot\text{OEt}_2$ (15.51 mL, 123.454 mmol) and $\text{CF}_3\text{CH}_2\text{OH}$ (4.67 mL, 64.132 mmol). The reaction was monitored by TLC. After 1 h saturated $\text{NaHCO}_3_{(\text{aq})}$ (50 mL) was added at $-78\text{ }^\circ\text{C}$ and warmed to $25\text{ }^\circ\text{C}$. The solution was basified until pH 9 with saturated $\text{NaHCO}_3_{(\text{aq})}$ then THF (100 mL) and Boc_2O (3.504 g, 16.033 mmol) was added and allowed to stir at $25\text{ }^\circ\text{C}$ for 12 h. The solvent was removed under reduced pressure. The aqueous residue was extracted with EtOAc/hexanes (2 x 300 mL) mixture. The combined organic layers were washed with brine, dried over Na_2SO_4 , and concentrated under reduced pressure. The crude material was purified by flash chromatography (5% \rightarrow 20%EtOAc/Hexanes) on silica gel (320 mL) yielding *tert-butyl ((2R,3R,6R)-6-allyl-2-methyltetrahydro-2H-pyran-3-yl)carbamate* (2.35 g, 38%) as a colorless oil.

Spectroscopic data for *tert-butyl ((2R,3R,6R)-6-allyl-2-methyltetrahydro-2H-pyran-3-yl)carbamate* matches known literature; *Chem. Euro. J.*, **2011**, *17*, 895.



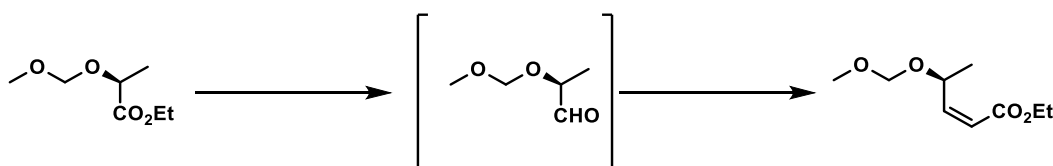
Preparation of (2R,3R,6R)-6-allyl-N,2-dimethyltetrahydro-2H-pyran-3-amine: To a 3-neck 250-mL round bottom flask under a nitrogen atmosphere was added THF (50 mL) and began cooling to 0 °C (external temperature). LAH (0.509 g, 13.41 mmol) was added at 0 °C. Starting amine (0.5 g, 1.960 mmol in 8 mL THF) was added dropwise at 0 °C, then brought to reflux and stirred for 14 h. Reaction progress was monitored by TLC. Removed the heat and allowed the solution to cool to 25 °C. Added THF (20 mL) and cooled the solution to 0 °C. Added EtOAc dropwise until gas production stopped followed by NaOH_(aq) (1.0 M) until solid formation stopped. Filtered the solution through a pad of celite and removed the solvent under reduced pressure. Added saturated NaHCO_{3(aq)} and stirred for 15 min. Extracted aqueous residue with CH₂Cl₂ (2 x 100 mL). Combined organic layers were washed with brine and dried over Na₂SO₄. Solvent was removed under reduced pressure yielding secondary amine as a yellow oil. Material was used crude in next step.



Preparation of ethyl (S)-2-(methoxymethoxy)propanoate: To a 250-mL 3-neck round bottom flask under a nitrogen atmosphere was added THF (60.4 mL) and cooled to 0 °C (external temperature). NaH (1.63 g, 40.63 mmol) was added in one portion followed by ethyl-(S)-lactate (4.80 mL, 42.32 mmol) dropwise at 0 °C. After 2 h MOMCl (3.21 mL, 42.32 mmol) was added dropwise at 0 °C and warmed to 25 °C. Reaction progress was monitored by TLC. After 16 h, saturated NH₄Cl_(aq) (50 mL) was added dropwise at 0 °C followed by THF (50 mL) and allowed to warm to 25 °C. The solution was transferred to a 500 mL round bottom flask and the solvent was removed under reduced pressure. The aqueous residue was extracted with EtOAc (2 x 100

mL). The combined organic layer was washed with brine and dried over Na₂SO₄. Yielding ethyl (*S*)-2-(methoxymethoxy)propanoate (3 g, 86%) as a colorless oil.

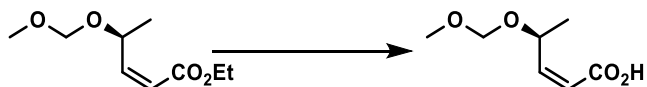
Spectroscopic data for ethyl (*S*)-2-(methoxymethoxy)propanoate matches known literature; *Org. Biomol. Chem.*, **2006**, *4*, 2932.



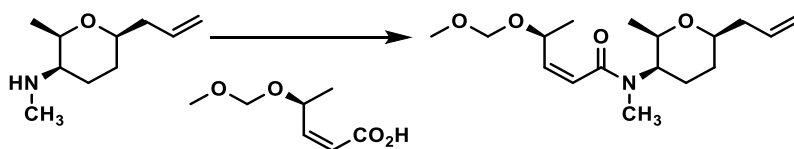
Preparation of *ethyl (S)-(Z)-4-(methoxymethoxy)pent-2-enoate*: To a 100-mL round bottom flask (FLASK A) with starting ester (2.1 g, 12.923 mmol) under a nitrogen atmosphere was added CH₂Cl₂ (25.86 mL) and the solution was cooled to -78 °C (external temperature). To a 500-mL round bottom flask (FLASK B) with phosphonate (6.15 g, 14.23 mmol) under a nitrogen atmosphere was added THF (14.23 mL) and the solution cooled to 0 °C (external temperature). KO^tBu (1.52 g, 13.58 mmol) was added in one portion to FLASK B at 0 °C and the solution was stirred at that temperature DIBALH (20.69 mL, 20.69 mmol) was added dropwise at -75 °C to FLASK A and stirred at that temperature. The reaction was monitored by ¹H NMR. After 3 h FLASK B was cannulaed into FLASK A at -75 °C and the reaction was warmed to 25 °C. After 24 h, Na₃C₆H₅O₇(aq) (60 mL, 1.0 M) solution was added dropwise at 0 °C and stirred until the layers were clear (5 h). The layers were separated, and the aqueous layer was extracted with EtOAc (2 x 20 mL). The combined organic layers were washed with brine, dried over Na₂SO₄, and the solvent was removed under reduced pressure. Crude material was purified by flash chromatography (7.5% → 30% EtOAc/Hexanes) on silica gel (240 mL) yielding ethyl (*S*)-(*Z*)-4-(methoxymethoxy)pent-2-enoate (0.810 g, 33%) as a colorless oil.

Data for *ethyl ((S)-(Z)-)-4-(methoxymethoxy)pent-2-enoate*: $R_f = 0.32$ (10% EtOAc/hexanes); IR (neat): $\nu_{max} = 2980, 2937, 2889, 1718, 1648, 1408, 1189, 1096, 1028, 920,$

822 cm^{-1} ; $[\alpha]_{\text{D}}^{24}$ -40.9 (c 1.0, CH_2Cl_2); ^1H NMR (400MHz, CDCl_3 , 298K): δ = 6.198-6.148 (dd, J = 11.6, 8.0Hz, 1H), 5.794-5.761 (dd, J = 12.0, 1.2Hz, 1H), 5.336-5.267 (m, J = 7.6, 6.8Hz, 1H), 4.645-4.595 (m, J = 13.2Hz, 2H), 4.191-4.137 (q, J = 7.2Hz, 2H), 3.356 (s, 3H), 1.315-1.261 (apt q, J = 7.2, 6.8Hz, 6H); ^{13}C NMR (400 MHz, CDCl_3 , 293 K) 165.9, 151.7, 119.8, 95.3, 69.8, 60.5, 55.6, 20.8, 14.4; HRMS (ES⁺) calcd for $\text{C}_9\text{H}_{16}\text{O}_4$ $[\text{M}+\text{Na}]^+$ 211.09408 found 211.09387.



Preparation of acid ((S)-Z)-4-(methoxymethoxy)pent-2-enoic acid: To a 25-mL round bottom flask with starting enoate (40.0 mg, 0.2127 mmol) was added EtOH (0.269 mL) and $\text{NaOH}_{(\text{aq})}$ (0.548 mL, 1.0 M) at 25 °C (external temperature) and the solution was stirred open to air at temperature. Reaction progress was monitored by TLC. After 2 h the solution was acidified with $\text{HCl}_{(\text{aq})}$ (10% v/v) until pH 1. The solvent was removed the under reduced pressure and the aqueous residue was extracted with CH_2Cl_2 (2 x 20 mL). The combined organic layers were washed with brine and dried over Na_2SO_4 . The crude material was carried forward without further purification.

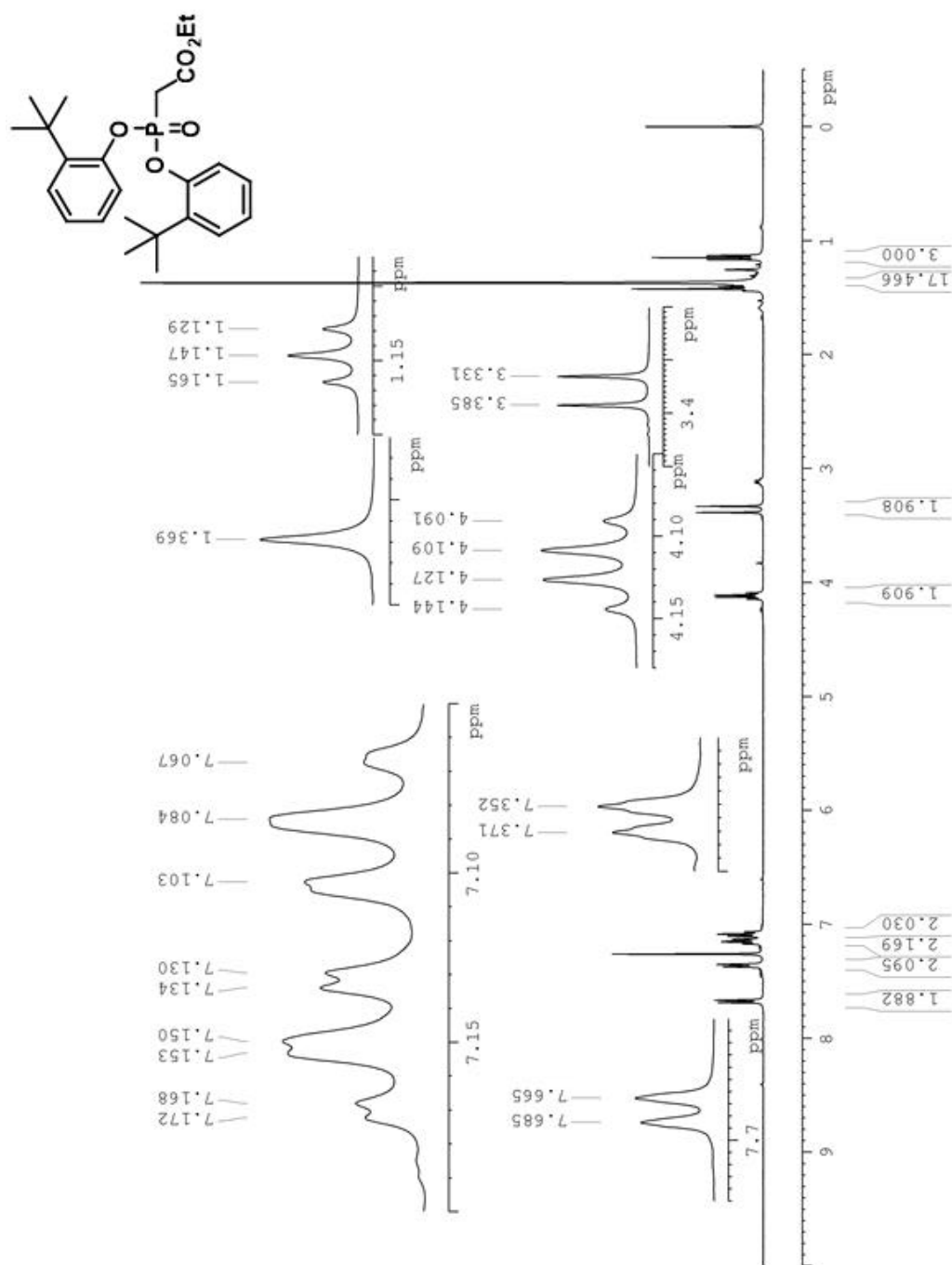


Preparation of (S,Z)-N-((2R,3R,6R)-6-allyl-2-methyltetrahydro-2H-pyran-3-yl)-4-(methoxymethoxy)-N-methylpent-2-enamide: To a 25-mL round bottom flask (FLASK A) with previously prepared acid (10.3 mg, 0.0643 mmol) and HATU (21.98 mg, 0.0578 mmol) under a nitrogen atmosphere was added MeCN (0.129 mL) at 25 °C (external temperature). To a 10-mL round bottom flask (FLASK B) with starting amine (10.88 mg, 0.0643 mmol) under a nitrogen atmosphere was added MeCN (0.075 mL) at 25 °C. DIPEA (0.0278 mL, 0.1608 mmol) was added

dropwise to FLASK A followed by FLASK B via cannula at 25 °C. Reaction progress was monitored by TLC. After 12 h, saturated $\text{NH}_4\text{Cl}_{(\text{aq})}$ (3 mL) was added dropwise at 25 °C and stirred for 0.5 h. The solvent was removed under reduced pressure and the aqueous residue was extracted with CH_2Cl_2 (2 x 10 mL). The combined organic layers were washed with brine and dried over Na_2SO_4 . The crude material was purified by flash chromatography (20% \rightarrow 100% EtOAc/Hexanes) on silica gel (5 mL) yielding ((*S*)-(*Z*))-*N*-((2*R*,3*R*,6*R*)-6-allyl-2-methyltetrahydro-2*H*-pyran-3-yl)-4-(methoxymethoxy)-*N*-methylpent-2-enamide (0.9mg, 5%) as a colorless oil.

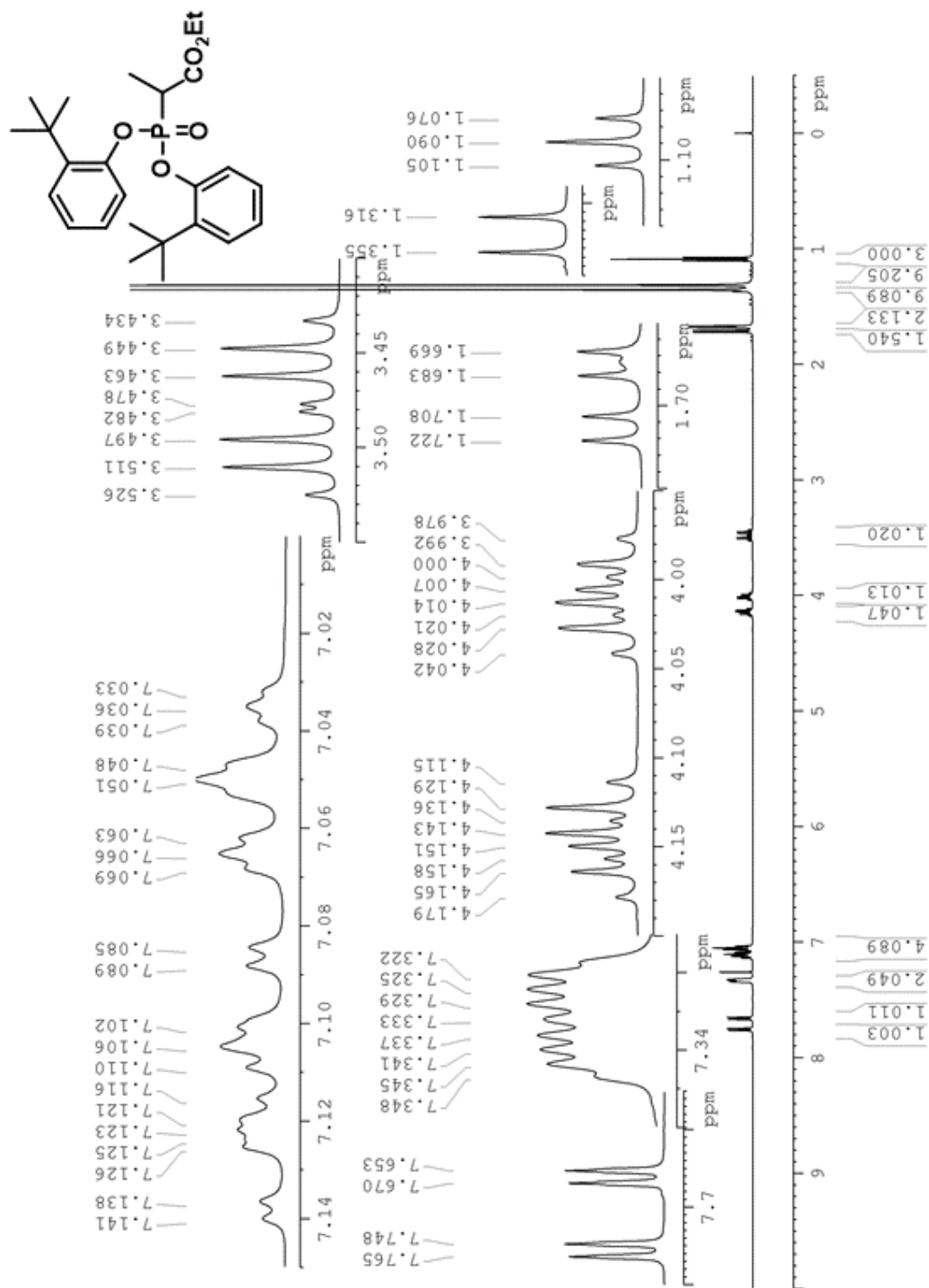
Spectroscopic data for (((*S*)-(*Z*))-*N*-((2*R*,3*R*,6*R*)-)-6-allyl-2-methyltetrahydro-2*H*-pyran-3-yl)-4-(methoxymethoxy)-*N*-methylpent-2-enamide: $R_f = 0.71$ (60% EtOAc in hexanes); IR (neat): $\nu_{\text{max}} = 2976, 2932, 2856, 1627, 1441, 1410, 1372, 1315, 1210, 1157, 1097, 1072, 1030, 918, 845 \text{ cm}^{-1}$; $[\alpha]_{\text{D}}^{24} -104.0$ (c 1.0, CH_2Cl_2); $^1\text{H NMR}$ (400 MHz, CDCl_3 1% CD_3OD , 298 K): $\delta = 6.40\text{-}6.35$ (dd, $J = 15.2, 1.2 \text{ Hz}$, 1H), $6.17\text{-}6.14$ (dd, $J = 11.6, 1.2 \text{ Hz}$, 1H), $6.01\text{-}5.98$ (d, $J = 11.6 \text{ Hz}$, 1H), $5.88\text{-}5.77$ (m, 2H), $5.09\text{-}5.03$ (m, 2H), $4.82\text{-}4.75$ (m, 1H), $4.71\text{-}4.60$ (m, 2H), $4.58\text{-}4.56$ (d, $J = 6.8 \text{ Hz}$, 1H), $4.52\text{-}4.50$ (m, 1H), $3.79\text{-}3.70$ (dq, $J = 6.5, 3.3 \text{ Hz}$, 2H (rotamers)), $3.65\text{-}3.62$ (apt pentet, $J = 5.2, 2.8, 2.4 \text{ Hz}$, H14 rotamer), $3.50\text{-}3.42$ (m, H11 & rotamer), 3.23 (s, N- CH_3 /rotamer), 3.19 (s, N- CH_3 /rotamer), $2.39\text{-}2.30$ (m, H10 & rotamer), $2.27\text{-}2.18$ (m, H10 & rotamer), $2.04\text{-}1.89$ (m, H13 & rotamer), $1.65\text{-}1.54$ (m, H12 & rotamer), $1.33\text{-}1.29$ (apt dd, $J = 6.4 \text{ Hz}$, H5' & rotamer), $1.17\text{-}1.15$ (apt dd, $J = 6.4 \text{ Hz}$, H 16 & rotamer) ppm; $^{13}\text{C NMR}$ (400 MHz, CDCl_3 , 293 K) $168.2, 168.0, 142.6, 141.8, 134.5, 134.4, 123.7, 123.1, 95.0, 94.7, 75.6, 75.4, 55.5, 55.4, 47.6, 41.0, 40.8, 35.3, 32.2, 29.8, 29.3, 28.0, 27.0, 26.8, 21.2, 21.0, 18.2$ ppm; HRMS (ES+) calcd for $\text{C}_{14}\text{H}_{24}\text{O}_3\text{N}$ $[\text{M}+\text{H}]^+$ 312.21693 found 312.21651.

Appendix B NMR Spectra

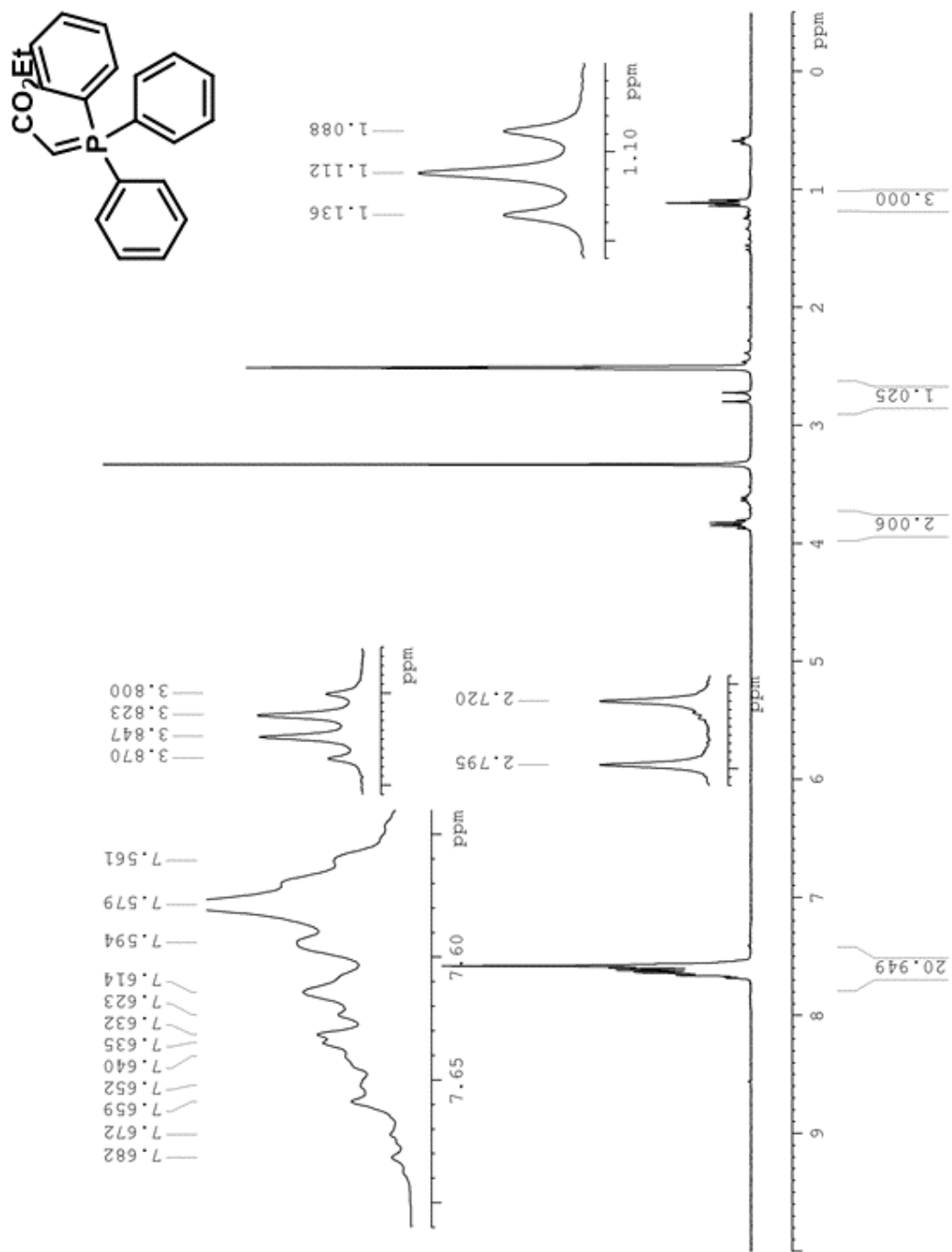


Appendix Figure 1: ¹H NMR spectrum of ethyl 2-(bis(2-(tert-butyl)phenoxy)phosphoryl)acetate (CDCl₃,

400MHz, 1H 298 K)

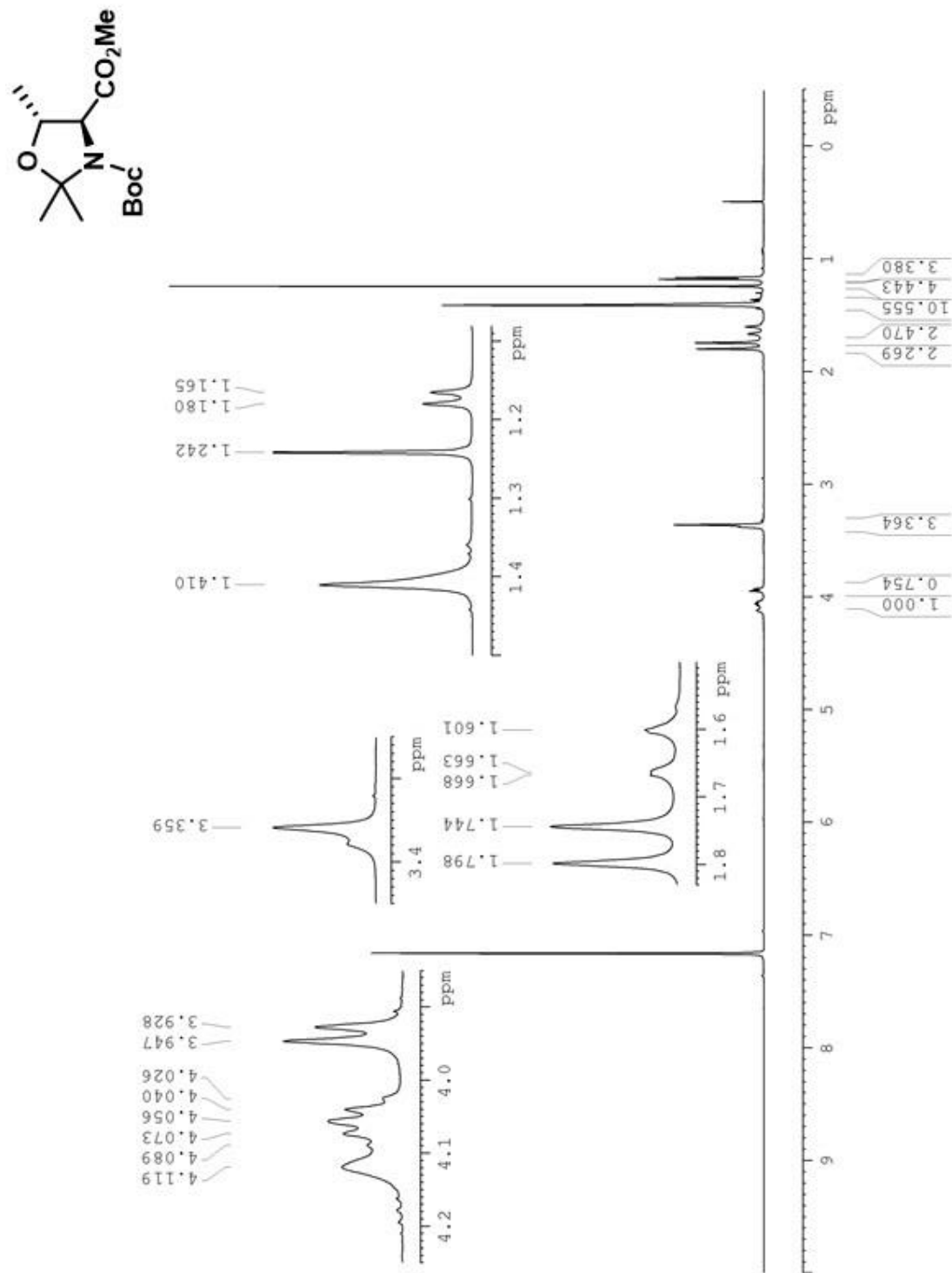


Appendix Figure 2: ¹H NMR spectrum of ethyl 2-(bis(2-(tert-butyl)phenoxy)phosphoryl)propanoate (CDCl₃, 400MHz, 1H 298 K)

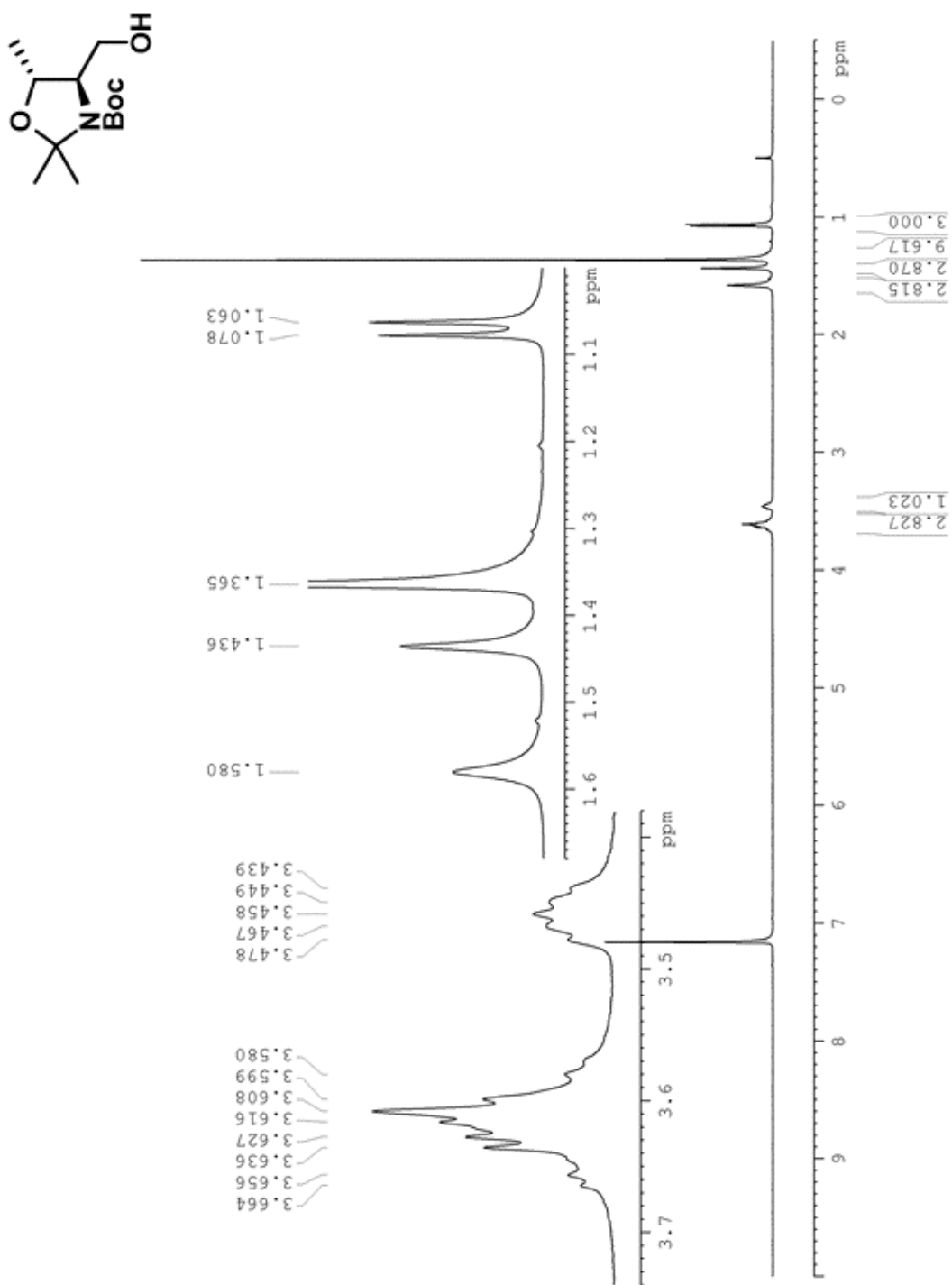


Appendix Figure 3: ^1H NMR spectrum of ethyl 2-(triphenyl- λ^5 -phosphaneylidene)acetate (CDCl_3 , 400MHz,

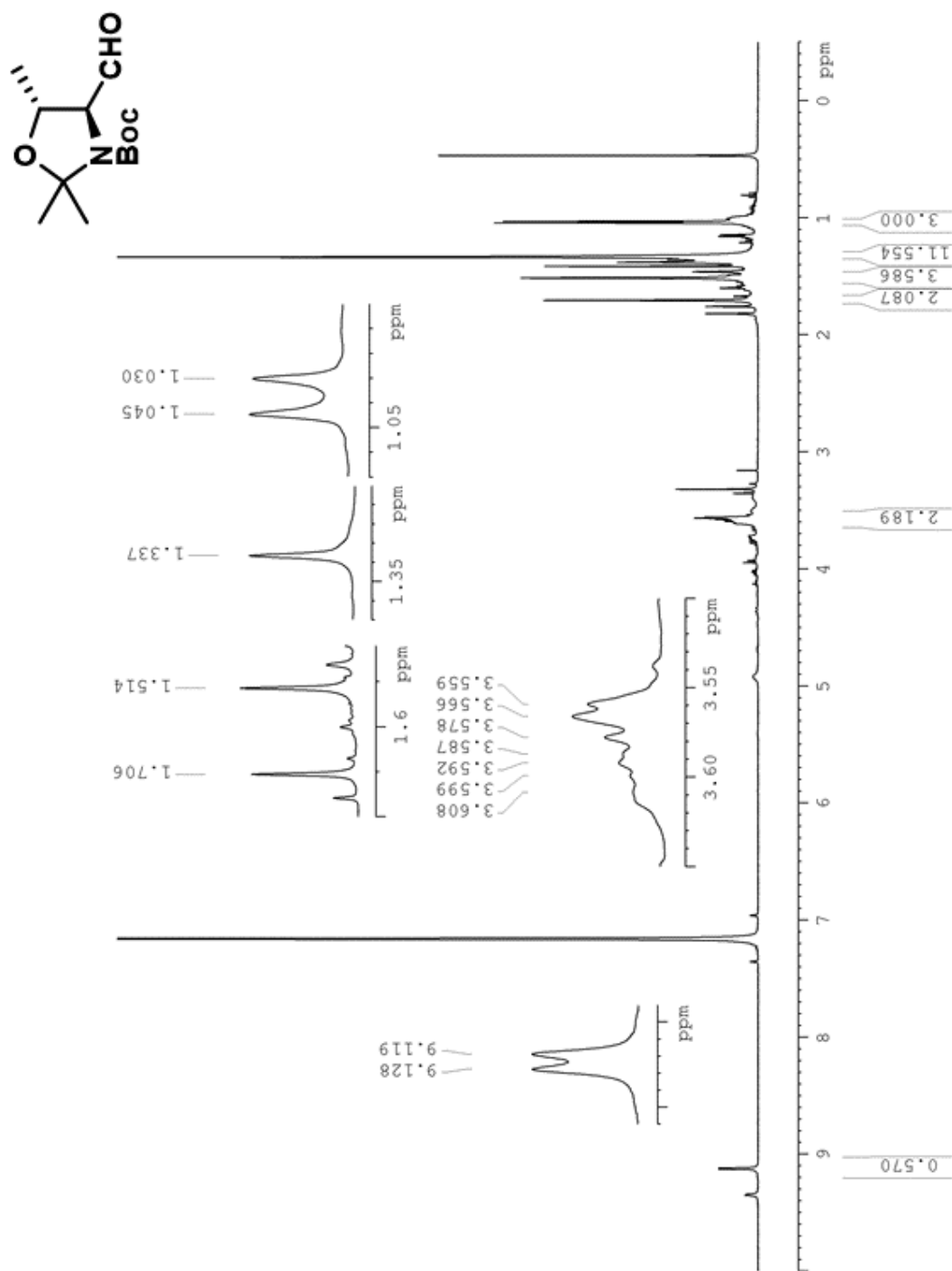
^1H 298 K)



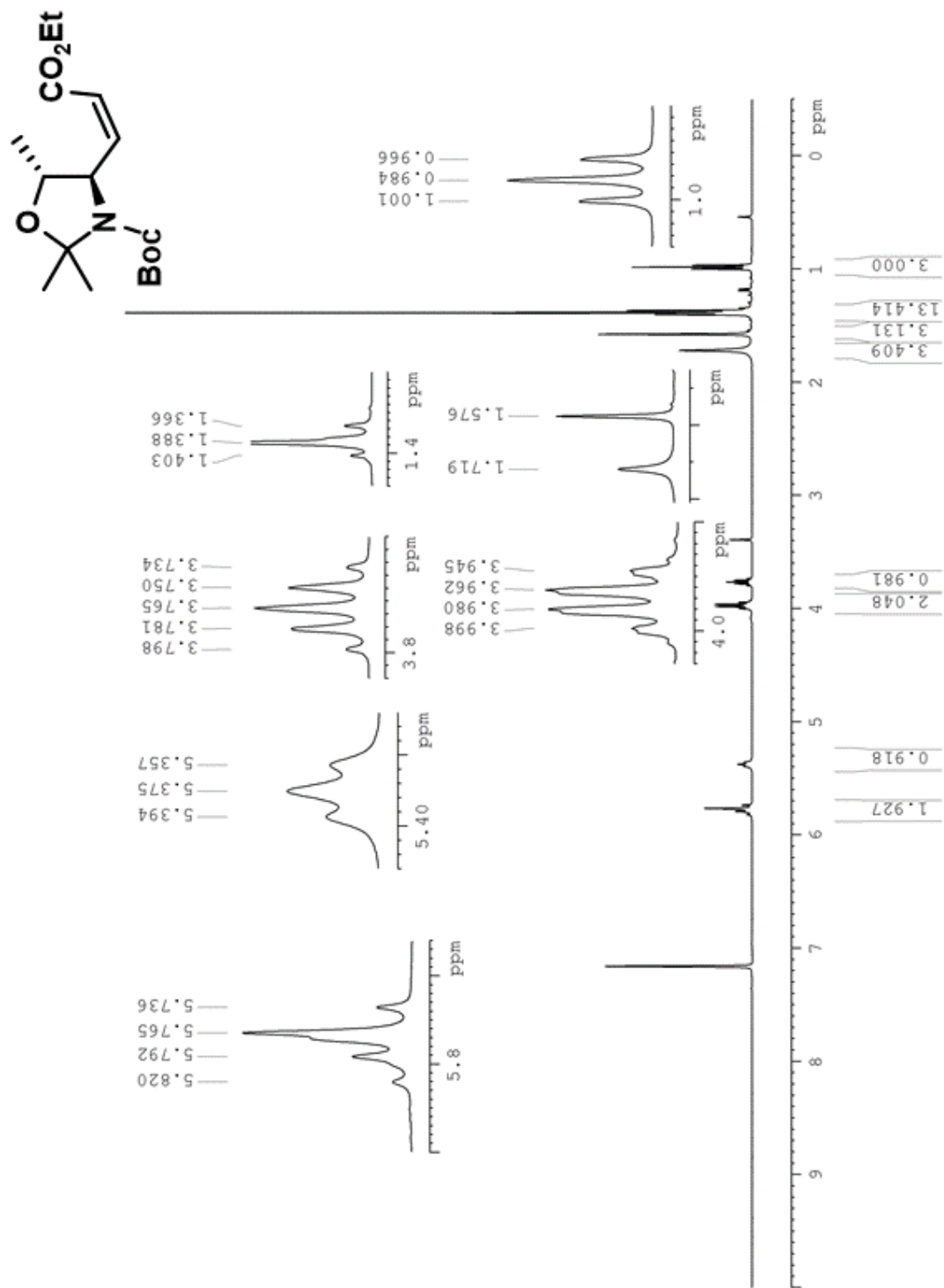
Appendix Figure 4: ¹H NMR spectrum of 3-(tert-butyl) 4-methyl (4S,5R)-2,2,5-trimethyloxazolidine-3,4-dicarboxylate (C₆D₆, 400MHz, 1H 338 K)



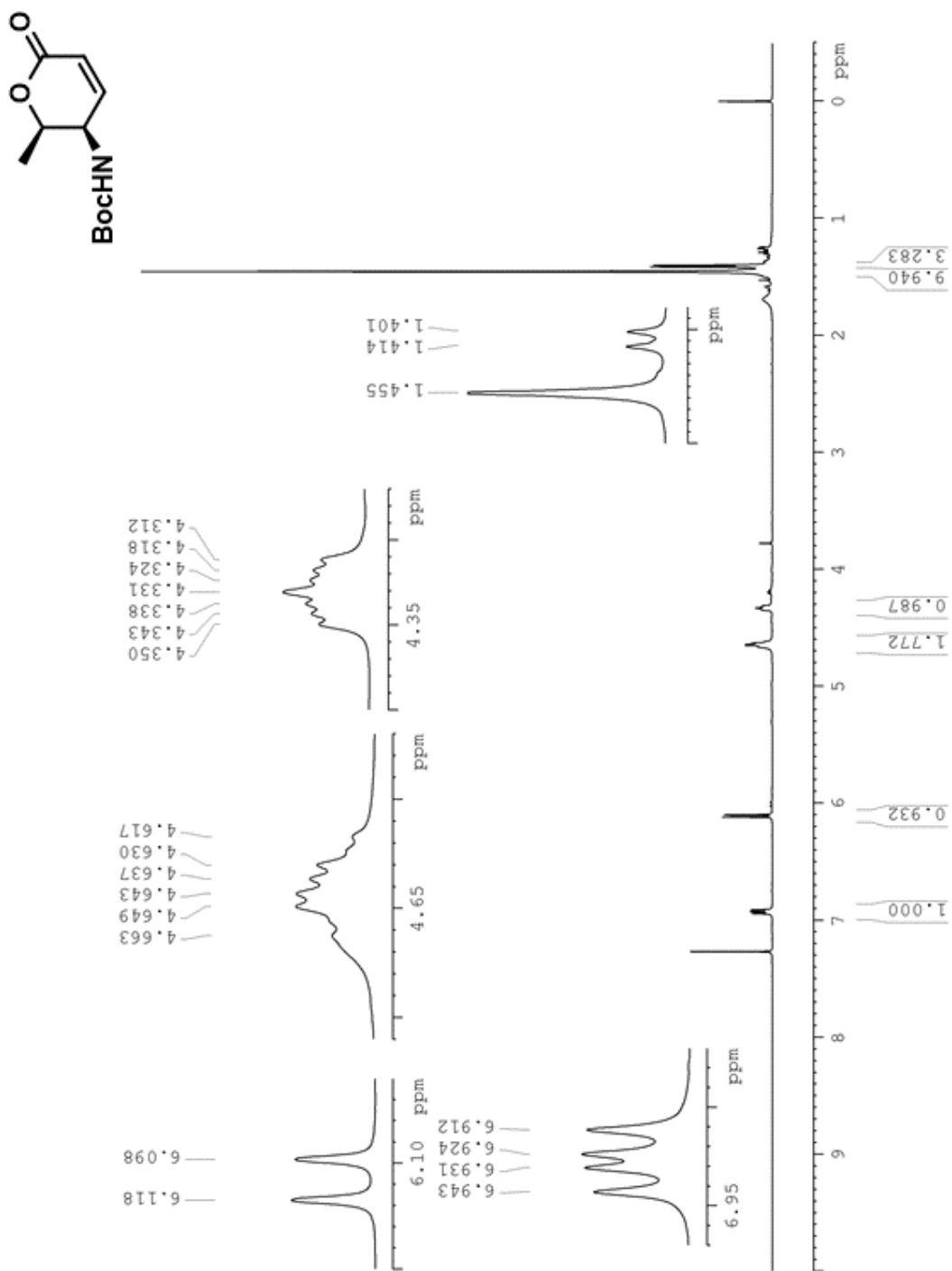
Appendix Figure 5: ¹H NMR spectrum of tert-butyl (4R,5R)-4-(hydroxymethyl)-2,2,5-trimethyloxazolidine-3-carboxylate (C₆D₆, 400MHz, ¹H 338 K)



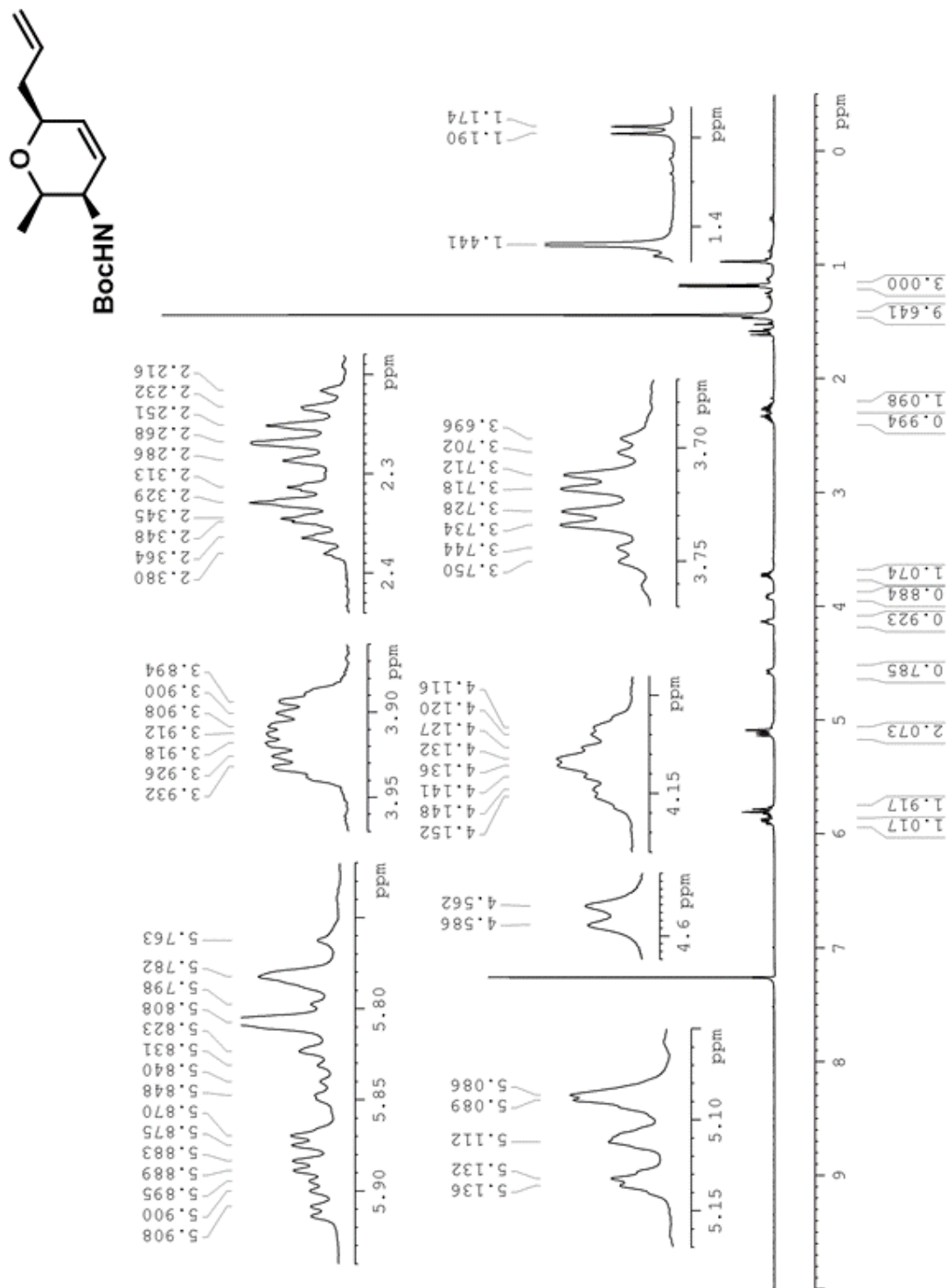
Appendix Figure 6: ¹H NMR spectrum of tert-butyl (4S,5R)-4-formyl-2,2,5-trimethyloxazolidine-3-carboxylate (C₆D₆, 400MHz, 1H 338 K)



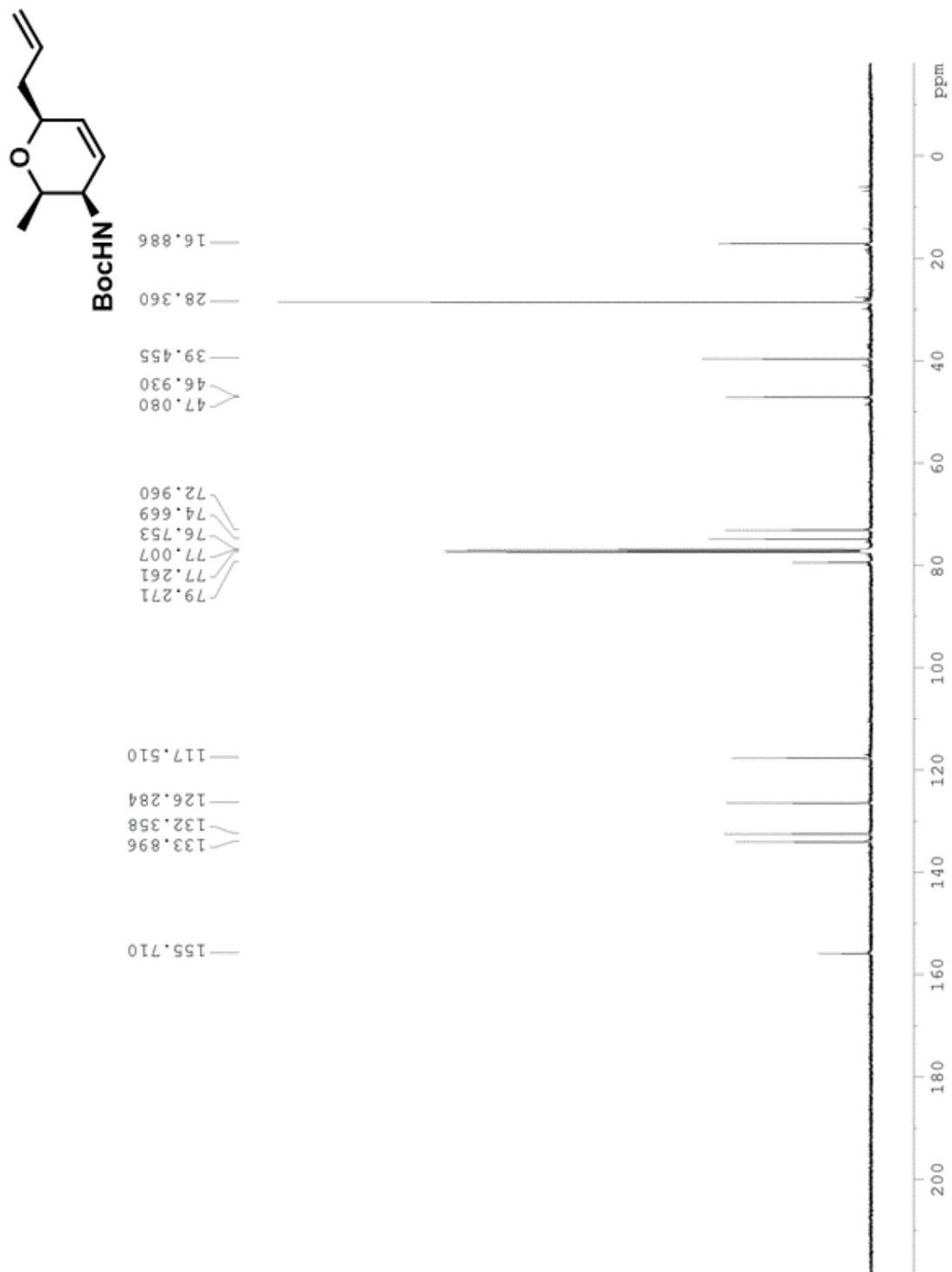
Appendix Figure 7: ¹H NMR spectrum of tert-butyl (4R,5R)-4-((Z)-3-ethoxy-3-oxoprop-1-en-1-yl)-2,2,5-trimethyloxazolidine-3-carboxylate (C6D6, 400MHz, 1H 343 K)



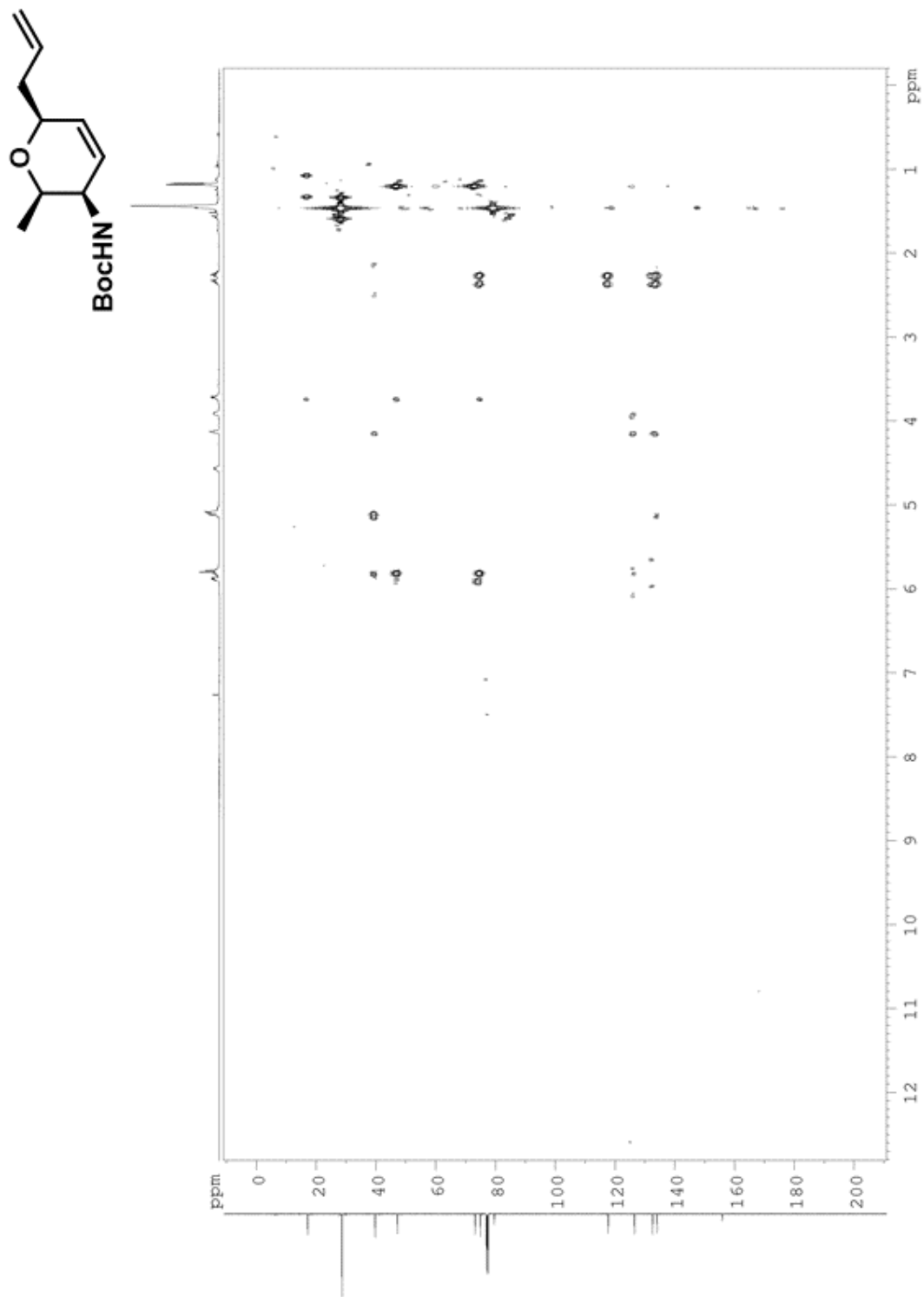
Appendix Figure 8: ¹H NMR spectrum of tert-butyl ((2R,3R)-2-methyl-6-oxo-3,6-dihydro-2H-pyran-3-yl)carbamate (CDCl₃, 500MHz, 1H 298 K)



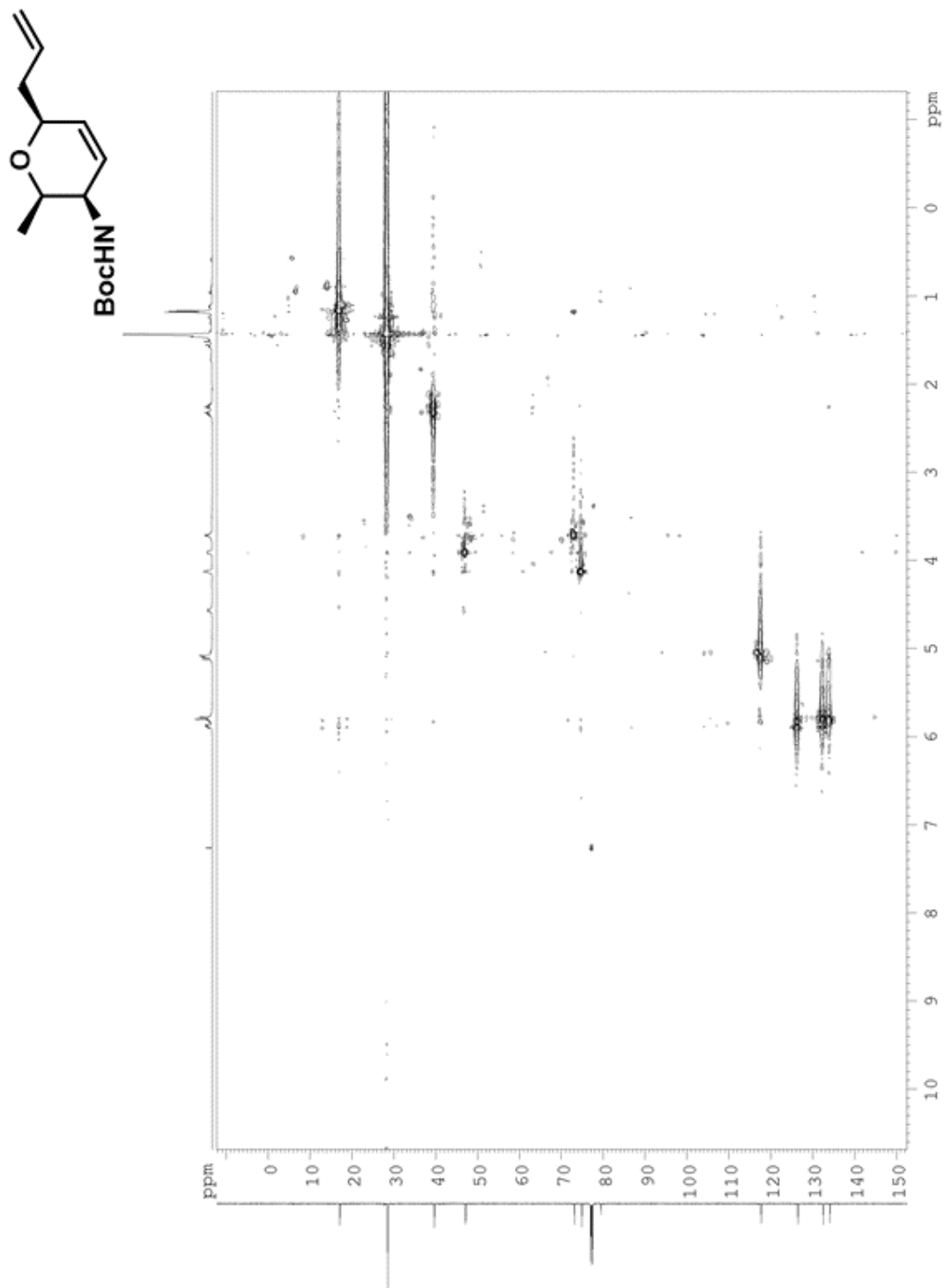
Appendix Figure 9: ¹H NMR spectrum of tert-butyl ((2R,3R,6S)-6-allyl-2-methyl-3,6-dihydro-2H-pyran-3-yl)carbamate (CDCl₃ with 1% CD₃OD, 400MHz, 1H 298 K)



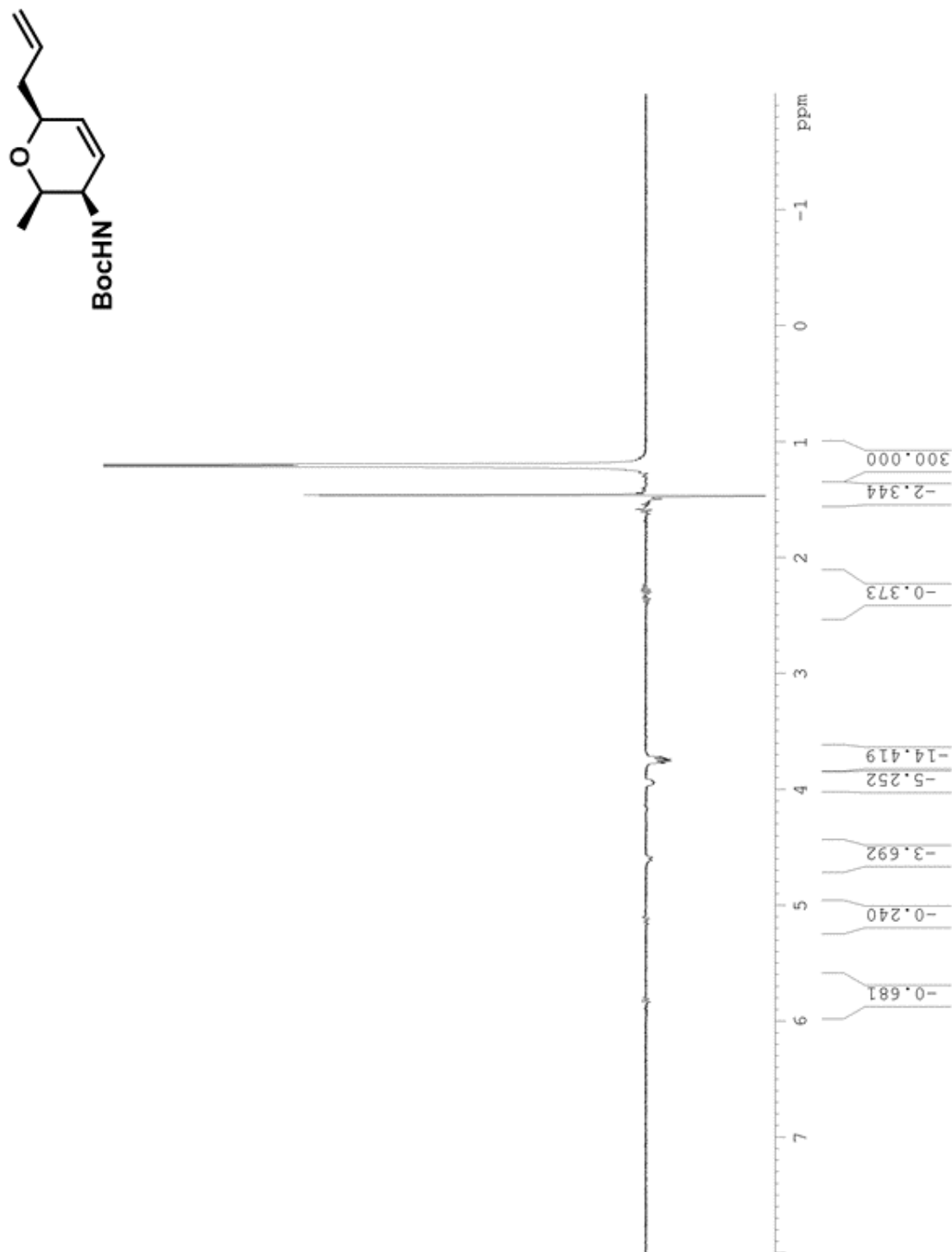
Appendix Figure 10: ¹³C NMR spectrum of tert-butyl ((2R,3R,6S)-6-allyl-2-methyl-3,6-dihydro-2H-pyran-3-yl)carbamate (CDCl₃ with /1% CD₃OD, 500400MHz, 1H 298 K)



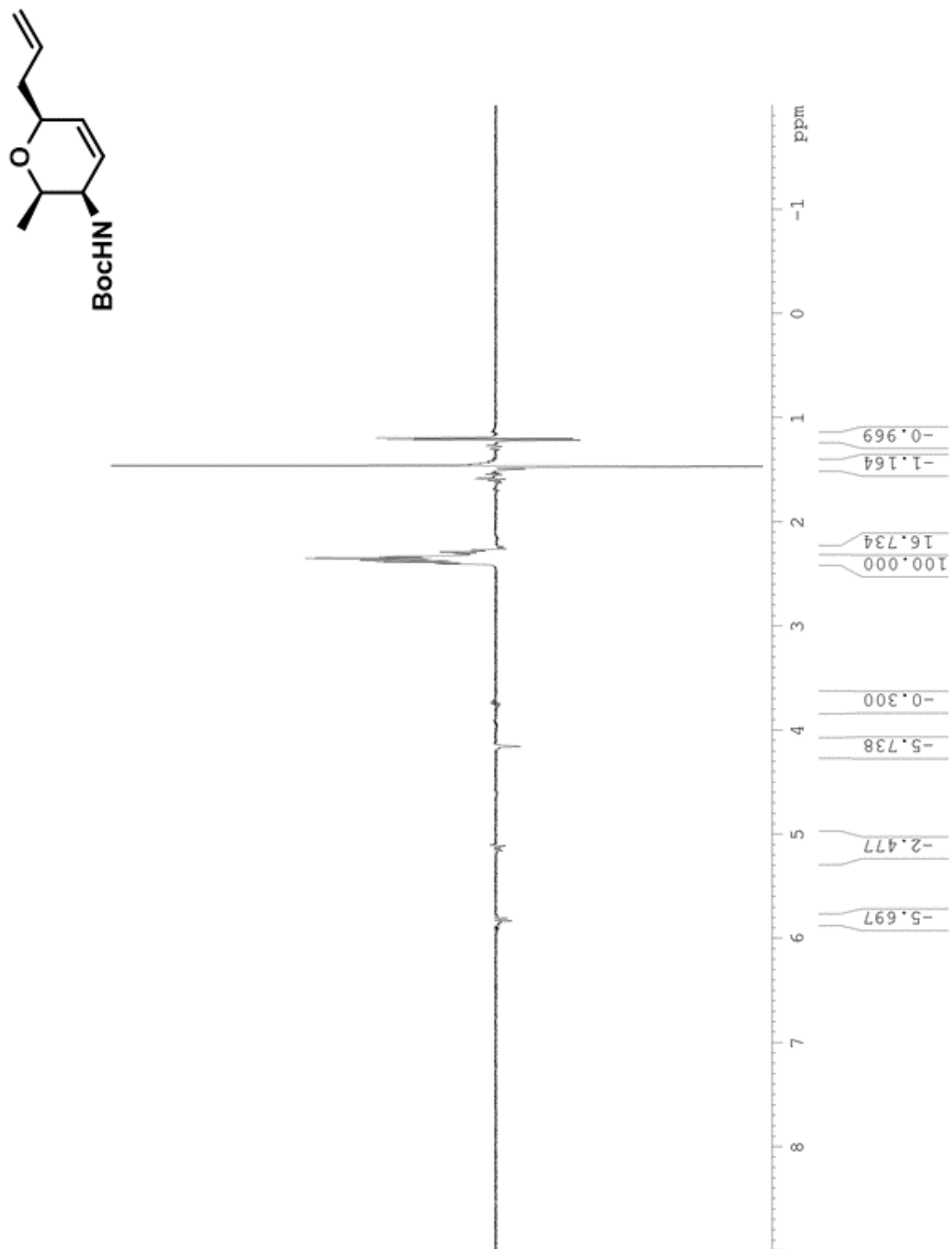
Appendix Figure 11: HMBC NMR spectrum of tert-butyl ((2R,3R,6S)-6-allyl-2-methyl-3,6-dihydro-2H-pyran-3-yl)carbamate (CDCl₃ with /1% CD₃OD, 500MHz, HMBC 298 K)



Appendix Figure 12: HSQC NMR spectrum of tert-butyl ((2R,3R,6S)-6-allyl-2-methyl-3,6-dihydro-2H-pyran-3-yl)carbamate CDCl_3 with /1% CD_3OD , 500MHz, HSQC 298 K)



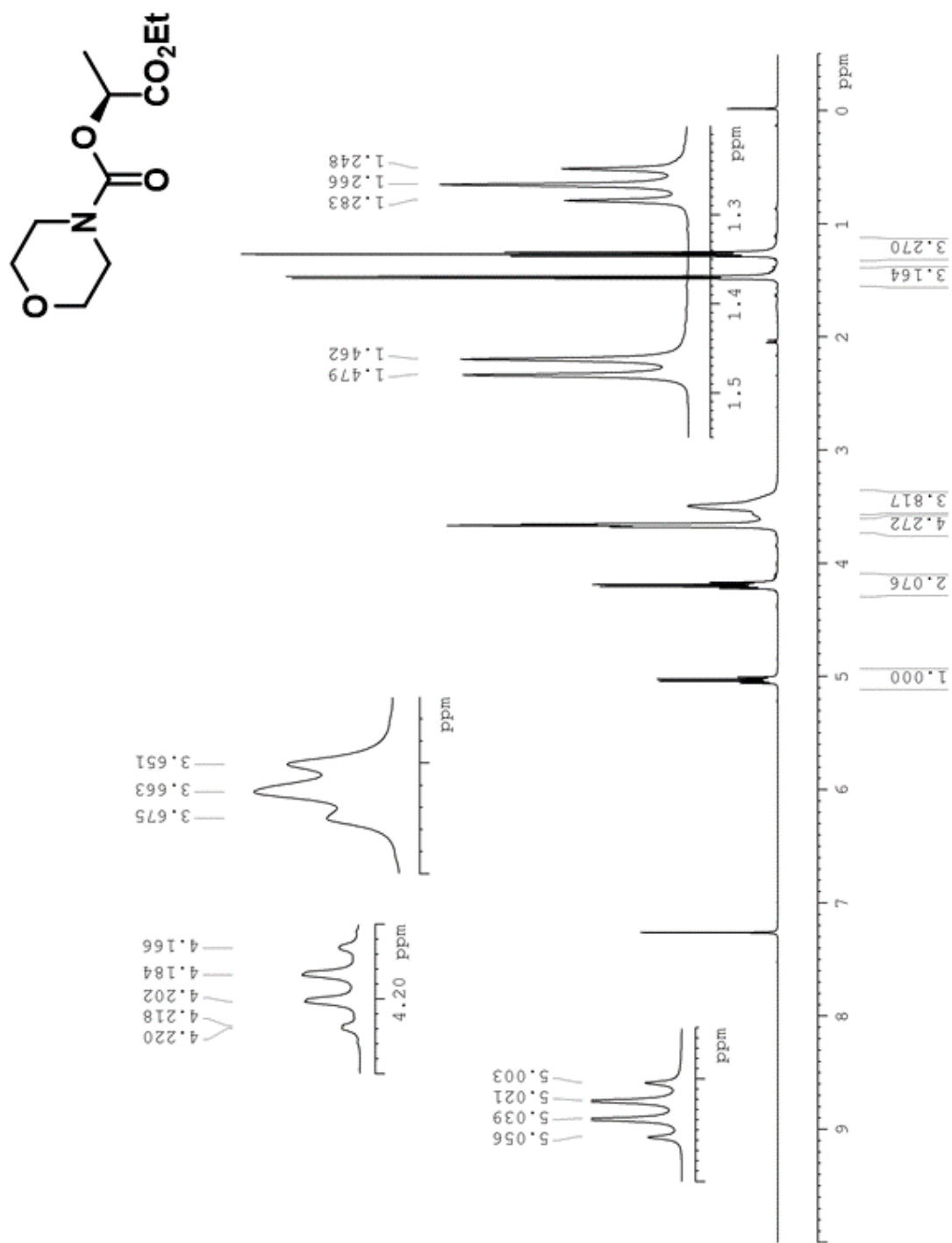
Appendix Figure 13: NOE irradiated at 1.15 ppm NMR spectrum of tert-butyl ((2R,3R,6S)-6-allyl-2-methyl-3,6-dihydro-2H-pyran-3-yl)carbamate CDCl₃ with /1% CD₃OD, 400MHz, 298 K)



Appendix Figure 14: NOE irradiated at 2.25 ppm NMR spectrum of tert-butyl ((2R,3R,6S)-6-allyl-2-methyl-3,6-dihydro-2H-pyran-3-yl)carbamate (CDCl₃ w/ith 1% CD₃OD, 400MHzpp, 298 K)

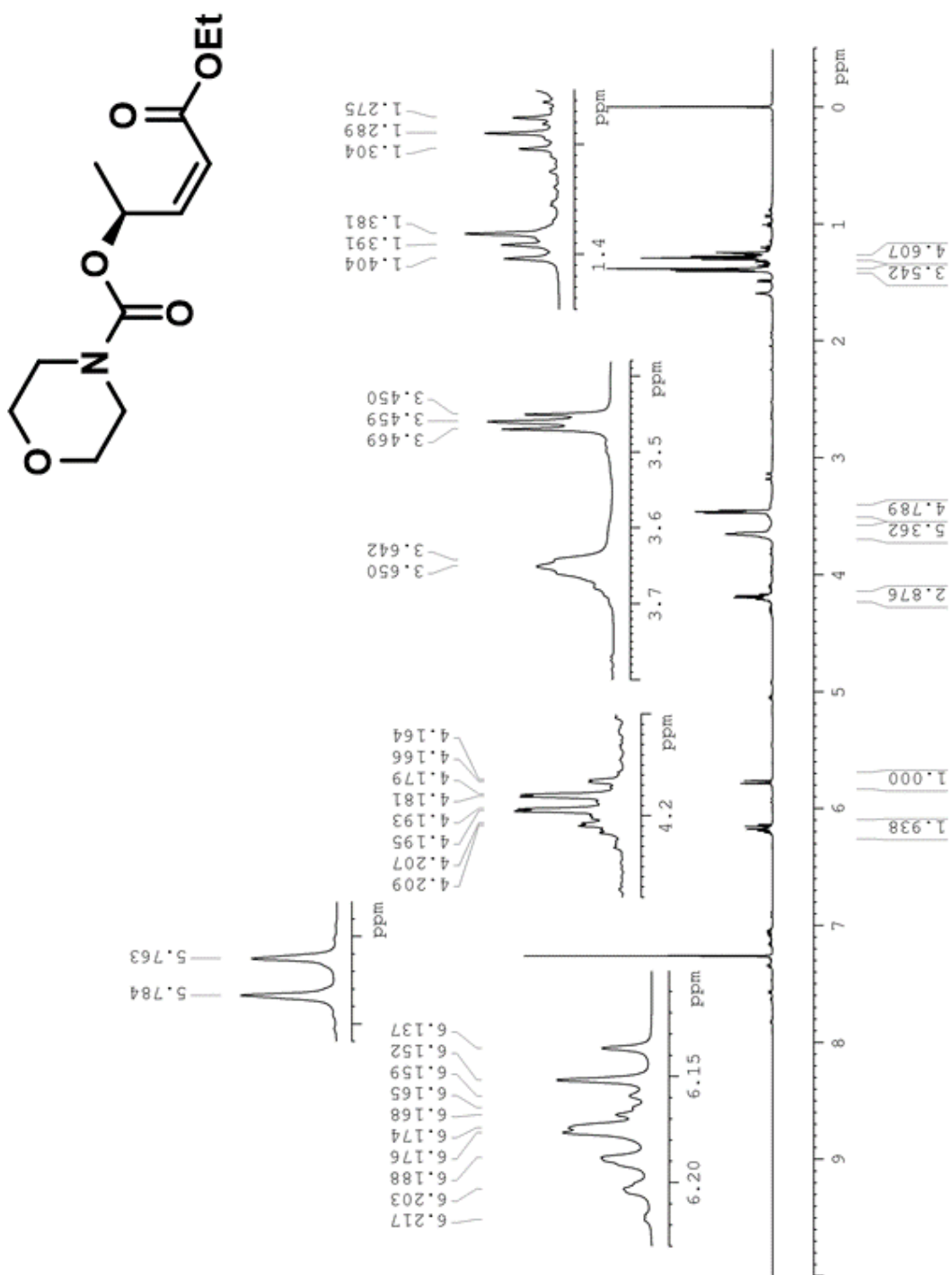


Appendix Figure 16: NOE irradiated at 4.15 ppm NMR spectrum of tert-butyl ((2R,3R,6S)-6-allyl-2-methyl-3,6-dihydro-2H-pyran-3-yl)carbamate (CDCl₃ with /1% CD₃OD, 400MHz, 298 K)

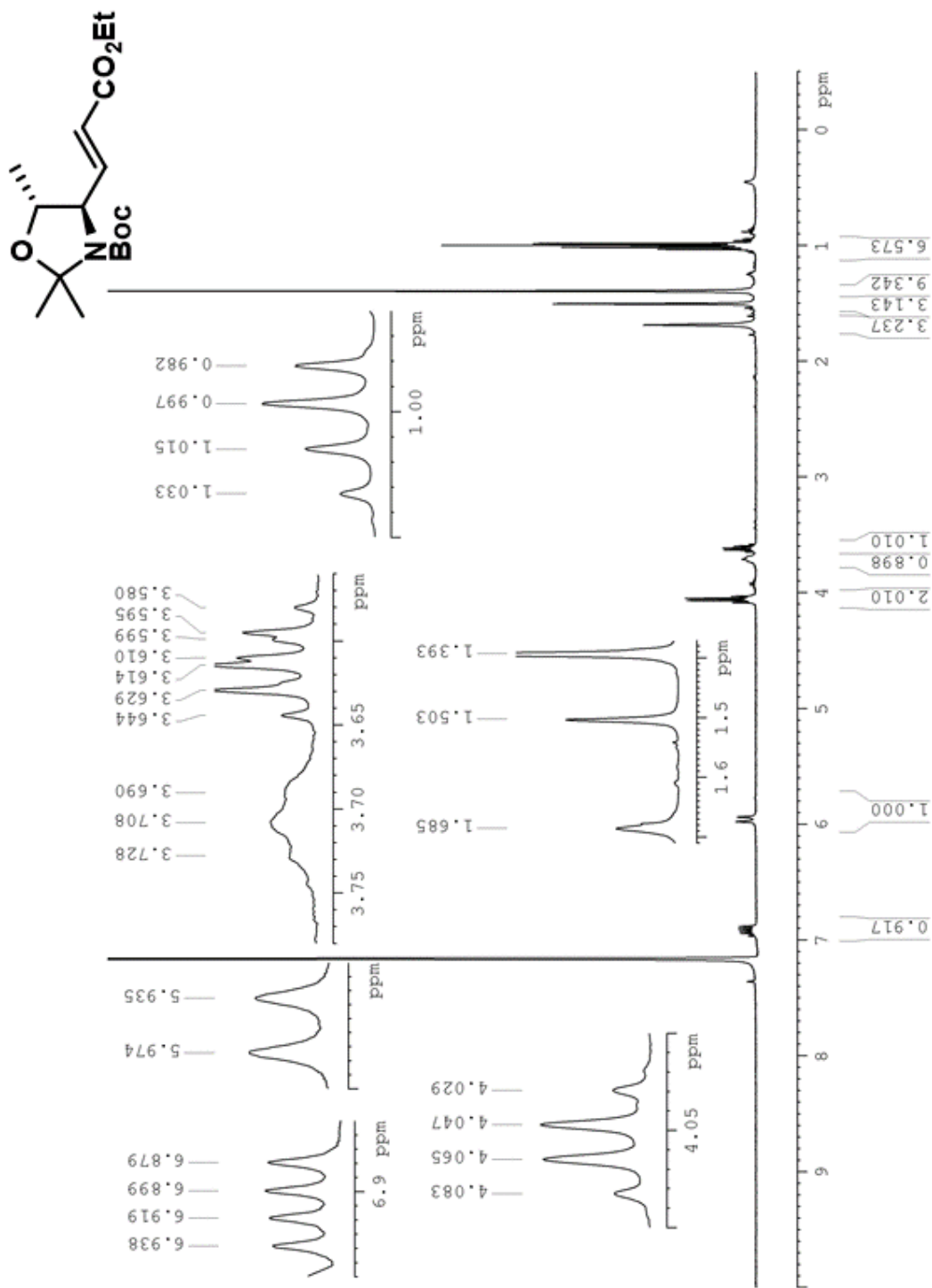


Appendix Figure 18: ¹H NMR of (S)-1-ethoxy-1-oxopropan-2-yl morpholine-4-carboxylate (CDCl₃, 400MHz,

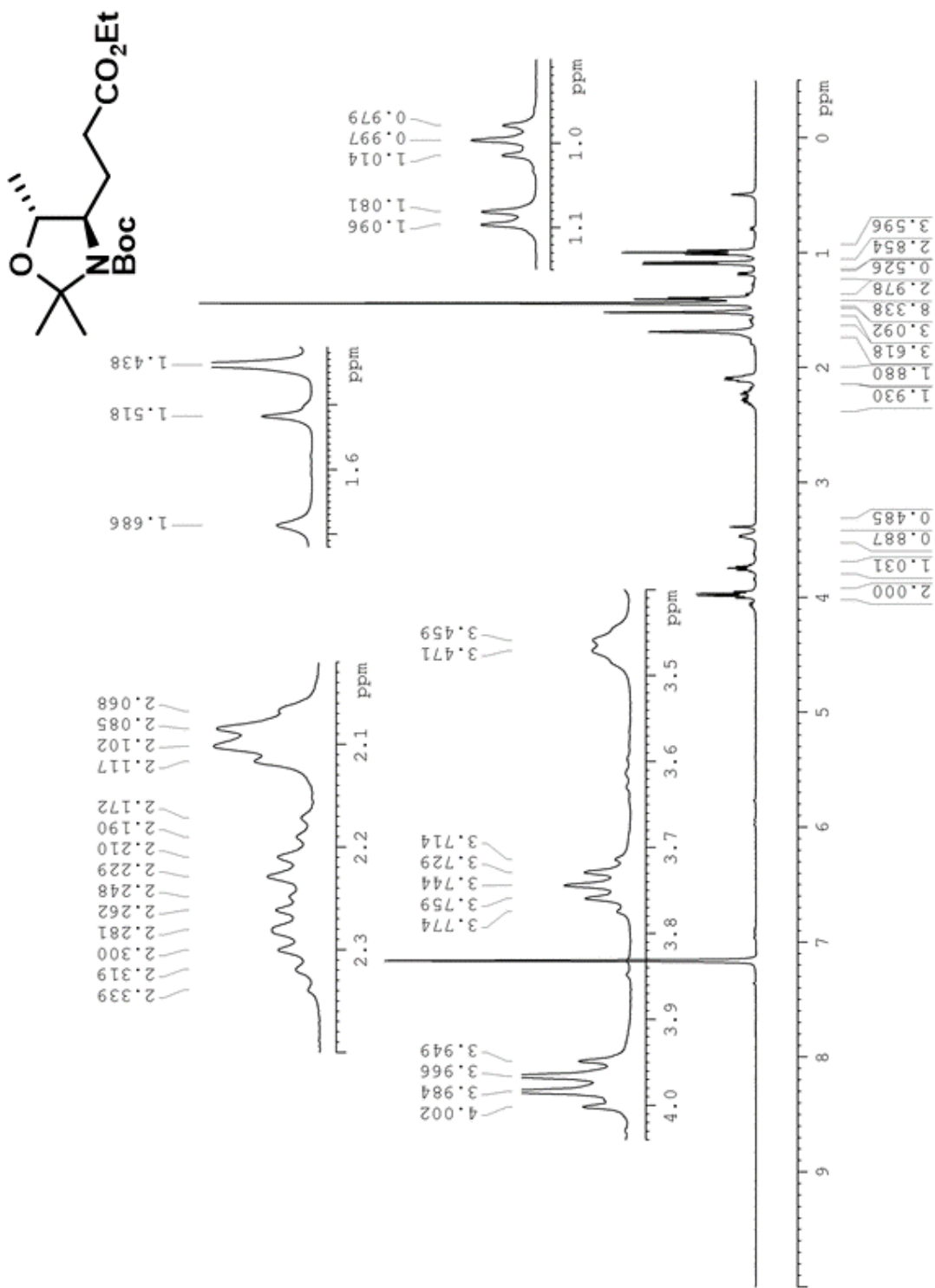
298 K)



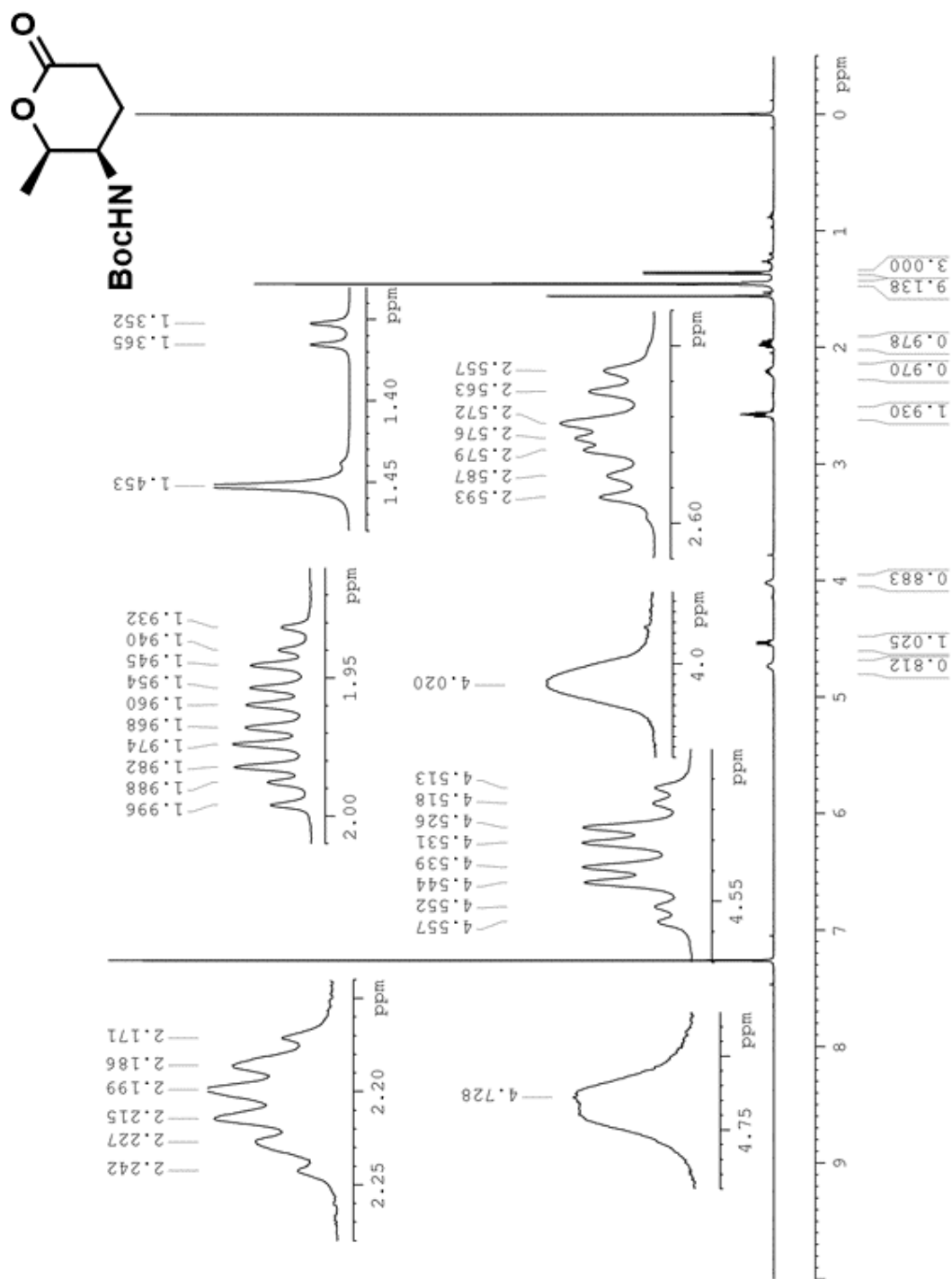
Appendix Figure 19: ¹H NMR of (S)-(Z)-5-ethoxy-5-oxopent-3-en-2-yl morpholine-4-carboxylate (CDCl₃, 500MHz, 298 K)



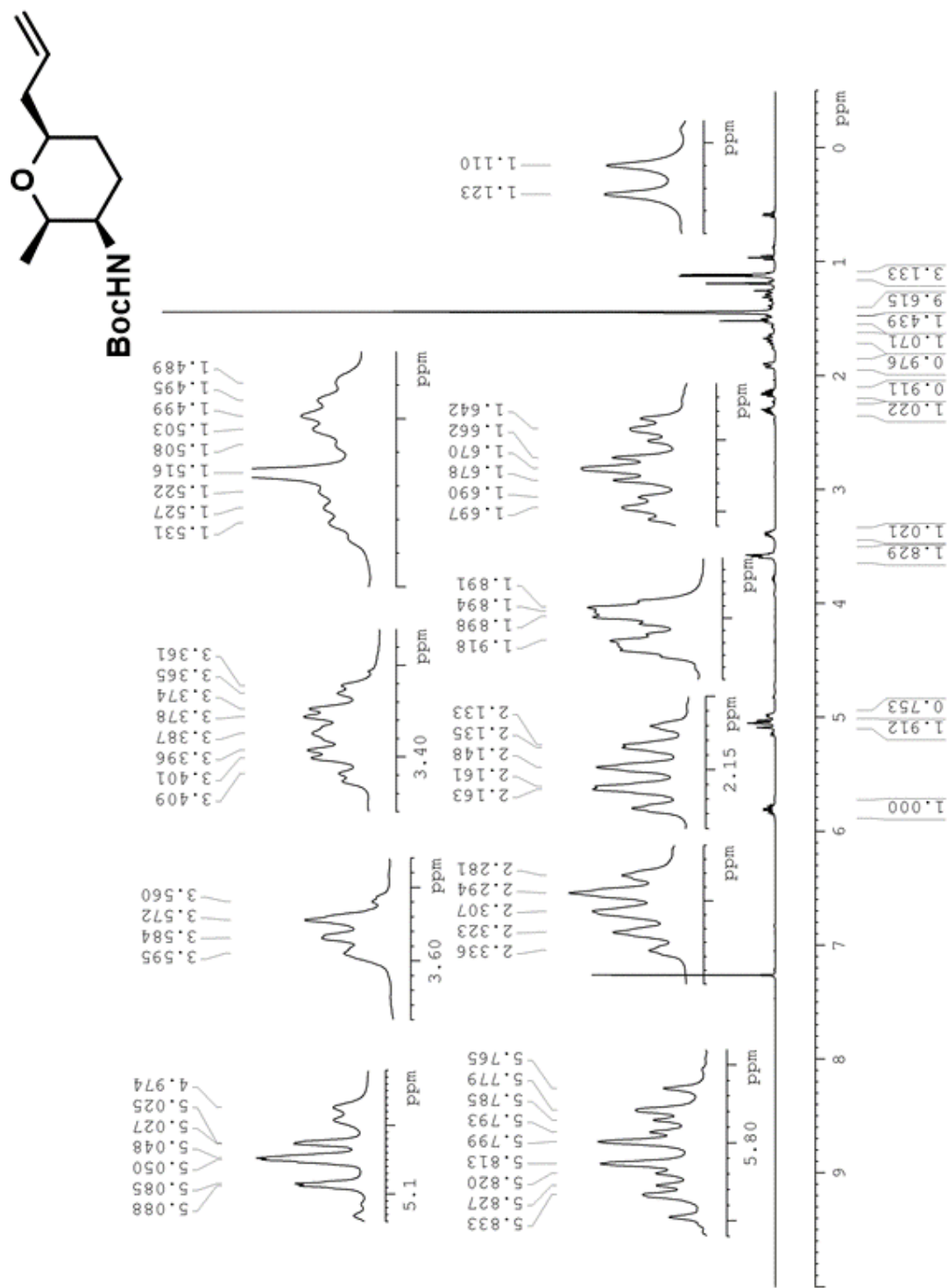
Appendix Figure 20: ¹H NMR of tert-butyl (4R,5R)-4-((E)-3-ethoxy-3-oxoprop-1-en-1-yl)-2,2,5-trimethyloxazolidine-3-carboxylate (C₆D₆, 400MHz, 338 K)



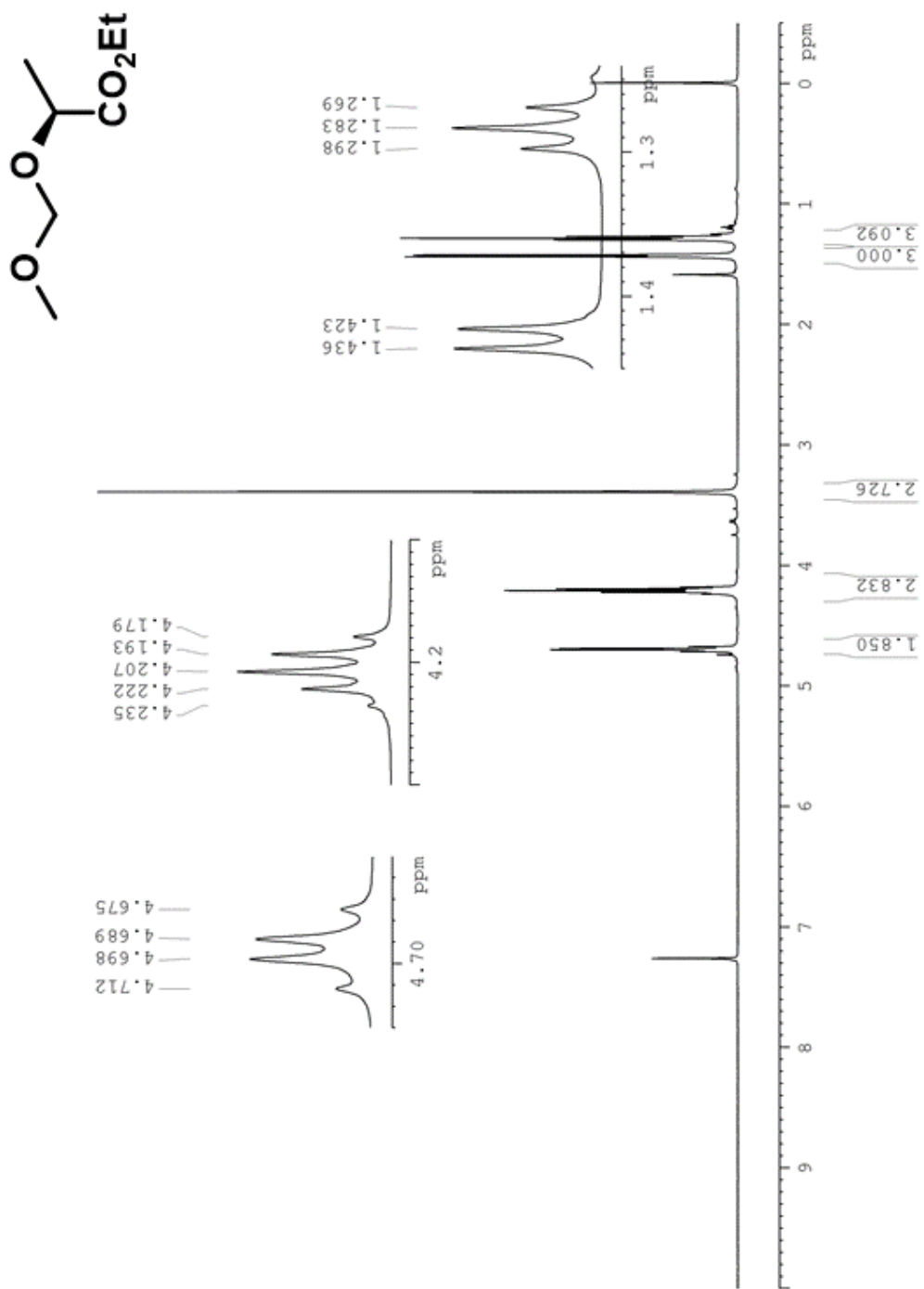
Appendix Figure 21: ¹H NMR of tert-butyl tert-butyl (4R,5R)-4-(3-ethoxy-3-oxopropyl)-2,2,5-trimethyloxazolidine-3-carboxylate (C₆D₆, 400MHz, 338 K)



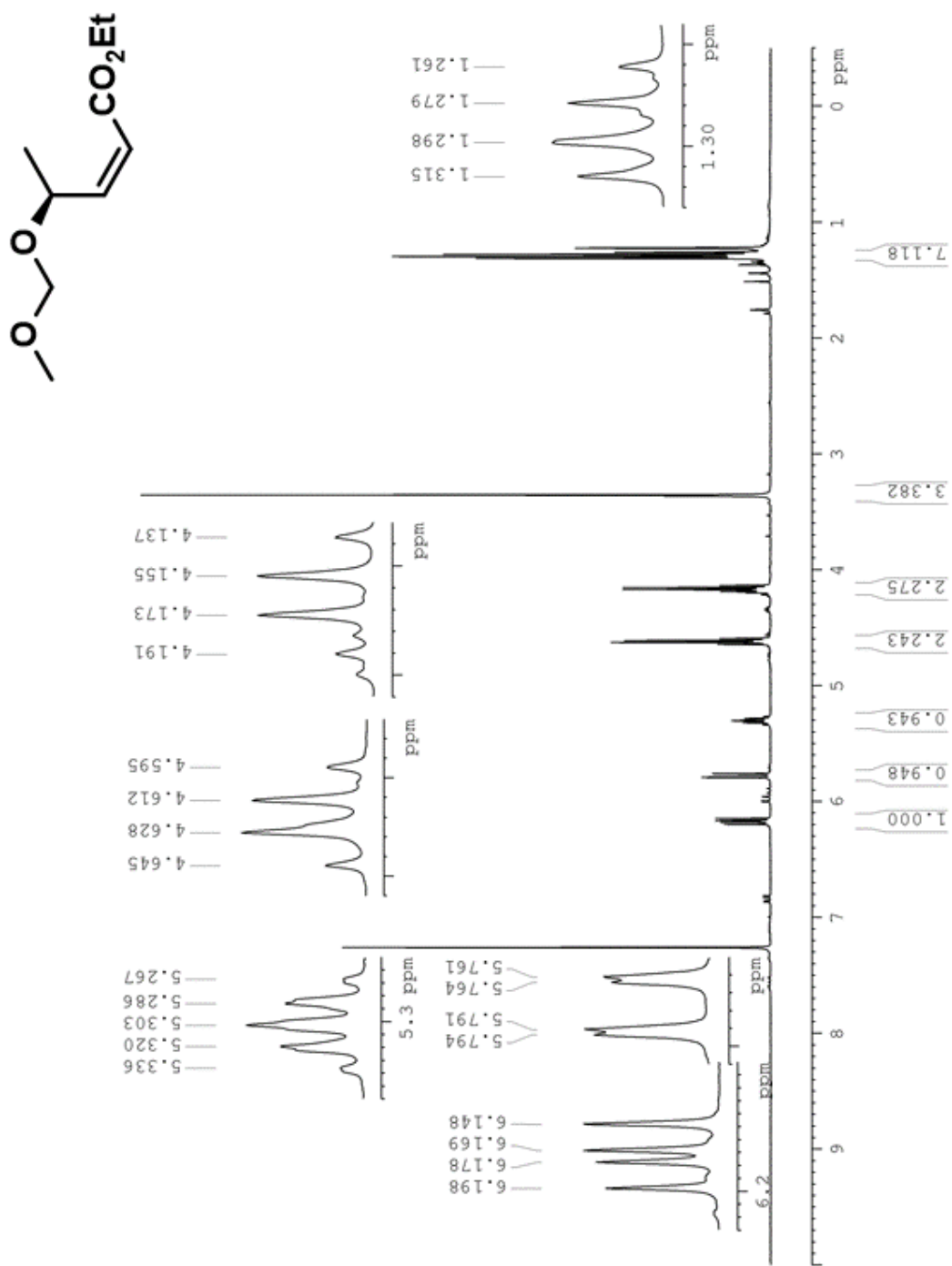
Appendix Figure 22: ^1H NMR of tert-butyl ((2R,3R)-2-methyl-6-oxotetrahydro-2H-pyran-3-yl)carbamate (CDCl₃, 500MHz, 298 K)



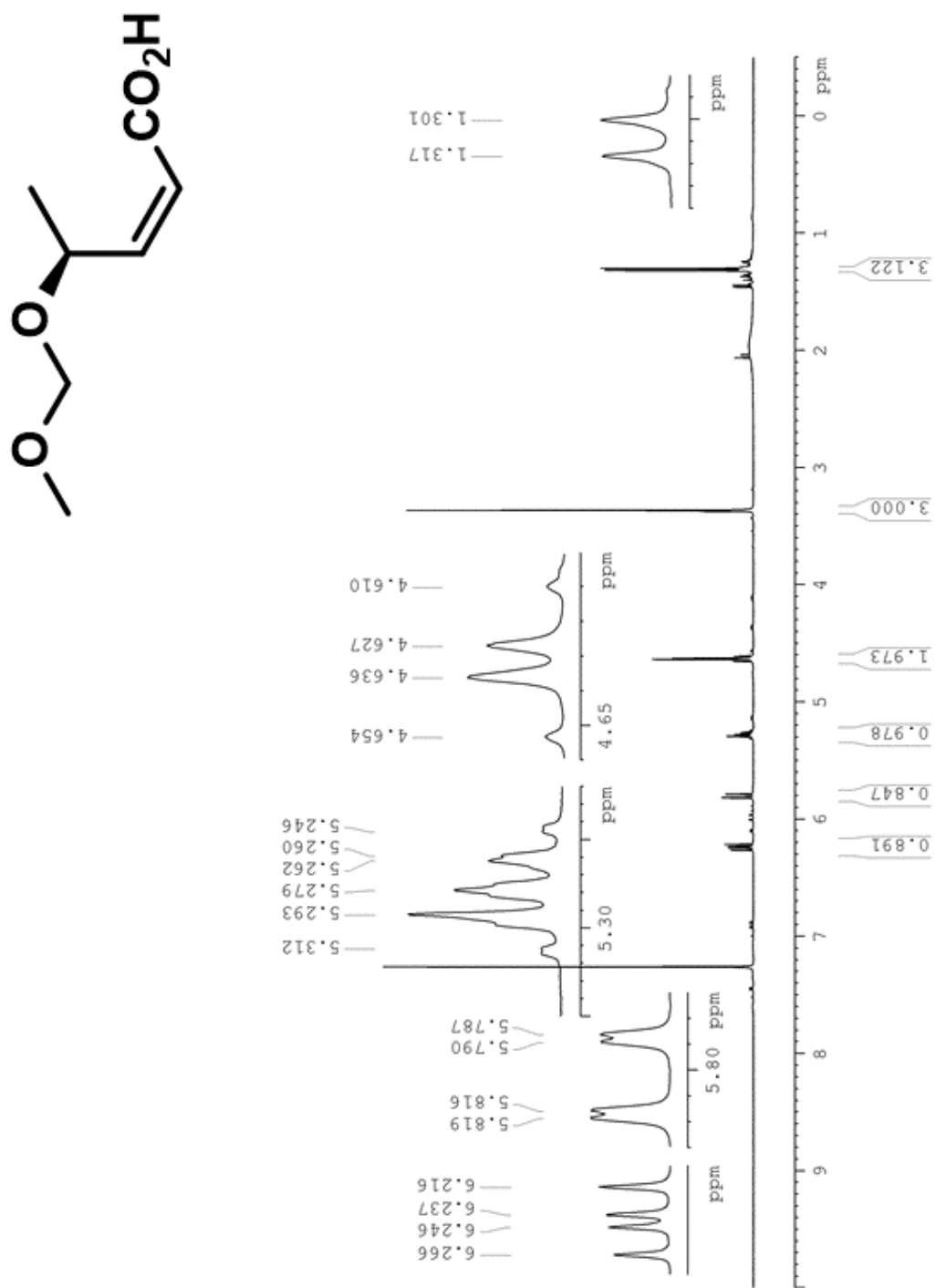
Appendix Figure 23: ¹H NMR of tert-butyl ((2R,3R,6R)-6-allyl-2-methyltetrahydro-2H-pyran-3-yl)carbamate (CDCl₃, 500MHz, 298 K)



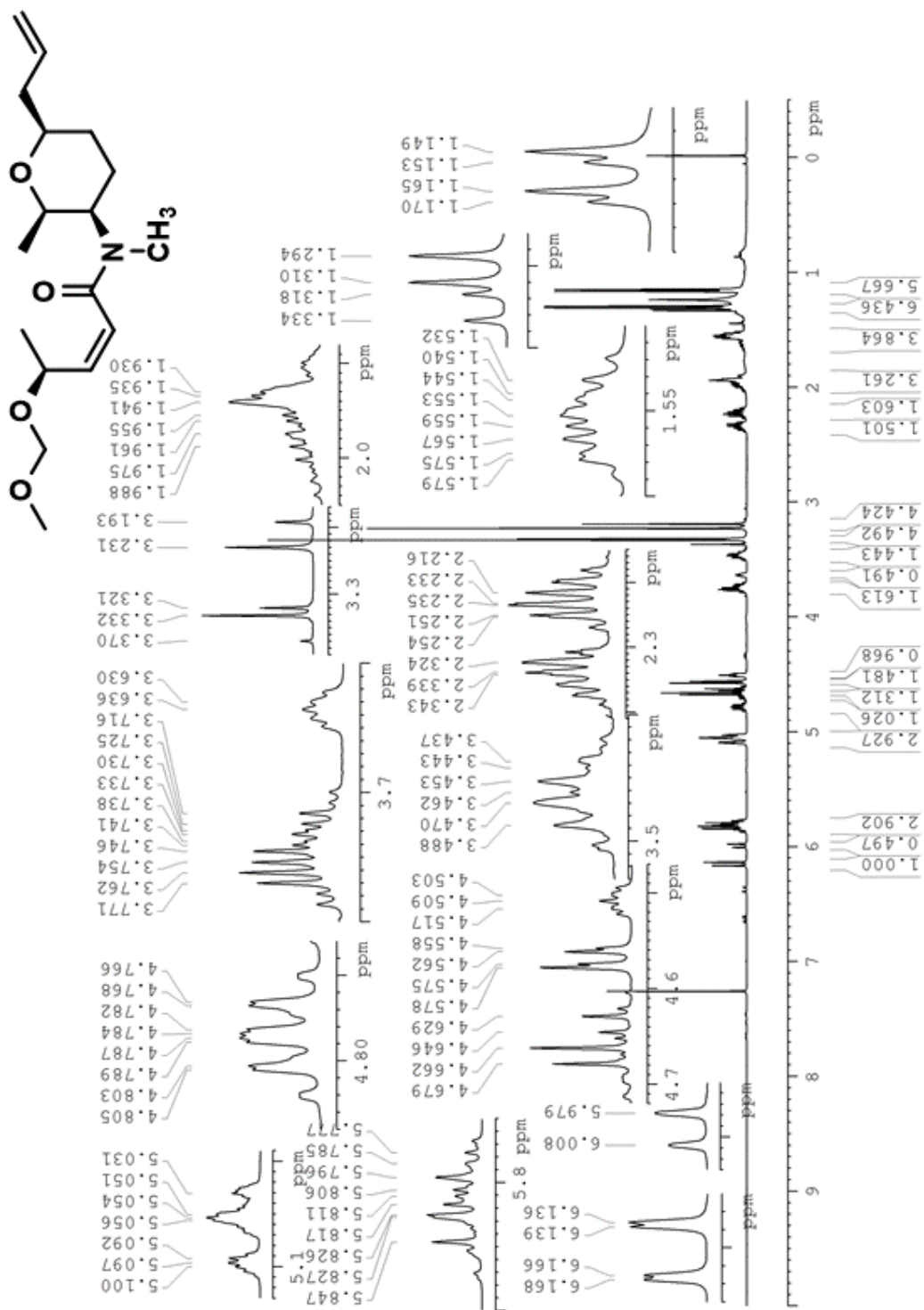
Appendix Figure 24: ¹H NMR of S-2-(methoxymethoxy)propanoate (CDCl₃, 500MHz, 298 K)



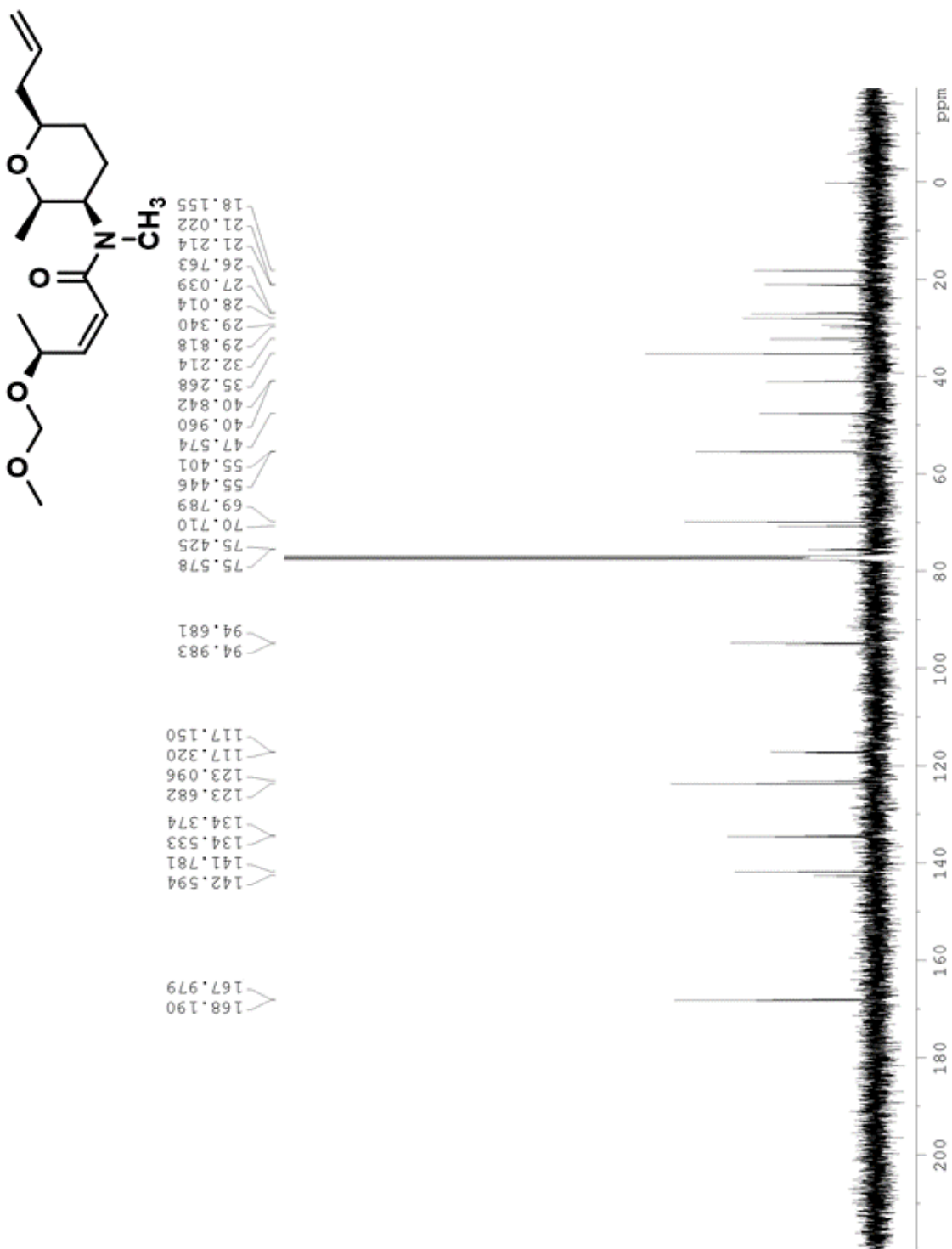
Appendix Figure 25: ¹H NMR of (S)-(Z)-4-(methoxymethoxy)pent-2-enoate (CDCl₃, 400MHz, 298K)



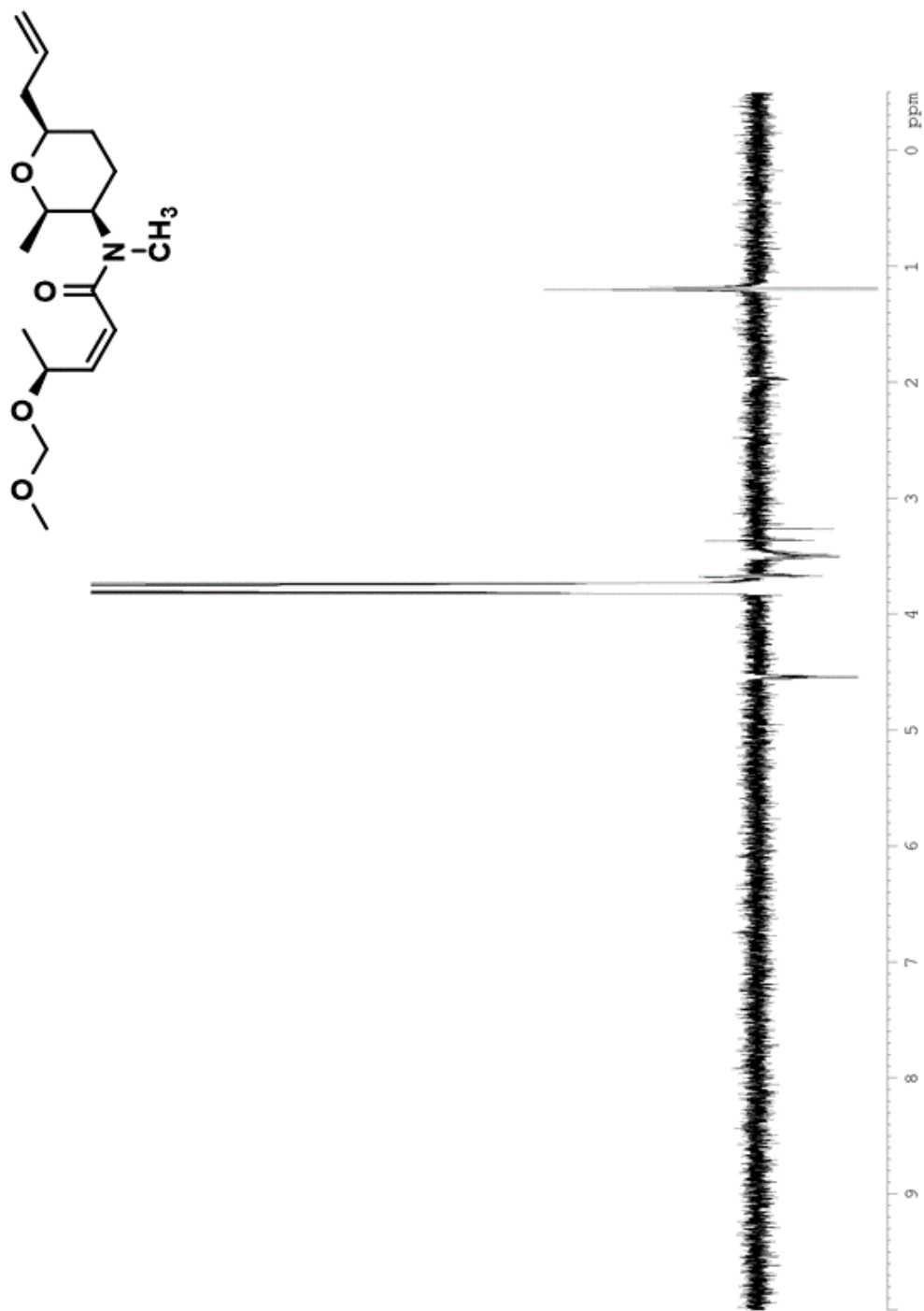
Appendix Figure 26: ¹H NMR of ((S)-(Z)-4-(methoxymethoxy)pent-2-enoic acid (CDCl₃, 400MHz, 298 K)



Appendix Figure 27: ¹H NMR of (((S)-(Z))-N-((2R,3R,6R))-6-allyl-2-methyltetrahydro-2H-pyran-3-yl)-4-(methoxymethoxy)-N-methylpent-2-enamide (CDCl₃, 400MHz, 298 K)



Appendix Figure 28: ^{13}C NMR of (((S)-(Z))-N-((2R,3R,6R))-6-allyl-2-methyltetrahydro-2H-pyran-3-yl)-4-(methoxymethoxy)-N-methylpent-2-enamide (CDCl_3 , 400MHz, 298 K)



Appendix Figure 29: NOE irradiated at 3.7623ppm NMR of (((S)-(Z))-N-((2R,3R,6R))-6-allyl-2-methyltetrahydro-2H-pyran-3-yl)-4-(methoxymethoxy)-N-methylpent-2-enamide (CDCl₃, 400MHz, 298 K)

Bibliography

- (1)Pan, Q.; Shai, O.; Lee, L. J.; Frey, J.; Blencowe, B. J. *Nat Genet* **2008**, *40*, 1413.
- (2)Berget, S. M.; Moore, C.; Sharp, P. A. *Proc. Natl. Acad. Sci. U. S. A.* **1977**, *74*, 3171.
- (3)Chow, L. T.; Gelinas, R. E.; Broker, T. R.; Roberts, R. J. *Cell* **1977**, *12*, 1.
- (4)Darnell, J. E. *Science* **1978**, *202*, 1257.
- (5)Knapp, G.; Beckmann, J. S.; Johnson, P. F.; Fuhrman, S. A.; Abelson, J. *Cell* **1978**, *14*, 221.
- (6)Rappsilber, J.; Ryder, U.; Lamond, A. I.; Mann, M. *Genome Res* **2002**, *12*, 1231.
- (7)Jurica, M. S.; Moore, M. J. *Molecular Cell* **2003**, *12*, 5.
- (8)Berglund, J. A.; Chua, K.; Abovich, N.; Reed, R.; Rosbash, M. *Cell* **1997**, *89*, 781.
- (9)Black, D. L.; Chabot, B.; Steitz, J. A. *Cell* **1985**, *42*, 737.
- (10)Ruskin, B.; Zamore, P. D.; Green, M. R. *Cell* **1988**, *52*, 207.
- (11)Wu, S. P.; Romfo, C. M.; Nilsen, T. W.; Green, M. R. *Nature* **1999**, *402*, 832.
- (12)Konarska, M. M.; Sharp, P. A. *Cell* **1987**, *49*, 763.
- (13)Parker, R.; Siliciano, P. G.; Guthrie, C. *Cell* **1987**, *49*, 229.
- (14)Boesler, C.; Rigo, N.; Anokhina, M. M.; Tauchert, M. J.; Agafonov, D. E.; Kastner, B.; Urlaub, H.; Ficner, R.; Will, C. L.; Lührmann, R. *Nature Communications* **2016**, *7*, 11997.
- (15)Raghuathan, P. L.; Guthrie, C. *Curr Biol* **1998**, *8*, 847.
- (16)Chan, S. P.; Kao, D. I.; Tsai, W. Y.; Cheng, S. C. *Science* **2003**, *302*, 279.
- (17)Lardelli, R. M.; Thompson, J. X.; Yates, J. R.; Stevens, S. W. *Rna* **2010**, *16*, 516.
- (18)Agafonov, D. E.; Kastner, B.; Dybkov, O.; Hofele, R. V.; Liu, W. T.; Urlaub, H.; Lührmann, R.; Stark, H. *Science* **2016**, *351*, 1416.

- (19)Bertram, K.; Agafonov, D. E.; Dybkov, O.; Haselbach, D.; Leelaram, M. N.; Will, C. L.; Urlaub, H.; Kastner, B.; Luhrmann, R.; Stark, H. *Cell* **2017**, *170*, 701.
- (20)Schwer, B.; Guthrie, C. *Embo J* **1992**, *11*, 5033.
- (21)Zhan, X. C.; Yan, C. Y.; Zhang, X. F.; Lei, J. L.; Shi, Y. G. *Cell Res* **2018**, *28*, 1129.
- (22)Zhang, X. F.; Yan, C. Y.; Hang, J.; Finci, L. I.; Lei, J. L.; Shi, Y. G. *Cell* **2017**, *169*, 918.
- (23)Arenas, J. E.; Abelson, J. N. *P Natl Acad Sci USA* **1997**, *94*, 11798.
- (24)Schwer, B.; Gross, C. H. *Embo J* **1998**, *17*, 2086.
- (25)Gozani, O.; Potashkin, J.; Reed, R. *Mol Cell Biol* **1998**, *18*, 4752.
- (26)Gozani, O.; Feld, R.; Reed, R. *Gene Dev.* **1996**, *10*, 233.
- (27)Corrionero, A.; Minana, B.; Valcarcel, J. *Gene Dev.* **2011**, *25*, 445.
- (28)Malcovati, L.; Karimi, M.; Papaemmanuil, E.; Ambaglio, I.; Jadersten, M.; Jansson, M.; Elena, C.; Galli, A.; Walldin, G.; Della Porta, M. G.; Raaschou-Jensen, K.; Travaglino, E.; Kallenbach, K.; Pietra, D.; Ljungstrom, V.; Conte, S.; Boveri, E.; Invernizzi, R.; Rosenquist, R.; Campbell, P. J.; Cazzola, M.; Lindberg, E. H. *Blood* **2015**, *126*, 233.
- (29)Moore, M. J.; Wang, Q. Q.; Kennedy, C. J.; Silver, P. A. *Cell* **2010**, *142*, 625.
- (30)Kim, J. H.; Sim, S. H.; Ha, H. J.; Ko, J. J.; Lee, K.; Bae, J. *Febs Lett* **2009**, *583*, 2758.
- (31)Bae, J.; Leo, C. P.; Hsu, S. Y.; Hsueh, A. J. W. *J Biol Chem* **2000**, *275*, 25255.
- (32)Paoletta, B. R.; Gibson, W. J.; Urbanski, L. M.; Alberta, J. A.; Zack, T. I.; Bandopadhyay, P.; Nichols, C. A.; Agarwalla, P. K.; Brown, M. S.; Lamothe, R.; Yu, Y.; Choi, P. S.; Obeng, E. A.; Heckl, D.; Wei, G.; Wang, B.; Tsherniak, A.; Vazquez, F.; Weir, B. A.; Root, D. E.; Cowley, G. S.; Buhrlage, S. J.; Stiles, C. D.; Ebert, B. L.; Hahn, W. C.; Reed, R.; Beroukhim, R. *Elife* **2017**, *6*, e23268.

- (33) Nakajima, H.; Sato, B.; Fujita, T.; Takase, S.; Terano, H.; Okuhara, M. *J. Antibiot.* **1996**, *49*, 1196.
- (34) He, H. Y.; Ratnayake, A. S.; Janso, J. E.; He, M.; Yang, H. Y.; Loganzo, F.; Shor, B.; O'Donnell, C. J.; Koehn, F. E. *J. Nat. Prod.* **2014**, *77*, 1864.
- (35) Kaida, D.; Motoyoshi, H.; Tashiro, E.; Nojima, T.; Hagiwara, M.; Ishigami, K.; Watanabe, H.; Kitahara, T.; Yoshida, T.; Nakajima, H.; Tani, T.; Horinouchi, S.; Yoshida, M. *Nat. Chem. Biol.* **2007**, *3*, 576.
- (36) Kotake, Y.; Sagane, K.; Owa, T.; Mimori-Kiyosue, Y.; Shimizu, H.; Uesugi, M.; Ishihama, Y.; Iwata, M.; Mizui, Y. *Nat. Chem. Biol.* **2007**, *3*, 570.
- (37) Hasegawa, M.; Miura, T.; Kuzuya, K.; Inoue, A.; Won Ki, S.; Horinouchi, S.; Yoshida, T.; Kunoh, T.; Koseki, K.; Mino, K.; Sasaki, R.; Yoshida, M.; Mizukami, T. *Acs Chem. Biol.* **2011**, *6*, 229.
- (38) Thompson, C. F.; Jamison, T. F.; Jacobsen, E. N. *J. Am. Chem. Soc.* **2000**, *122*, 10482.
- (39) Thompson, C. F.; Jamison, T. F.; Jacobsen, E. N. *J. Am. Chem. Soc.* **2001**, *123*, 9974.
- (40) Horigome, M.; Motoyoshi, H.; Watanabe, H.; Kitahara, T. *Tetrahedron Lett.* **2001**, *42*, 8207.
- (41) Motoyoshi, H.; Horigome, M.; Watanabe, H.; Kitahara, T. *Tetrahedron* **2006**, *62*, 1378.
- (42) Motoyoshi, H.; Horigome, M.; Ishigami, K.; Yoshida, T.; Horinouchi, S.; Yoshida, M.; Watanabe, H.; Kitahara, T. *Biosci. Biotech. Biochem.* **2004**, *68*, 2178.
- (43) Albert, B. J.; Sivaramakrishnan, A.; Naka, T.; Koide, K. *J. Am. Chem. Soc.* **2006**, *128*, 2792.
- (44) Albert, B. J.; Sivaramakrishnan, A.; Naka, T.; Czaicki, N. L.; Koide, K. *J. Am. Chem. Soc.* **2007**, *129*, 7206.
- (45) Shahi, S. P.; Koide, K. *Angewandte Chemie-International Edition* **2004**, *43*, 2525.
- (46) Meta, C. T.; Koide, K. *Org. Lett.* **2004**, *6*, 1785.

- (47)Bickart, P.; Carson, F. W.; Jacobus, J.; Miller, E. G.; Mislow, K. *J. Am. Chem. Soc.* **1968**, *90*, 4869.
- (48)Ghosh, A. K.; Chen, Z. H. *Org. Lett.* **2013**, *15*, 5088.
- (49)Ghosh, A. K.; Chen, Z. H.; Effenberger, K. A.; Jurica, M. S. *J. Org. Chem.* **2014**, *79*, 5697.
- (50)Ghosh, A. K.; Reddy, G. C.; MacRae, A. J.; Jurica, M. S. *Org. Lett.* **2018**, *20*, 96.
- (51)Osman, S.; Albert, B. J.; Wang, Y.; Li, M.; Czaicki, N. L.; Koide, K. *Chem.-Eur. J.* **2011**, *17*, 895.
- (52)Albert, B. J.; McPherson, P. A.; O'Brien, K.; Czaicki, N. L.; DeStefino, V.; Osman, S.; Li, M. S.; Day, B. W.; Grabowski, P. J.; Moore, M. J.; Vogt, A.; Koide, K. *Mol. Cancer. Ther.* **2009**, *8*, 2308.
- (53)Gao, Y.; Koide, K. *Acs Chem. Biol.* **2013**, *8*, 895.
- (54)Cretu, C.; Agrawal, A. A.; Cook, A.; Will, C. L.; Fekkes, P.; Smith, P. G.; Luhrmann, R.; Larsen, N.; Buonamici, S.; Pena, V. *Molecular Cell* **2018**, *70*, 265.
- (55)Talele, T. T. *J Med Chem* **2016**, *59*, 8712.
- (56)Blanksby, S. J.; Ellison, G. B. *Accounts Chem Res* **2003**, *36*, 255.
- (57)Gentles, R. G.; Ding, M.; Bender, J. A.; Bergstrom, C. P.; Grant-Young, K.; Hewawasam, P.; Hudyma, T.; Martin, S.; Nickel, A.; Regueiro-Ren, A.; Tu, Y.; Yang, Z.; Yeung, K. S.; Zheng, X. F.; Chao, S.; Sun, J. H.; Beno, B. R.; Camac, D. M.; Chang, C. H.; Gao, M.; Morin, P. E.; Sheriff, S.; Tredup, J.; Wan, J.; Witmer, M. R.; Xie, D. L.; Hanumegowda, U.; Knipe, J.; Mosure, K.; Santone, K. S.; Parker, D. D.; Zhuo, X. L.; Lemm, J.; Liu, M. P.; Pelosi, L.; Rigat, K.; Voss, S.; Wang, Y.; Wang, Y. K.; Colonno, R. J.; Gao, M.; Roberts, S. B.; Gao, Q.; Ng, A.; Meanwell, N. A.; Kadow, J. F. *J Med Chem* **2014**, *57*, 1855.

- (58) Rigat, K. L.; Lu, H.; Wang, Y. K.; Argyrou, A.; Fanslau, C.; Beno, B.; Wang, Y.; Marcinkeviciene, J.; Ding, M.; Gentles, R. G.; Gao, M.; Abell, L. M.; Roberts, S. B. *J Biol Chem* **2014**, *289*, 33456.
- (59) Kim, J. Y.; Shin, W. K.; Jaladi, A. K.; An, D. K. *Tetrahedron* **2018**, *74*, 4236.
- (60) Abe, T.; Haga, T.; Negi, S.; Morita, Y.; Takayanagi, K.; Hamamura, K. *Tetrahedron* **2001**, *57*, 2701.
- (61) Kim, M. S.; Choi, Y. M.; An, D. K. *Tetrahedron Lett.* **2007**, *48*, 5061.
- (62) Ducry, L.; Roberge, D. M. *Org. Process Res. Dev.* **2008**, *12*, 163.
- (63) Uhlig, N.; Martins, A.; Gao, D. T. *Org. Process Res. Dev.* **2020**, *24*, 2326.
- (64) Fulop, Z.; Bana, P.; Greiner, I.; Eles, J. *Molecules* **2021**, *26*, 10.
- (65) Magano, J.; Dunetz, J. R. *Org. Process Res. Dev.* **2012**, *16*, 1156.